UNIVERSITEIT VAN PRETORIA
UNIVERSITY OF PRETORIA
YUNIBESITHI YA PRETORIA

THE EFFECT OF PREWETTING ON THE RESIDENCE TIME DISTRIBUTION AND HYDRODYNAMIC PARAMETERS IN TRICKLE BED REACTORS

Nadine Wales

Submitted in partial fulfilment of the requirements of the Degree Master of Engineering (Chemical Engineering), in the Faculty of Engineering, Built Environment and Information Technology.

University of Pretoria, Pretoria

November 2006

The Effect of Prewetting on the Residence Time Distribution and Hydrodynamic Parameters in Trickle Bed Reactors

By

Nadine Wales

Professor Mike Heydenrych

Department of Chemical Engineering

Master of Engineering (Chemical Engineering)

Residence time distributions have become an important analytical tool in the analysis of many types of flow systems. Residence time distributions have proven to be effective for analysing trickle bed reactors, as it allows determination of parameters under operating conditions allowing no interference of these conditions. By studying the residence time distribution a great amount of information can be obtained and therefore used to determine a number of hydrodynamic parameters.

Due to recent findings that prewetting has a tremendous effect on a number of hydrodynamic parameters such as holdup, wetting efficiency and pressure drop, it is therefore the aim of this study to investigate the effect of trickle flow morphology or prewetting on a trickle bed reactor. The residence time distribution is obtained whereby hydrodynamic parameters are determined and therefore the effect the flow morphology has on various hydrodynamic parameters is highlighted. A number of methods were used to determine these parameters, namely that of the best-fit method, whereby the PDE model was used, and the method of moments.

Operating conditions included varying gas and liquid flow rates for porous and non-porous catalyst particles at atmospheric pressure. The different prewetting procedures used during this work included the following:

- Non-wetted
- Levec-wetted
- Super-wetted

From this investigation the following conclusions were made:

- Prewetting has a great effect on the hydrodynamic parameters of trickle bed reactors
- The differences in prewetting can be attributed to differing flow morphologies for the different prewetted beds i.e. the dominant flow morphology for a non-wetted bed is that of rivulets and for prewetted beds that of film flow
- It was also found that at low liquid flow rates the flow morphology in prewetted beds changes from film flow to a combination of rivulet and film flow
- The different flow morphologies for prewetted and non prewetted beds was confirmed by the residence time distributions and various parameters obtained there from
- At low liquid flow rates the flow morphology becomes a more predominant factor in creating the tailing effect present in residence time distribution for prewetted beds
- The tailing effect in residence time distributions is a result of both internal diffusion and liquid flow morphology, where the liquid flow morphology is the more dominant factor
- The use of residence time distributions to determine a number of hydrodynamic parameters proved to be very useful and accurate by means of different methods, i.e. method of moments and best-fit method
- Differences in the liquid holdup determined from the method of moments and the weighing method confirmed that different flow morphologies exist for different prewetted beds
- An increase in the dispersion coefficient with prewetting was observed indicating that the amount of micro mixing is different for the different prewetted beds
- Differences in residence times and high values for the dynamic holdup, for the porous packing, confirmed that the PDE model does not model well the porous packing response curves due to the lack of internal diffusion and internal holdup in this model

- The dynamic-static mass transfer showed that film flow, as in prewetted beds, results in slower mass transfer as opposed to rivulet flow and therefore it is concluded that prewetting results in different flow morphologies.

Following this study it is recommended that a residence time distribution model be used or developed that incorporates the effects of internal diffusion and internal holdup as present in porous catalyst particles. In addition, it was found that very few correlations could accurately predict hydrodynamic parameters due to the absence of the effect of prewetting and therefore it is recommended that correlations be developed that incorporate the effect of prewetting.

KEYWORDS: prewetting, residence time distribution, pressure drop, liquid holdup, wetting efficiency, piston dispersion exchange model, best-fit method, method of moments, trickle flow

Acknowledgements

The support of Sasol Research and Development and the efforts of Arno de Klerk, towards the Reactor Engineering Focus Group at the University of Pretoria, are hereby acknowledged.

Table of Contents

Nomenclature

ΔP	Pressure drop, kPa
Δz	Differential reactor length, m
a	Specific interfacial area between dynamic and static phases, m^{-1}
a_C	Area of catalyst, m^2
A_C	Cross-sectional area, m^2
a_{LS}	Liquid-solid interfacial area, m^2
a_V	Packing geometrical area, m^2
C, C_D	Concentration in dynamic phase, $kmol/m^3$
C_A	Concentration of liquid reactant, $kmol/m^3$
C_{AD}	Concentration of adsorbing species, $kmol/m^3$
C_i	Concentration of tracer, $kmol/m^3$
C_S	Concentration in static phase, $kmol/m^3$
D_A	Dispersion coefficient, m^2/s
D_{EFF}	Effective diffusivity, m^2/s
d_h	Hydraulic diameter $\left[16\frac{\varepsilon_B^3}{(9\pi(1-\varepsilon_B)^2)}\right]^{0.33} d_p$, m
d_P	Particle diameter, m
E(t)	Normalised residence time distribution, dimensionless
E_1, E_2	Ergun constants, dimensionless
F	Function of packing defined by equation 2.29, dimensionless
F(t)	External cumulative residence time distribution, dimensionless
F_i	Internal pore filling, dimensionless
f_{LGG}	Two-phase frictional factor, dimensionless

G	Gas mass flux, kg/m^2 s
g	Gravitational acceleration m^2/s
Ga	Galileo number $\frac{d_P^3 \rho^2 g \varepsilon_B}{\mu^2 (1-\varepsilon_B)}$, dimensionless
H	Ratio of dynamic to total liquid holdup, dimensionless
H_D	Dynamic holdup, dimensionless
H_L, H_T	Total liquid holdup, dimensionless
H_{RTD}	Total liquid holdup determined from the residence time distribution, dimensionless
H_{weigh}	Total liquid holdup determined from the weighing method, dimensionless
k	True reaction rate constant, s^{-1}
K_A	Equilibrium adsorption constant, kg/m^3
k_{ad}	Adsorbing reaction rate constant, s^{-1}
k_L	Mass transfer coefficient between dynamic and static phases, m/s
k_{LS}	Mass transfer coefficient between liquid and sold, m/s
L	Liquid mass flux, kg/m^2 s
N_o	Number of moles tracer injected, kmol
N	Number of transfer units between dynamic and static phases, dimensionless
Pe_L	Liquid Peclet number, dimensionless
Q	Volumetric flow rate, m^3/s
r	Radius, m
Re	Reynolds number $\frac{\rho U d_P}{\mu}$, dimensionless

r_p	Particle radius, m
S_{ext}	External surface area of particle, m^2
t	Time, s
u	Velocity, m/s or mm/s
V	Volume of packed bed, m^3
V_P	Particle volume, m^3
V_R	Volume of empty column, m^3
v_{SL}	Liquid velocity, m/s
We	Weber number $\frac{L^2 d_P}{\rho_L \sigma_L}$ or $\frac{G^2 d_P}{\rho_G \sigma_G}$ for liquid and gas phases respectively, dimensionless
Z	Reactor length, m

Greek symbols

τ	Average residence time, s
S	Degree of stagnancy, dimensionless
δ	Film thickness, m
χ	Holdback as defined in equation 2.18, dimensionless
Φ	Internal cumulative residence time distribution, dimensionless
τ_{LS}	Liquid-solid shear stress, Pa
δ_{LG}	Two-phase frictional pressure drop, kg/ m^2 s^2
ϕ	Internal residence time distribution as in equation 2.19, dimensionless
χ^2	Lockhart-Martinelli parameter as defined in equation 2.24, dimensionless
α	Angle up to which catalyst is covered with liquid

β	Liquid saturation, dimensionless
ε_B	Bed porosity, dimensionless
ε_p	Particle porosity, dimensionless
η_{CE}	Wetting efficiency, external contacting efficiency, dimensionless
$\lambda(t)$	Intensity function, dimensionless
μ_L, μ_G	Viscosity of liquid and gas phases, respectively, cP
μ_n	n^{th} moment, dimensionless
ρ	Density, kg/m^3
σ_V	Standard deviation, dimensionless
Φ_{TB}	Thiele modulus

Subscripts

APP	Apparent
D	Dynamic
EFF	Effective
G	Gas
GS	Gas-solid interactions
L	Liquid phase
LFR	Liquid filled reactor
LG	Gas-liquid interactions
LS	Liquid-solid interactions
M	Mixture
S	Solid
S	Static
T	Total
TBR	Trickle bed reactor

CHAPTER 1

Introduction

Trickle bed reactors are packed beds of catalyst with a cocurrent flow of liquid and gas reactants. The use of these three phase reactors has become widespread in the petroleum industry, wastewater treatment, coal liquefication and other applications in chemical processing. An advantage of using trickle bed reactors is that it has a smaller power requirement to that of other reactors, such as slurry reactors (Mills & Dudukovic, 1981).

In order to model these types of reactors a number of parameters are defined, such two-phase pressure drop, liquid holdup and wetting efficiency. Models used normally describe the flow within the trickle bed reactor in terms of averaged bed hydrodynamic parameters. These parameters are predicted by using the gas and liquid properties as well as the flow rates and the bed properties such as bed and particle porosity. A number of studies have been performed on each of these hydrodynamic parameters and it is evident that tremendous scatter exists between the data of different authors.

It is thought that this scatter is mainly due to the different operating conditions used in experimental work. In addition, the flow history has proven to have a tremendous effect on the nature of trickle bed reactors (as evident by different prewetting modes) and therefore on the hydrodynamic parameters (Loudon, 2005; Kan & Greenfield, 1979). This hysteresis effect has been explained in terms of the flow morphology occurring within trickle bed reactors.

Residence time distributions, as obtained from tracers, have become an important analytical tool in the analysis of flow systems such as reactors and biological systems. Residence time distributions have been effective for especially analysing trickle bed reactors, as it allows determination of parameters under operating conditions and therefore there is no interference of these conditions. By studying the residence time distribution a great amount of information can be obtained and therefore used to determine a number of hydrodynamic parameters. In addition, the residence time distribution gives an indication of the flow history of a trickle bed reactor.

The aim of this study is to investigate the effect of trickle flow morphology (prewetting) on a trickle bed reactor by obtaining the residence time distribution and in turn determining the effect the flow morphology has on various hydrodynamic parameters. Operating conditions include that of different gas and liquid flow rates for the different prewetting modes and using porous and non-porous catalyst particles. By means of the residence time distribution, the liquid holdup as well as the wetting efficiency is determined. The pressure drop is also determined but not by means of the residence time distriution. The holdup determined from the residence time distribution is compared to that obtained by another method for reasons of giving an indication of the accuracy of residence time distributions.

CHAPTER 2

Literature Study

2.1. Distribution of Residence Time

Using the distribution of residence time distributions for the analysis of chemical reactors was first proposed as far back as 1935 (Fogler, 1999:811). However the concept of residence time distributions were further developed by Danckwerts (1953) when he gave structure by defining the various distributions of interest.

The residence time distribution (RTD) of a reactor is a characteristic way of identifying the mixing occurring within a chemical reactor. For example, an ideal plug flow reactor exhibits no axial mixing and this is illustrated in the shape of the residence time distribution. Not all residence time distributions are unique to a certain type of reactor (Fogler, 1999:812) and therefore different reactors can yield the same residence time distribution.

2.1.1. Measurement of the RTD

The RTD is determined experimentally by injecting a chemical that is inert, called a tracer, into the reactor at some initial time. The concentration of the tracer is then measured in the effluent stream as a function of time. To ensure that the tracer truly reflects the behaviour of the reactant mixture flowing through the reactor, it is important that the tracer have certain characteristics such as:

- Having properties similar to the reactor mixture
- Be soluble in the reacting mixture
- Should not absorb on the surfaces of the reactor.

Commonly used tracers include colour, conductive or radioactive materials as they allow for the easy measurement or detection in the effluent stream.

The method of injecting the tracer is very important for the determination of the RTD. The two most used methods of injection is a pulse input and a step input. Injection with a pulse input is briefly described, as this is the method that will be used in the experimental work. With a pulse input an amount of tracer is injected into the feed stream entering the reactor in a very short period of time.

For a pulse input the residence time distribution function, E(t) can be defined.

$$E(t) = \frac{Q\,C(t)}{N_O} \tag{2.1}$$

In 2.1, Q is the volumetric flow rate of the effluent, N_O is the amount of tracer that was injected into the reactor and C(t) is the effluent concentration-time curve, known as the C curve in RTD analysis. The function E(t), also known as the exit-age distribution function, describes the time spent in the reactor by different fluid elements. Usually N_O is not known directly and can be obtained by the summation of all tracer amounts between the times the tracer was injected up to infinity. In addition, the volumetric flow rate is usually constant. From 2.1, the RTD function can therefore be defined differently, as in 2.2.

$$E(t) = \frac{C(t)}{\int_0^\infty C(t)\; dt} \tag{2.2}$$

The integral in the denominator of 2.2 is the area under the concentration curve.

It is important to state that drawbacks do exist when the method of injection is by means of a pulse input. Difficulties of the pulse input lie with obtaining a reasonable pulse at the entrance of the reactor. It must be ensured that the time or period of injection be small when compared to the residence times of the chemical reactor. In addition, there must be, at the most, a small amount of dispersion occurring between the point of injection and the entrance to the reactor. If these aspects can be overcome, the RTD can be obtained simply and directly.

In the case of certain types of reactors, especially in trickle bed reactors, a long tail is observed in the concentration-time curve. This occurrence can create large inaccuracies in the analysis of the RTD function. The tail in the concentration-time curve affects the denominator in 2.2, i.e. the integration of the C(t) curve. To overcome this, it has been suggested by authors to extrapolate the tail and analytically continue the calculation or the tail can be approximated as an exponential decay (Fogler, 1999:817).

2.1.2. RTD Parameter Estimation Techniques

Once residence time distributions are obtained at different operating conditions and physical properties of the reactor system, it is required to interpret the RTD curves and is an integral part in the success of tracing testing. RTD curves are approximated and thereby reduced to a number of parameters, in order to correlate reactor performance to operating conditions. There are a number of techniques in obtaining the RTD parameters:

- ***Method of moments*****.** This technique obtains the solution of the differential equations of the RTD curves. The n-th moment obtained from an ideal stimulus is given by:

  $$\mu_n = \int_0^\infty t^n \, E(t)\, dt, \qquad n = 0, 1, 2, 3... \tag{2.3}$$

  The conditions of E(t) do not guarantee the existence of the moments greater than the second ($n \geq 2$) (Buffham & Mason, 1993). However when an ideal stimulus is not obtainable the moments need to incorporate this. Mills & Dudukovic (1989) proposed the following for the n-th moments for a non-ideal stimulus:

  $$\begin{aligned} \mu_n &= \mu_{n,out} - \mu_{n,in} \\ &= \int_0^\infty t^n \, E(t)\, dt - \int_0^\infty t^n \, I(t)\, dt \end{aligned} \tag{2.4}$$

  The appropriate moments of the RTD data provides an indication of various aspects of flow in the reactor bed. The zeroth moment is related to the amount of tracer injected and therefore the mass balance. For the mass balance to be satisfied the zeroth moment must equal one ($\mu_o = 1$). The first moment indicates the liquid holdup. The liquid holdup is then determined from 2.5.

$$H_L = \mu_1 \frac{Q}{V} \qquad (2.5)$$

The second moment is an indication to the deviation from plug flow. The determination of the second and higher moments from experimental RTD curves are sensitive to the measurement error in the tail of the E(t) curve as well as the value of time (t) chosen as the truncation point or upper limit of the integration as in 2.3 and 2.4 (Buffham & Mason, 1993). Therefore the moments higher than the second are difficult to determine owing to the uncertainty of the RTD tails.

The method of moments is a means of testing models to match experimental data (Buffham & Mason, 1993) by determining the moments from the RTD data as well as from the model. The theory and validity of the model is confirmed if the model and experimental moments agree.

- ***Numerical comparison of experimental and theoretical RTD response curves (curve fitting).*** This technique requires the use of an RTD model that best describes the behaviour of the flow within the reactor system; such RTD models will be discussed later. The model that best fits the experimental RTD data is obtained by determining the parameter values that minimise a suitable objective function. An objective function would be one such as the minimisation of the mean square deviation between the experimental and calculated values of the response curves. The value of the optimisation function will be an indication of the quality of fit between the experimental data and model and can determine the choice of model to be used. This technique is more thorough, but if there are more than two parameters, the optimisation techniques require complex, iterative computations and may give rise to indefinite solutions (Gianetto et al., 1978).

- ***Graphical comparison of particular values of the theoretical and experimental RTD curves.***

- ***Method of convolution/deconvolution.*** (Mills & Dudukovic, 1989) For these methods it is assumed that the experimental response data has been normalised to give the forcing function (i.e. the stimuli/input response) and the system output response. The forcing function represents the tracer response of the non-ideal tracer injection and sampling system, which for an ideal system would be described by the Dirac function. For the case of deconvolution, the impulse response of the packed bed E(t) is determined by the inversion of the convolution integral operator using the input and output system responses. A more detailed description is provided in Mills & Dudukovic, (1989).

The choice of method to be used to determine the RTD parameters is important as it influences the value of the various parameters. This influence was discussed in the work of Sicardi et al., (1980), in the case of different RTD models. The parameter values are indeed very sensitive to the identification method as was reported by Sicardi et al., (1980). In their work, the method of moments gave fairly good results, however moments greater than the first were sensitive to the cutting off of the response curves at low concentrations. Sicardi et al., (1980) also investigated the curve fitting technique and it was found to perform considerably better than the method of moments. It must be added that the parameters were subject to the optimisation function. From this it can be said that if a model exists that accurately describes the reactor system and the only reason for any discrepancies is due to experimental errors the method of curve fitting is the best option. The objective function can be chosen so as to suit the error range. In addition the nature of errors can be identified by the reproduction of experiments (Buffham & Mason, 1993). On the other hand when the model does not accurately describe the experimental data a problem arises as the meaning of the parameters lie in the model description. For this reason it is better suited to opt for the method of moments.

2.1.3. RTD Models for Non-Ideal Reactors (TBR)

In the literature there exist many mathematical models for the hydrodynamics in trickle bed reactors whereby the model parameters are verified or obtained from residence time distribution data of the liquid phase in a trickle bed reactor.

Since the residence time distribution does not provide a unique description of the flow patterns and mixing occurring within a reactor, an approach whereby models are used to determine mixing, i.e. macro and micro mixing (Robinson & Tester, 1986), are essential. Difficulties do arise when flow models are constructed as parameters are introduced into the model equations. If the model parameters do not have a specific meaning, i.e. physical meaning, the modelling becomes a step in curve fitting and the true meaning behind the flow model becomes lost. Following this, it can be stated that different models will give different values for model parameters fitted to the same experimental data. For this reason it is important to consider what models will best represent experimental RTD data. It is at this point that certain guidelines are given when developing models for non-ideal reactors (Fogler, 1999:872):

- The model must be mathematically tractable, i.e. the equations used to describe a reactor should be solved without a great use of human or computer time.
- The model must realistically describe the characteristics of the non-ideal reactor, physically, mathematically and chemically.
- The model must not have more than two adjustable variables.

A very simple model was proposed by Henry & Gilbert (1973) and includes only liquid holdup to incorporate hydrodynamic effects. The liquid holdup is calculated from the mean residence time obtainable from RTD data as in (2.6).

$$\tau = \frac{H_L V}{Q_L} \tag{2.6}$$

Another type of hydrodynamic model, i.e. dispersion type, can be used to model trickle bed reactors. These models are also verified on the basis of RTD data. Three types of dispersion models are most commonly used in literature. These are the:

- Piston Dispersion (PD) model
- Piston Exchange (PE) model or Cross Flow model
- Piston Dispersion Exchange (PDE) model

The piston dispersion model, models a trickle bed reactor as a liquid phase, plug flow, packed bed reactor accounting for longitudinal dispersion. An additional hydrodynamic factor included is that of total liquid holdup. It has been found that the PD model does not interpret RTD data very well and the reason for this is that the physical phenomenon is too complex to be described only by the dispersion coefficient (Gianetto et al., 1978). The PD model is shown.

Mass balance of tracer in the bulk fluid over a differential reactor length Δz:
Accumulation rate = (Rate in due to convection + Rate in due to dispersion) - (Rate out due to convection + Rate out due to dispersion)

$$H_L A_C \Delta z \frac{dC}{dt} = -D_A A_C \left.\frac{dC}{dz}\right|_z + v_{SL} A_C C\big|_Z - \left(-D_A A_C \left.\frac{dC}{dz}\right|_{z+\Delta z} + v_{SL} A_C C\big|_{z+\Delta z} \right) \tag{2.7}$$

Even though the PD model is a widely used model (Danckwerts, 1953; Tsamatsoulis & Papyannakos, 1994) due to its simplicity and it owning a single parameter, it is felt that the use of a single parameter to model or describe the hydrodynamics of a trickle bed reactor is oversimplified. It is for this reason that various workers have employed different dispersion type models, such as the PE and PDE models, to explain trickle bed hydrodynamics (Tsamatsoulis & Papyannakos, 1994; Nigam, Illuita and Larachi, 2002; Sicardi, Baldi and Specchia, 1980a).

The piston exchange model is derived from the assumption that the liquid phase is divided into two parts. The one part or phase is that of flowing liquid in plug flow and the other is a stagnant liquid phase that is in contact with the flowing liquid. Mass exchange between these phases occurs. The piston exchange model is shown in (2.8) and (2.9). Mass balances are done over both phases, i.e. the dynamic phase and stagnant phase.

Mass balance of tracer in the dynamic liquid phase over a differential reactor length Δz:

Accumulation rate = (Rate in due to convection) - (Rate out due to convection) - (Exchange rate between dynamic and stagnant phases)

$$H_D A_C \Delta z \frac{dC_D}{dt} = H_D v_{SL} A_C C_D\big|_z - H_D v_{SL} A_C C_D\big|_{z+\Delta z} - H_L A_C k_L a (C_D - C_S) \tag{2.8}$$

Mass balance of tracer in the stagnant liquid phase over a differential reactor length Δz:

Accumulation rate = Exchange rate between dynamic and stagnant phases

$$H_S A_C \Delta z \frac{dC_S}{dt} = H_L A_C k_L a (C_D - C_S) \tag{2.9}$$

From (2.8) and (2.9) it can be seen that the PE model includes the parameters of total, dynamic and stagnant liquid holdup. The total holdup is the sum of the dynamic and stagnant liquid hold-ups. It has been shown that the PE model is sufficient for calculations and scale-up of trickle bed reactors (Gianetto et al., 1978) however according to Tsamatsoulis & Papyannakos (1994) the response to an impulse tracer input may not include the static liquid phases. Contrary to this, Van Swaaij (1969) showed that, by comparison of the measured total holdup and holdup deduced from the mean residence time that no stagnant regions existed that are not accessible to the tracer.

It has been reported that two main mechanisms are the cause for spreading in residence time distributions of trickle bed reactors. These mechanisms include that of a diffusion process and mass exchange with stagnant liquid phases (Van Swaaij, 1969). Due to this observation it is important to use a RTD model that incorporates both mechanisms, such a model would be a combination of the PE and PD models, namely the PDE model. The PDE model accounts for plug flow with longitudinal dispersion as well as for the mass transfer occurring between the dynamic and stagnant phases. Total liquid holdup and dynamic or static liquid holdup are also considered. The PDE model is shown in equations (2.10) and (2.11).

Mass balance of tracer in the dynamic liquid phase over a differential reactor length Δz:

Accumulation rate = (Rate in due to dispersion + Rate in due to convection) - (Rate out due to dispersion + Rate out due to convection) - (Exchange rate between dynamic and stagnant phases)

$$H_D A_C \Delta z \frac{dC_D}{dt} = \left(-H_D A_C D_A \left.\frac{dC_D}{dz}\right|_z + H_D v_{SL} A_C \left. C_D \right|_z \right) - \left(-H_D A_C D_A \left.\frac{dC_D}{dz}\right|_{z+\Delta z} + H_D v_{SL} A_C \left. C_D \right|_{z+\Delta z} \right) - H_L A_C k_L (C_D - C_S) \tag{2.10}$$

Mass balance of tracer in the stagnant liquid phase over a differential reactor length Δz:

Accumulation rate = Exchange rate between dynamic and stagnant phases

$$H_S A_C \Delta z \frac{dC_S}{dt} = H_L A_C k_L (C_D - C_S) \tag{2.11}$$

Adding to the suitability of the PDE as well as the PE model is the fact that the presence of stagnant liquid phases has been shown by workers (Sicardi et al., 1980a) and that other models are linked to them, for example the PDE model plus intraparticle diffusion. It would seem reasonable that the PDE model would be the most suitable for trickle bed reactors in order to determine the RTD parameters, however the PDE model leads to incorrect estimation of the

Peclét number when porous particles are used (Illiuta, Larachi & Grandjean, 1999d).

It is known that when porous particles are used in trickle bed reactors, the RTD shape is distorted as a result of intraparticle tracer diffusion, tracer adsorption and desorption (Charpentier et al., 1971; Midoux & Charpentier, 1973) and therefore needs to be incorporated into an RTD model. This was done in the work of Illiuta et al., (1999d) and Nigam, Iliuta & Larachi (2002). Nigam et al., (2002) and Illiuta et al., (1999d) extended the PDE model to include the effects of pore diffusion as the intraparticle diffusion contributes to the long tails of the RTD for trickle bed reactors. The concentration change within the particle was described by a diffusion equation and the following assumptions (Illiuta et al., 1996a) were used in their analysis:

- Particles are fully wetted
- Mass transfer between static and intraparticle liquid is neglected
- The area covered by the static liquid is negligible.

The liquid structure for this model is represented in figure 2.1 and includes:

- Mass transfer between the dynamic and static phases
- Mass transport between the dynamic phases and wetted particles
- Mass transport between the static phases and wetted particles
- Intraparticle mass transfer.

This model has proven to significantly match experimental data for trickle bed reactors. This new model, however, overlooks the important aspect of partial wetting that is known to have an effect on the conversion of a trickle bed reactor (Colombo, Baldi & Sicardi, 1976).

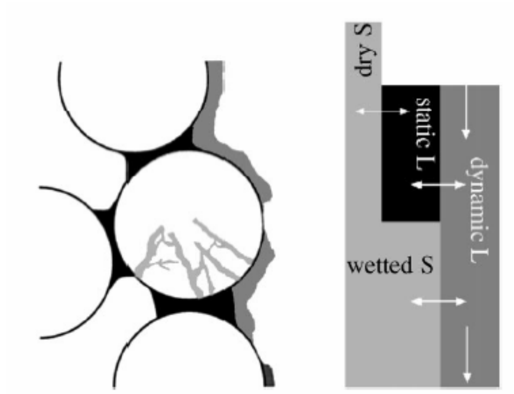

Figure 2.1 - Flow structure of the liquid trickle flow in trickle bed reactors (Illiuta et al., 1999d)

In order to incorporate the wetting efficiency in hydrodynamic models Colombo et al., (1976) proposed a model assuming total external wetting, as the effective wetted area cannot be easily determined and would be difficult to use in trickle bed analysis. Therefore if a partially effective area exists, an evaluation of the apparent internal diffusivity would be less than the actual internal diffusivity. It is reasoned that the mean path of a molecule, diffusing through a porous particle that is partially externally wetted is larger than that in a particle with complete external wetting (Colombo et al., 1976). Figure 2.2 illustrates this concept. The ratio of the apparent to actual internal diffusivity is related to the effective wetted area or fraction of the external catalyst area, i.e. wetting efficiency.

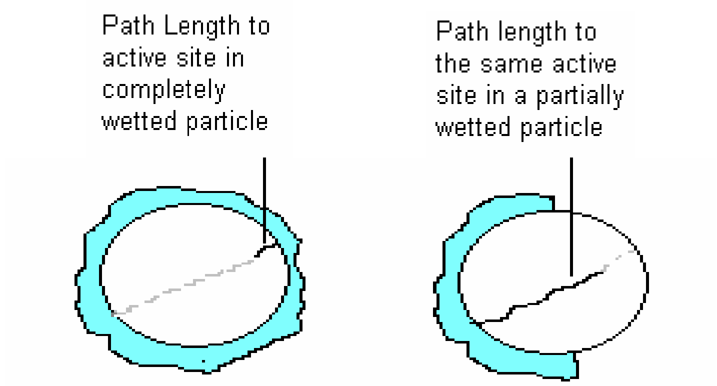

Figure 2.2 - Effect of partial external wetting on effective diffusivity (Colombo et al., 1976)

Colombo et al., (1976) determined the internal wetting and interparticle diffusivity as a function of liquid flow rate in a trickle bed reactor using an analysis of the residence time distribution. The procedure was repeated for a liquid filled reactor in order to determine the interparticle diffusivity for totally wetted particles. Assuming total external and internal wetting, the following RTD model was proposed.

Mass balance of tracer in the bulk fluid over a differential reactor length Δz:

Accumulation rate = (Rate in due to dispersion + Rate in due to convection) -

(Rate out due to dispersion +Rate out due to convection)-

(Rate of diffusion over catalyst particle)

$$H_L A_C \Delta z \frac{dC}{dt} = \left(-D_A A_C \left.\frac{dC}{dz}\right|_z + v_{SL} A_C \left. C \right|_z \right) - \left(-D_A A_C \left.\frac{dC}{dz}\right|_{z+\Delta z} + v_{SL} A_C \left. C \right|_{z+\Delta z} \right) - aD_{eff} A_C \Delta z \left.\frac{dC_i}{dr}\right|_{r=r_P} \qquad (2.12)$$

Mass balance of tracer over the particle, assuming total wetting, over a differential particle radius Δr:

Accumulation rate = Rate of diffusion over particle - Rate of adsorption

$$\varepsilon_P \left(4\pi r^2\right) \Delta r \frac{dC_i}{dt} = D_{eff}(4\pi) \left[r^2 \left.\frac{dC_i}{dr}\right|_r + r^2 \left.\frac{dC_i}{dr}\right|_{r+\Delta r} \right] - \left(4\pi r^2\right) \Delta r \left(1-\varepsilon_P\right) \frac{dC_{AD}}{dt} \qquad (2.13)$$

In addition it can be said that if equilibrium is obtained quickly, the kinetics can be neglected and the adsorbing concentration is:

$$C_{AD} = k_{AD} C_i \qquad (2.14)$$

From this model the effective diffusivity (D_{eff}) can be determined from residence time distribution data. If this model is applied to a liquid filled reactor, the wetting efficiency can be determined for a trickle bed reactor (as discussed in section 2.4).

2.1.4. Important Features in Residence Time Distributions

As already stated, the use of RTD models to describe the experimental data has its drawbacks. For this reason, the need for more precise terms or 'descriptions' is required to describe physical features occurring in the flow system. Such features have been described in various articles (Naor & Shinnar, 1963; Robinson & Tester, 1986) and are:

- ***Measure of Spread.*** The spread in residence times is an important feature of interest as it gives an indication of the deviation from plug flow in the flow system. An indication of the spread in residence times is through the coefficient of variation or otherwise known as the relative standard deviation (Naor & Shinnar, 1963). The standard deviation is defined as

$$\sigma_V^2 = \int_0^\infty (t - t_E)^2 \; E(t) \; dt = \mu_2 - \mu_1^2 \tag{2.15}$$

  Where t_E is the apparent residence time of the outlet concentration profile.

- ***Stagnancy.*** Authors often relate this property as segregation, short-circuiting or dead water. Stagnancy occurs in systems whereby the total flow divides into flow components connected in parallel and one of the components has a much larger average residence time than the others. This is further explained by means of an example: when a reactor is filled with porous packing, whereby fluid flows near plug flow, the porous packing affects the residence time distribution due to a fraction of the fluid diffusing through the packing and back. In such a case the relative standard deviation may equal to one, though only slight back mixing occurs. Similar results would be obtained if the reactor could contain stagnant regions.

  It has been attempted by workers to measure stagnancy by utilising higher moments, such as the third moment with respect to the skewness (mean), however the skewness is not suitable for this. In the work of Van Deemter (1961), whereby he compared the skewness of different distribution functions, he concluded that the skewness is not characteristic of the physical properties of a reactor system. Stagnancy was therefore, through more advanced concepts, quantified with a distribution known as the Intensity function, $\lambda\,(t)$ (Naor & Shinnar, 1963):

$$\lambda\,(t) = \frac{E(t)}{1-F(t)} \tag{2.16}$$

In (2.16) E(t) is the residence time distribution as defined earlier and F(t) is the external cumulative residence time distribution defined by:

$$F(t) = \int_0^\infty E(t)\,dt \tag{2.17}$$

The intensity function is an escape probability for the molecules remaining in the system at time t (Robinson & Tester, 1986). From the definition of the intensity function, Naor & Shinnar (1963) defined stagnancy as: *A system with stagnancy is one in which the escape probability decreases in time over some interval.* It is therefore evident that if the intensity function curve decreases over some range of time, this is an indication of stagnant zones or sluggish flow zones.

In addition to the intensity function to measure the stagnancy, Danckwerts (1953) defined a parameter known as the holdback, which is also used to determine the extent of stagnancy. The holdback is defined as (rewritten by Robinson & Tester, 1963):

$$\chi = \frac{1}{\tau}\int_0^\tau F(t)\,dt \tag{2.18}$$

τ is the mean residence time as defined in (2.6). It was shown in the work of Danckwerts (1953) that the holdback is the fraction of internal flow with age greater than the mean residence time. When the holdback equals zero, this corresponds to pure plug flow and as the holdback tends to 1, the reactor contents are almost totally stagnant (Robinson & Tester, 1963).

- ***Internal Residence Time Distribution.*** It is useful to use distribution functions that describe the internal conditions of a system. Such a distribution is known as the internal residence time distribution function. This function is related to the interior flow pattern and was first defined by Buffham (1983) as:

$$\phi(t) = \frac{t}{\tau} E(t) \tag{2.19}$$

  The internal RTD is simply also determined from inlet-outlet tracer experiments and does not provide additional information above the external RTD, E(t). The internal RTD is merely a new method used to investigate tracer experiments and is found useful for the characterisation of flow maldistribution.

In the work of Robinson & Tester (1986), they proposed a new quantitative definition of sluggish flow or stagnancy through the use of the internal RTD. They also showed how the internal RTD and its related cumulative distribution function are used to describe the interior flow patterns. The internal cumulative RTD is defined:

$$\begin{aligned}\Phi(t) &= \int_0^t \phi(t)\, dt \\ &= \frac{1}{\tau}\int_0^t t\, E(t)\, dt\end{aligned} \tag{2.20}$$

The importance of the internal RTD is that it describes the eventual residence times, therefore the internal flow velocities of the different fluid elements and this is important for systems where a large degree of flow maldistribution occurs (Robinson & Tester, 1986). With this in place, a definition of the degree of stagnancy was established based on $\Phi(t)$:

$$\begin{aligned}S(c\tau) &= 1 - \Phi(t) \\ &= \frac{1}{\tau}\int_{c\tau}^{\infty} t\, E(t)\, dt\end{aligned} \tag{2.21}$$

The variable c was defined as a cut-off residence time above which the contents are seen as sluggish, approximately 1.5 or 2 times the mean residence time (Robinson & Tester, 1986). The definition of stagnancy, as in (2.21), is physically explained by means of an example: S(2τ) represents the fraction of internal contents that remain in the system for a time greater than twice the mean residence time.

In order to define the interior flow patterns within a system, the internal and external cumulative RTD functions, $\Phi(t)$ and F(t) respectively, are used. In the work of Robinson & Tester, they demonstrated the use of $\Phi(t)$ and F(t) by analysing an idealised flow model, one of complete segregated flow. The $\Phi(t)$ and F(t) functions are compared as shown in figure 2.3.

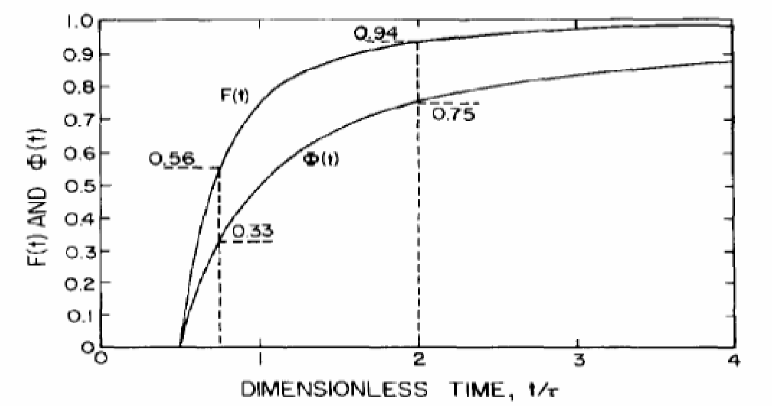

Figure 2.3 – Comparison of $\Phi(t)$ and F(t) curves for the case of laminar flow of a newtonian fluid through a cylindrical tube (Robinson & Tester, 1986)

The point on the F(t) curve at t = 0.75τ indicates that 56% of the injected tracer travels throughput the reactor with a residence time of 0.75τ or less. The $\Phi(t)$ curve indicates that the fast moving fluid is moving through only 33% of the total volume of the reactor.

2.2. Liquid Holdup

An important hydrodynamic parameter for the design and modelling of trickle-bed reactors is that of liquid holdup. It is important for reasons of up-scaling to ensure that that the liquid holdup is maintained at the optimum value (Ellman et al., 1990). Liquid holdup has been investigated by a number of workers (Iliuta & Thyrion, 1997; Ellman et al., 1990; Al-Dahhan & Dudukovic, 1994 and 1998). The liquid holdup is not an isolated hydrodynamic parameter but has an effect on a number of other parameters, namely (Ellman et al., 1990 and Al-Dahhan & Dudukovic, 1994):

- Pressure Drop
- Transfer of heat from the catalyst particles
- The thickness of the liquid film surrounding the catalyst particles
- The heat capacity of the reactor to absorb heat that is generated during exothermic reactions
- The mean residence time of the liquid phase
- Liquid-solid mass transfer, i.e. the degree of wetting, and gas-liquid mass transfer is determined by the liquid holdup, as it is the holdup that determines the mean residence time of the liquid
- Axial dispersion coefficient

Liquid holdup is defined as the volume fraction of liquid in the bed or as a liquid saturation. Liquid saturation is defined as the total volume of liquid held in the reactor bed per unit void volume. In this work the liquid holdup will not be defined as the liquid saturation.

For a reactor packed with porous catalyst particles, the total holdup can be divided into an external and internal holdup or otherwise known as the intraparticle and interparticle holdup, respectively. The external holdup can further be classified as containing the dynamic and static holdup. The dynamic holdup is the liquid volume in the reactor, which is continually being drained or renewed. The dynamic holdup can be determined by means of a weighing method.

The static holdup, also known as the capillary holdup, is defined as the liquid volume contained at contact points between the catalyst particles as well as between the particles and the walls of the reactor. This liquid volume contained at the contact points is considered stagnant. The static holdup seems to cause deviations from ideal plug flow within trickle-bed reactors. Van Swaaij, (1969) attributed the spread in residence times to the mass exchange occurring with the stagnant areas contained in the static holdup. The static holdup can also be determined by means of a weighing method once the reactor has allowed to drain completely. For non-porous catalyst particles, residual liquid holdup is defined as the volume of liquid that remains in the bed once the liquid flow has stopped and the reactor has completely drained. Residual holdup is analogous to static holdup for porous catalyst particles.

2.2.1. Determining Liquid Holdup

Dynamic and static holdups play an important role in the hydrodynamics and the mass transfer steps occurring within the reactor. It is therefore important to be able to determine these parameters and is possible by means of a number of methods. As already mentioned, weighing methods can be utilised to determine these components of the total holdup. For example by shutting of the inlet and outlet streams of the reactor and then draining the reactor to obtain the drained liquid. This liquid is then weighed which gives the dynamic holdup. The liquid remaining in the column is then determined as the residual holdup for non-porous catalyst particles and as the static plus internal holdup for porous catalyst particles. More recently tracer techniques are being utilised to determine the total holdup. The tail of the RTD is attributed to the presence of the static holdup and is therefore used to determine the static liquid holdup and in turn the dynamic holdup (Ellman et al., 1990) when the total holdup is determined from the first moment as in equation 2.6. The holdups determined from the different methods of weighing and tracer techniques do differ. It is thought that the tracer technique is not as representative as the weighing method as the tracer is not totally accessible to the entire packed bed.

2.2.2. Liquid Holdup Correlations

A number of studies have been performed on the hydrodynamics of trickle-bed reactors and especially focusing on the holdup since it is regarded as a very essential parameter. With these extensive studies a number of correlations have been proposed to predict liquid holdup in trickle-bed reactors, however there is still a lot of uncertainty regarding these holdup predictions, as they are limited to certain ranges of experimental conditions. In addition, the prewetting procedure has a great influence on the holdup as concluded from the work of Loudon (2005) and the reason for this is due to the dependency of the holdup on the liquid flow morphology (Loudon, 2005). Due to the large number of correlations available only a few will be discussed and only a few of these will be tested against the holdup data obtained in this work.

Charpentier et al., (1971) proposed a stratified pore model that can be used to predict the dynamic liquid holdup. For this model the single-phase flow pressure drops are required. Using this model, it was found that the experimentally determined holdups and the predicted values did not agree. This was attributed to the presence of a static liquid holdup (Charpentier et al., 1971). In the development of this model the following assumptions were made (Charpentier et al., 1971):

- Static pressure is uniform in a cross-sectional area perpendicular to flow, i.e. $\Delta P)_G = \Delta P)_L$ and therefore equation 2.22 holds

$$\left(\frac{\Delta P}{\Delta z}\right)' = \left(\frac{\Delta P}{\Delta z}\right)'_{FG} - g\rho_G = \left(\frac{\Delta P}{\Delta z}\right)'_{FL} - g\rho_L \qquad (2.22)$$

- The frictional pressure drop of each rivulet can be expressed in terms of the bed characteristics, the fluid properties and the single phase pressure drops as determined from Ergun's equation
- The flow of rivulets through the catalyst pores is stratified meaning the different phases (gas and liquid) flow independently
- Frictional pressure drop at the fluid interfaces are negligible

With these assumptions in place, equation 2.22 can be rewritten to include the holdup parameter as in equation 2.23.

$$\left(\frac{\Delta P}{\Delta z}\right)' = H_D\left(\frac{\Delta P}{\Delta z}\right)'_{FL} + (1-H_D)\left(\frac{\Delta P}{\Delta z}\right)'_{FG} - g\rho_M$$

$$with \quad \rho_M = H_D\rho_L + (1-H_D)\rho_G \tag{2.23}$$

This model accurately predicted, with an average difference of 25% from the experimental holdup, the predicted holdup. This was a great improvement from previous correlations were the average difference was about 75%. In addition this model can be used to predict holdup for a number of packing types.

The stratified pore model can be classified as one of two types of correlations i.e. correlations which relate the dynamic holdup to the Lockhart-Martinelli parameter, χ as shown in equation 2.24 (Ellmann et al., 1990).

$$\chi^2 = \frac{\left(dP/dz\right)_L}{\left(dP/dz\right)_G} = \left(\frac{L}{G}\right)^2\left(\frac{\rho_G}{\rho_L}\right)^{1.1}\left(\frac{\mu_L}{\mu_G}\right)^{0.2} \tag{2.24}$$

The second types of correlation are those that correlate the total or dynamic holdup with dimensionless groups that characterise the flow.

The above correlation of Charpentier et al., (1971) and similar correlations that relate the dynamic holdup to the Lockhart-Martinelli parameter were proposed not considering the effect of different hydrodynamic regimes, such as the high and low interaction regimes. Ellman et al., (1990), however, introduced the different regimes and proposed a new correlation.

Ellman et al., (1990) argued that the Lockhart-Martinelli type predictions do not consider the properties of the gas and liquid as well as the properties of the packing. It was by these workers that it was shown that the Lockhart-Martinelli parameter may be developed to give equation 2.25.

$$\chi = \left(\frac{L}{G}\right)\left(\frac{\rho_G}{\rho_L}\right)^{0.5}\left(\frac{\mu_L}{\mu_G}\right)^{0.1} \approx \left(\frac{L}{G}\right)\left(\frac{\rho_G}{\rho_L}\right)^{0.5} = \left(\frac{We_L}{We_G}\right)^{0.5} = \chi_L \qquad (2.25)$$

χ_L is the ratio of phase inertial forces. The ratio of the phase inertial forces was seen to be proportional to the dynamic saturation by the plot of the dynamic saturation versus the phase inertial force ratio. The Weber number introduces the variables of the liquid viscosity and surface tension; the dynamic saturation is proportional and inversely proportional to these variables, respectively. In order to incorporate the influence the packing properties have on the holdup, the specific area of the packing, the hydraulic diameter and the bed void fraction are clumped into a dimensionless group. By considering their experimental results, Ellman et al., (1990) found that the liquid holdup tends to an upper value that is unity at low pressures and 0.7 at higher pressures. Additional considerations taken included (Ellman et al., 1990):

- Liquid flow tends to zero at non-zero gas flow
- With increasing liquid flow, a minimum value is expected and may not be unity since gas pockets could be trapped
- Distribution of the gas and liquid influences the maximum holdup value.

On the basis of these considerations a correlation for the dynamic holdup was developed having limits at zero and at unity. The correlation makes provision for operation in the different hydrodynamic regimes. The correlation is shown in equations 2.26.

$$\begin{aligned} \beta_D &= 10^{\kappa} \\ \kappa &= 0.001 - \frac{R}{\xi^S} \qquad (2.26) \\ \xi^S &= \chi_L^m \operatorname{Re}_L^n We_L^P \left(\frac{a_C d_h}{1-\varepsilon_B}\right)^q \end{aligned}$$

The Lockhart-Martinelli parameter is defined as in equation 2.25. For the Low interaction regime the following constants are given:
R=0.42, S=0.48, m=0.5, n=-0.3, p=0 and q=0.3.

Ellman et al., (1990) reported that with a wide variation of important variables the prediction of holdup correlates well within an error limit of 50%.

These correlations that relate the dynamic holdup to the Lockhart-Martinelli parameter were proposed not considering the effect of increased gas and liquid flow rates. With an increase in the gas and liquid flow rates a different kind of interaction occurs and therefore momentum transfer is by means of different mechanisms. The Lockhart -Martinelli parameter is based on the assumption that the flow of the liquid and gas phases run independently and therefore the interaction between these phases are not taken into account. These interaction effects will indeed have an effect on the liquid holdup.

In the work of Specchia & Baldi, (1977) liquid holdup was determined for foaming and non-foaming systems as well as considering the different hydrodynamic regimes. They found that their data agreed well with the predicted values using the correlation of Charpentier et al., (1971) for the non-foaming systems but not for the foaming systems in the high interaction regime. On the other hand for the low interaction regime, the predicted values from the correlation of Charpentier et al., (1971) and similar correlations did not agree with the experimental values of Specchia & Baldi (1977). For this reason Specchia & Baldi (1977) considered a different approach whereby the two phase frictional pressure drop is determined by accounting for the gas flowing within a packed bed and is restricted by the presence of the liquid. The influence of the liquid holdup is also accounted for. Specchia & Baldi (1977) stated that the free section of a column that is available for gas to flow through is proportional to the volume of open spaces not occupied by the dynamic and static holdups i.e. $\varepsilon_P(1-\beta_S-\beta_D)$. β_S and β_D are defined here as the static and dynamic liquid saturation, respectively. With this an equation for the two-phase frictional pressure drop is arrived at as in equation 2.27.

$$\delta_{LG} = k_1 \frac{\left[1-\varepsilon_P(1-\beta_S-\beta_D)\right]^2}{\varepsilon_P^3(1-\beta_S-\beta_D)^3}\mu_G u_G + k_2 \frac{\left[1-\varepsilon_P(1-\beta_S-\beta_D)\right]^2}{\varepsilon_P^3(1-\beta_S-\beta_D)^2}\rho_G u_G^2 \qquad (2.27)$$

The constants k_1 and k_2 depend on the packing size and shape for the dry packing. This equation can be used to determine the dynamic holdup only if the static holdup as well as the pressure drops is known. The static holdup is rarely known and therefore this equation is not very useful. For this reason, Specchia & Baldi (1977) derived another equation for the dynamic holdup by considering the packing type and the gas and liquid flow rates. It was assumed by them that the mechanism of momentum transfer does not change between trickling flow and the packing. With this assumption in place the dynamic holdup can be correlated assuming the gas flow rate is zero. This relation is a function of the Reynolds number, Galileo number and a function of the packing, as in equation 2.28.

$$\beta_{DO}(u_G = 0) = a(\mathrm{Re}_L)^b (Ga)^c F \tag{2.28}$$

F is a function of the packing and is related to the particle porosity, nominal packing diameter and the geometrical packing of the area, as in 2.29.

$$F = \left(\frac{a_V d_P}{\varepsilon_P} \right)^{0.65} \tag{2.29}$$

By fitting equations 2.28 and 2.29 to their data, Specchia & Baldi (1977) found a good fit when a=3.86, b=0.545, c=-0.42. The mean relative quadratic error was 22%. For a given type of packing and liquid flow rate, the dynamic holdup can be determined as a function of the gas flow rate and in turn the two-phase frictional pressure drop, as in equation 2.30.

$$\frac{\beta_D}{\beta_{DO}} = \left(\frac{\rho_L g + \delta_{LG}}{\rho_L g} \right)^{-0.42} \tag{2.30}$$

In the work of Holub et al., (1992) a more fundamental approach was taken to develop a holdup correlation. The approach was used to model two-phase flow in an ideal void configuration where the average bed properties are mapped to the void geometry (Holub et al., 1992). The void space is modelled by a single-walled slit of average half width (w), half wall thickness (δ) and an inclination angle to the vertical axis (ϕ), figure 2.3.

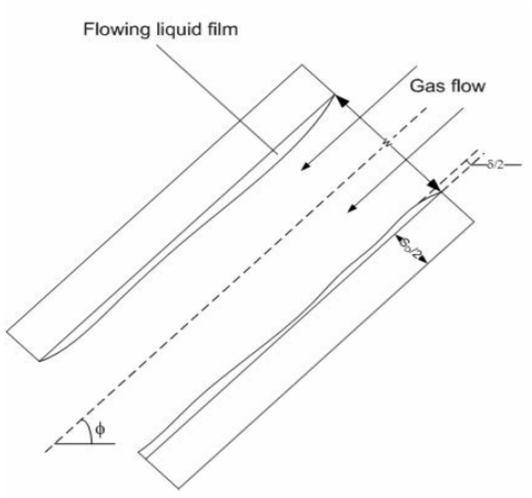

Figure 2.3 - Geometry of the slit model proposed by Holub et al., (1992), Van Houwelingen (2006)

Assumptions made are that of completely wetted walls with a uniform film thickness and that the central core contains gas. Performing the momentum balances over the slit, relating the slit dimensions to the bed properties and assuming the volumetric ratios are the same in the slit and the bed, a relationship between holdup and pressure drop is derived as in equation 2.31.

$$H_L = \varepsilon_B \left[\frac{E_1 \mathrm{Re}_L + E_2 \mathrm{Re}_L^2}{Ga_L \left(1 + (\Delta P / \Delta z) / \rho_L g\right)} \right]^{\frac{1}{3}} \qquad (2.31)$$

The constants E_1 and E_2 are the Ergun constants determined from single-phase pressure drop values.

By comparing this model to a number of widely used correlations, Holub et al., (1992) showed that it predicts holdup better in trickle-bed reactors than other models however large errors were found, this being an indication that the uniform distribution of the liquid assumed for the slit walls is not achievable. In addition, the averaging of bed properties could also lead to these large errors.

The discussed correlations and models for predicting liquid holdup are applicable for low pressures. At higher pressures, the liquid holdup can be very different to holdup obtained at lower and atmospheric pressures. When the gas and liquid flow rates increase an increase in pressure drop is observed. With this increase in pressures drop it is probable that gas-liquid interfacial areas decrease and therefore would affect the holdup. In the work of Larachi et al., (1991) a holdup correlation was determined for higher pressures. The authors found that the liquid holdup increases with an increase in pressure. This is explained by reasoning that as the pressure increases the gas density increases at a constant gas flow rate, and therefore the gas occupies less space within the reactor bed and this allows for more liquid holdup. In addition the authors also reasoned that the gas velocity decreases with a pressure increase and therefore reduced shear forces at the gas-liquid interfaces leading to larger liquid residence times. From their observations, Larachi et al., (1991) proposed an empirical correlation for predicting the total liquid holdup relevant for low and higher pressures. Their correlation makes use of the total liquid saturation instead of the total holdup, as shown in equation 2.32.

$$\begin{aligned} \beta_T &= 1 - 10^{-\gamma} \\ \gamma &= 1.22 \frac{We_L^{0.15}}{X_G^{0.15}\,\mathrm{Re}_L^{0.2}} \\ X_G &= \frac{G}{L}\sqrt{\frac{\rho_L}{\rho_G}} \quad and \quad We_L = \frac{L^2 d_P}{\rho_L \sigma_L} \end{aligned} \tag{2.32}$$

More recently, Nemec & Levec (2005) proposed a correlation to predict liquid holdup, specifically for trickling flow, based on the concept of relative permeability. The correlation has been based on a large number of experimental data obtained for wide range of operating conditions, including that of high pressures and different types of packing. It has also been stated by these authors that the correlation can predict liquid holdup within an error of 5%, regardless of the operating conditions. After extensive studies, Nemec & Levec (2005) proposed the liquid and gas-phase relative permeabilities, as in equations 2.33 and 2.34, respectively.

$$\begin{aligned} K_L &= \delta_L^{2.8} \qquad for \quad \delta_L \geq 0.3 \\ K_L &= 0.4\delta_L^{2.1} \quad for \quad \delta_L \prec 0.3 \\ where\ \delta_L &= \frac{H_T - H_S}{\varepsilon_B - H_S} \end{aligned} \tag{2.33}$$

$$K_G = 0.4 S_G^{3.6} \qquad for \;\; S_G \leq 0.64$$
$$K_G = S_G^{5.5} \qquad for \;\; S_G \succ 0.64 \tag{2.34}$$
$$where \; S = \frac{1 - H_T}{\varepsilon_B}$$

In order to determine the liquid holdup an iterative procedure is followed. Initially, the liquid holdup is guessed, the relative permaebilities of the different phases are determined from equations 2.33 and 2.34. Equation 2.35 is then used to solve for the holdup (H_T) till the equation is true.

$$\frac{1}{K_L}\left[E_1 \frac{\mathrm{Re}_L}{Ga_L} + E_2 \frac{\mathrm{Re}_L^2}{Ga_L}\right]\frac{\rho_L}{\rho_L - \rho_G} - \frac{1}{K_G}\left[E_1 \frac{\mathrm{Re}_G}{Ga_G} + E_2 \frac{\mathrm{Re}_G^2}{Ga_G}\right]\frac{\rho_G}{\rho_L - \rho_G} = 1 \tag{2.35}$$

E_1 and E_2 are the Ergun constants determined from pressure drop.

2.3. Pressure Drop

Pressure drop is another important hydrodynamic parameter for trickle bed reactors. The pressure drop over a trickle-bed reactor determines the cost required for pumping the gas and is especially important when a gas recycle stream is required. The pressure drop relates to the energy required to move the fluids through the entire system and is important in determining the performance or efficiency of the trickle-bed reactor (Al-Dahhan & Dudukovic, 1994) as well as determining the following:

- Energy losses
- Sizing of compression equipment
- Liquid holdup
- External contacting efficiency
- The gas-liquid interfacial area
- Mass transfer coefficients

Pressure drop and liquid holdup are interconnected parameters in trickle-bed reactors. A number of correlations couple these two parameters (Holub et al., 1992; Iliuta & Larachi, 2000). Van Houwelingen et al., (2006) stated that the liquid holdup in the bed is increased by liquid flow and decreased by the pressure drop, whereas the pressure drop over the bed is increased by increased holdup and by increased gas flow rates.

2.3.1. Pressure Drop Correlations

A number of pressure drop correlations have been proposed through out the years. Many of these make use of the liquid holdup in order to determine the pressure drop, however if the pressure drop can be directly and easily determined a number of correlations can be used to determine the liquid holdup.

In the work of Sato et al., (1973) the two-phase pressure drop was determined by means of using an energy balance, was correlated in terms of the Lockhart-Martinelli parameter and was based on their experimental data. It involves determining the pressure drop for single-phase flow, i.e. only liquid flow or gas flow. The pressure drop for each phase is determined as in equation 2.36.

$$\begin{aligned}
&\frac{\Delta P}{\Delta L} = \frac{f_v \mu U}{g\, d^{'2}} \frac{(1-\varepsilon)^2}{\varepsilon^3} \\
&f_v = 150 + 4.2\,\mathrm{Re}^{5/6} \\
&\mathrm{Re} = \frac{d^{'} U \rho}{\mu (1-\varepsilon)}
\end{aligned} \tag{2.36}$$

d’ is a modified particle diameter that incorporates the wall effect in the case of a large particle to column diameter ratio and is divided by the wall correction factor, M, as in equation 2.37.

$$\begin{aligned}
&d' = \frac{d}{M} \\
&M = 1 + \frac{4d}{6 d_{reactor} (1-\varepsilon)}
\end{aligned} \tag{2.37}$$

With the pressure drop known for the single-phase flow the pressure drop for two-phase flow can be determined by equation 2.38.

$$\begin{aligned}
&\phi_l = 1.30 + 1.85 \chi^{-0.85} \qquad for \;\; 0.1 \le \chi \le 20 \\
&\phi_l = \sqrt{\frac{\Delta P_{LG}}{\Delta P_L}} \quad and \quad \chi = \sqrt{\frac{\Delta P_L}{\Delta P_G}}
\end{aligned} \tag{2.38}$$

It is important to note that equation 2.38 is purely empirical and is only for the range as indicated in the second part of equation 2.38. In the work of Sato et al., (1973) the system of air and water was used, in addition no prewetting procedure was specified and therefore it is assumed that operations were performed on a non-wetted bed.

The above correlation is only valid for a very small range of system conditions and therefore may prove inaccurate. In addition the above correlation requires the determination of single-phase pressure drop and Ellman et al., (1988) described this as being inaccurate due to the single-phase liquid flow being very dependant on how well the reactor bed has been evacuated of any gas.

It was also noted by these authors that single-phase pressure drop data vary drastically at the same operating conditions and the same bed.

It was for these reasons that Ellman et al., (1988) proposed an improved correlation for the pressure drop and which was based on a database of about 4600 experimental results. The authors concluded that this would be applicable to industrial trickle bed reactors and includes operation at higher pressure drops. Following the reasoning to obtain equation 2.25 (as above and repeated here fore clarity)

$$\chi = \left(\frac{L}{G}\right)\left(\frac{\rho_G}{\rho_L}\right)^{0.5}\left(\frac{\mu_L}{\mu_G}\right)^{0.1} \approx \left(\frac{L}{G}\right)\left(\frac{\rho_G}{\rho_L}\right)^{0.5} = \left(\frac{We_L}{We_G}\right)^{0.5} = \chi_L \tag{2.25}$$

$\chi_L{}^2$ is the ratio of phase inertial forces and is fundamental in two-phase gas-liquid flow. Ellman et al., (1988) defined a two-phase friction factor as in equation 2.39.

$$f_{LGG} = \frac{\left(\Delta P/\Delta z\right)_{LG} d_H \rho_G}{2G^2} \tag{2.39}$$

A technique that correlates equation 2.39 to the data used by the authors yielded parameters required for the correlation and the final form is proposed as in equation 2.40.

$$\begin{aligned} f_{LGG} &= C(\chi_G \xi)^m + D(\chi_G \xi)^n \\ \xi &= \frac{\mathrm{Re}_L^2}{\left(0.001 + \mathrm{Re}_L^{1.5}\right)} \end{aligned} \tag{2.40}$$

The constants for equation 2.40 differ for the different interaction regimes. For the low interaction regime they are: C=200, D=85, m=-1.2, n=-0.5.

Larachi et al., (1991) proposed a new correlation that is also applicable for higher pressures and included a larger range of experimental data. Twelve different gas-liquid-solid systems were investigated. This correlation is merely a modification of the Ellman et al., (1988 & 1990) correlation. Parameters to describe the two-phase pressure were obtained by means of multiple regressions of the experimental data. The two-phase friction factor (as in equation 2.39) was used to determine the pressure drop as in equations 2.41.

$$
\begin{aligned}
f_{LGG} &= \frac{1}{\kappa^{1.5}}\left(31.3 + \frac{17.3}{\kappa^{0.5}}\right) \\
\kappa &= \left(\chi_G \operatorname{Re}_L We_L\right)^{0.25} \\
\chi_G &= \frac{G}{L}\sqrt{\frac{\rho_L}{\rho_G}} \\
We_L &= \frac{L^2 d_P}{\rho_L \mu_L}
\end{aligned}
\qquad (2.41)
$$

2.4. Wetting Efficiency

Wetting efficiency, also known as the external contacting efficiency, is the fraction of external catalyst particle that is exposed to the liquid flowing through a trickle bed reactor. The wetting efficiency is very important for the design and operation of trickle bed reactors as it has an influence on the internal and external mass transfer rates of the gas and liquid phases to the solid phase, therefore the wetting efficiency can affect the conversion as well as the reactor stability.

For non-volatile liquid reactants, the wetting efficiency will affect the rate of supply to the catalyst particles. When the reaction rate is fast, the controlling step will be the supply of the liquid to the catalyst. If the wetting efficiency is high the liquid supply will therefore be enhanced. An opposite effect to this is when the reactants are in the gas phase. The supply rate of reactants to the catalyst will be enhanced if there is incomplete wetting, i.e. a lower wetting efficiency. This contradiction occurs due to the complex nature of the hydrodynamics of trickle bed reactors.

A static wetting efficiency can also be defined due to the presence of static holdup. Due to liquid being trapped between the catalyst particle and the wall contact points (as described in section 2.5) and that this liquid is stagnant, it results in wetting the catalyst particles. The definition of static efficiency is therefore the external solid area fraction that is wetted by these static liquid holdups. In order to differentiate between the wetting efficiency obtained from reaction experimental methods and tracer response methods, Sicardi et al., (1980) was the first to define the concept of static wetting efficiency.

2.4.1. Determining Wetting Efficiency

A number of methods can be used to determine the wetting efficiency and which include destructive and non-destructive methods. Methods include that of (Mill & Dudukovic, 1981):

- ***Tracer response methods.*** This technique is the most popular for determining the wetting efficiency as it allows for this with the bed under operating conditions. A number of authors have proposed tracer response models in order to predict wetting efficiency. These include the work of Ramachandran et al., (1986) and Colombo et al., (1976). This method requires the use of a detailed residence time distribution model that can account for a number of parameters, such as liquid axial dispersion, diffusion at the solid catalyst particles, holdup and mass transfer. A different method that makes use of the moments obtained from a residence time distribution can also be used to determine the wetting efficiency

- ***Colourometric methods.*** This method involves the direct measurement of the contacted area that was coloured by means of permanent dye absorption. This method is vigorous as it can provide the shape and size of the wetted area on catalyst particles. Colourometrics involves introducing a liquid stream that contains a dye or colorant. The wetted fractions can be visually observed and therefore quantified. In the work of Van Houwelingen (2005) the analysis of the coloured catalyst particles included the placement of the catalyst particles in a grid; this was then photographed from both sides in a light box. These images were processed using a toolbox from Matlab to calculate the wetting efficiency for each particle.

- ***Reactive methods.*** For this method the wetting efficiency is supplementary from reaction conversion data through the use of reactor models. It is very useful in that it is a more direct determination of the wetting efficiency as the tracer-determined wetted area may be different to the chemically active wetted area; therefore this method determines the chemically active area fraction (Van Houwelingen, 2005).

- ***Methods making use of pressure drop readings.*** This is a very simple method that involves determining only three measurements: pressure drops through the bed for gas flow, gas-liquid flow and liquid flow, the bed void fraction and the liquid holdup. This method is based on a definition for wetting efficiency as in equation 2.42 (Baussaron et al., (2005).

$$\eta_{CE} = \frac{(\tau_{LS} a_{LS})}{\tau_{LS} a} \tag{2.42}$$

  τ_{LS} is the liquid solid shear stress in two-phase flow and a_{LS} is the liquid solid interfacial area. In the work of Baussaron et al., (2005) it was concluded that this method is unable to predict wetting efficiency with accuracy for a wide range of operating conditions.

2.4.2. Wetting Efficiency Correlations

Models that describe the response of a trickle bed reactor to an impulse have been proposed by Colombo et al., (1976), Ramachandran et al., (1986) and Mills & Dudukovic (1981). These models involve setting up mass balances for the tracer in the flowing liquid. In order to obtain the parameters from the models, the models can be fitted by a number of methods to the data. Instead of fitting the models to the data, a method of moments can be utilised. If this method is used it is very important that the response tail is accurate as the moments, especially moments greater than the first, is very sensitive to the accuracy of the tail. Any experimental noise present in the response tail will affect the moments.

Colombo et al., (1976) suggested that the wetting efficiency consists of two types of wetting:

- ***Internal wetting.*** Also known as pore filling, it is the volume of liquid internal to the catalyst pores and is a measure of the amount of active internal area as available for reaction. Often it is assumed that internal wetting is unity due to capillary forces.
- ***External effective wetting***. It is the external area of catalyst that is effectively contacted by flowing liquid. Mass transfer between the

internal and flowing liquid occurs at this surface. The external effective wetting may be different to the actual external wetting due to the presence of static liquid holdup.

The authors reasoned that the mean path of a molecule diffusing through porous catalysts with incomplete external wetting is greater than in a catalyst particle that is completely wetted on the exterior and therefore a ratio of the internal effective diffusivity for an incomplete wetted particle to that of a completely wetted particle is an indication of the catalyst wetting efficiency. Colombo et al 91976) therefore suggested equation 2.43.

$$\eta_{CE} = \frac{D_{EFF})_{pw}}{D_{EFF})_{cw}} = \frac{D_{EFF})_{TBR}}{D_{EFF})_{LF}} \qquad (2.43)$$

This ratio can also be determined by performing tracer analysis for a trickle bed reactor (i.e. partially wetted particle) and a liquid filled reactor (i.e. complete wetted particles) by making use of the residence time distribution model of Colombo et al., (1976) as described in section 2.1.3. It was concluded by Colombo et al., (1976) that the ratio of the effective diffusivities depends on the liquid velocity, packing size and the molecular diffusivity of the reactant and that a more accurate model should incorporate static liquid holdup.

Sicardi et al., (1980) proposed that the Thiele modulus for a partially wetted particle be used to derive a model for wetting efficiency. By making use of the Thiele modulus suggested by Dudukovic (1977) for completely filled pores (equation 2.44) an expression for the contacting efficiency in terms of the effective diffusivities was derived as in equation 2.45.

$$\varphi_{TB} = \frac{V_P}{\eta_{CE}\, S_{ext}} \sqrt{\frac{k}{D_{EFF}}} = \frac{V_P}{S_{ext}} \sqrt{\frac{k}{D_{EFF})_{TBR}}} \qquad (2.44)$$

$$\therefore \eta_{CE} = \sqrt{\frac{D_{EFF})_{TBR}}{D_{EFF})_{LFR}}} \qquad (2.45)$$

Mills & Dudukovic (1981) evaluated the wetting efficiency by means of tracer tests. They made use of the model proposed by Colombo et al., (1976); however they used the method of moments to determine the parameters. The effective diffusivities for a trickle bed reactor and a liquid filled reactor are obtained from first moments and the variance of an impulse response. It is assumed that, as in the work of Colombo et al., (1976), that internal wetting is complete. In addition, Mills & Dudukovic (1981) argued, not proven, that equation 2.43 holds. On assumption that the external wetting is incomplete the first moments is defined as in equation 2.46.

$$\begin{aligned}\mu_1 &= \frac{V_R}{Q_L}\left[H_T + F_i(1-\varepsilon_B)\varepsilon_P\,(1+\frac{K_a\rho_P}{\varepsilon_P}\right] \\ &= \frac{V_R H_T}{Q_L} + \frac{V_R(1-\varepsilon_B)K_a)_{app}\,\rho_P}{Q_L}\end{aligned} \tag{2.46}$$

In addition, by assuming that internal wetting is complete and therefore $K_a)_{app}= K_a$ and that the adsorption resistance is negligible, the variance is defined as in equation 2.47.

$$\frac{\sigma^2}{2\mu_2^2} = \frac{Q_L}{V_R H_{ext}}\frac{\gamma_1}{(1+\gamma_O)^2} + \frac{1}{Pe_L} \tag{2.47}$$

$$where \quad \gamma_1 = \gamma_i + \gamma_e$$

$$\gamma_i = \frac{(1-\varepsilon_B)\varepsilon_P}{H_{ext}}\left[1+\frac{K_a\rho_P}{\varepsilon_P}\right]^2 \frac{r^2\varepsilon_P}{15}\frac{1}{D_{EFF})_{APP=TBR}}$$

$$\gamma_e = \frac{(1-\varepsilon_B)\varepsilon_P}{H_{ext}}\left[1+\frac{K_a\rho_P}{\varepsilon_P}\right]^2 \frac{R^2\varepsilon_P}{15}\frac{5}{k_{LS}r}$$

$$\gamma_O = \frac{(1-\varepsilon_B)\varepsilon_P}{H_{ext}}\left[1+\frac{K_a\rho_P}{\varepsilon_P}\right]$$

It was shown by Mills & Dudukovic (1981) that the ratio of effective diffusivities for a trickle bed reactor and a liquid filled reactor is indeed a measure of wetting efficiency since the internal wetting was shown to be complete. It was however, concluded by them that the square root of this ratio is a better measure of wetting efficiency. This statement was confirmed by the work of Julcour-Lebique et al., (2006). Julcour-Lebique et al., (2006) concluded that the square root of the ratio of effective diffusivities gives better agreement at any wetting efficiency but is a more accurate estimation when the wetting efficiency is greater than 0.3.

Ramachandran et al., (1986) proposed an alternative model that models tracer diffusion in a spherical porous catalyst particle. Assumptions made were that of (Ramachandran et al., 1986):

- Tracer in the flowing liquid comes in contact with particles through the wetted area.
- The rate of transport through any static liquid is negligible.

The model follows the geometry of the catalyst particle and they assumed it to be covered with flowing liquid. Tracer diffusion within a porous particle is considered to be (Ramachandran et al., 1986);

- Actively wetted by flowing liquid in the geometry of a polar cap

$$0 < \theta < \alpha$$

- Remaining surface is covered with internal static liquid

$$\alpha < \theta < \pi$$

These considerations are illustrated in figure 2.4.

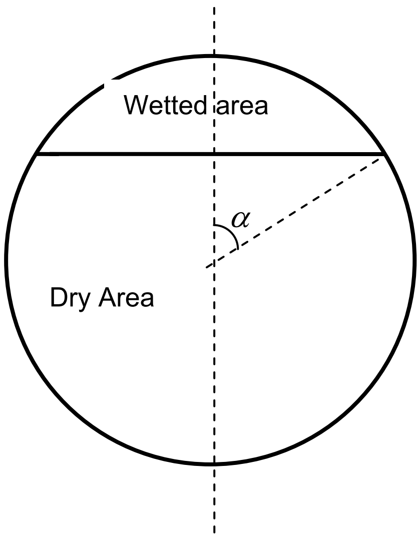

Figure 2.4 – Particle scale model of Ramachandran et al., (1986), Van Houwelingen (2006)

With the assumed particle geometry a mass balance (equation 2.48) is formed together with boundary conditions (equation 2.49).

$$\varepsilon_P \frac{\partial C_i}{\partial t} = D_{EFF}\left[\frac{1}{r^2}\frac{\partial}{\partial r}\left(r^2\frac{\partial C_i}{\partial r}\right) + \frac{1}{r^2 \sin\theta}\frac{\partial}{\partial \theta}\left(\sin\theta \frac{\partial C_i}{\partial \theta}\right)\right] \tag{2.48}$$

$$\begin{gathered} \lim_{r \to o}\left(r^2 \frac{\partial C_i}{\partial r}\right) = 0 \\ \theta = 0, \pi \quad \frac{\partial C_i}{\partial \theta} = 0 \\ r = R; \begin{bmatrix} D_{EFF}\dfrac{\partial C_i}{\partial r} = k_S(C_i - C_L) & 0 < \theta < \alpha \\ \dfrac{\partial C_i}{\partial r} = 0 & \alpha < \theta < \pi \end{bmatrix} \end{gathered} \tag{2.49}$$

By means of fitting the contact angle (α) to tracer response data, the wetting efficiency can be determined by equation 2.50.

$$\eta_{CE} = \frac{1 - \cos\alpha}{2} \tag{2.50}$$

An advantage of this model is that it does not require the determination of the effective diffusivities for both trickle bed reactors and liquid filled reactors. In the work of Ramachandran et al., (1986) it was concluded that the wetting efficiency from this model is comparable to that determined from the model of Colombo et al., (1976). It was also suggested that the ratio of effective diffusivities is a better estimation than the square root of the ratio of effective diffusivities.

The above correlations to estimate wetting efficiency use the ratio of $D_{EFF})_{TBR}/D_{EFF})_{LFR}$ raised to a power of 0.5 or 1. A new type of correlation proposed by Al-Dahhan & Dudukovic (1995) relates the wetting efficiency to operating conditions of pressure drop, gas flow rate and liquid flow rate. In the work of Al-Dahhan & Dudukovic (1995) it was reasoned that incomplete wetting efficiency is due to low liquid flow rates and that it increases with liquid velocity. Wetting efficiency correlations prior to this work neglected the effect of the liquid flow.

By using the model of Holub et al., (1992) as a basis the thickness of the liquid film surrounding catalyst particles can be expressed as the ratio of the total liquid holdup to that of the specific external area, as in equation 2.51.

$$\delta = \frac{H_T}{6(1-\varepsilon_B)/d_p} \tag{2.51}$$

Substituting the film thickness into equation 2.31 indicates the dependence of the film thickness on the pressure drop and liquid velocity. Al-Dahhan & Dudukovic (1995) therefore reasoned that the wetting efficiency can be determined from the film thickness and the liquid spreading and can be deduced from equations 2.31 and 2.51. Deductions made were that of (Al-Dahhan & Dudukovic, 1995):

- As the dimensionless pressure drop increases the liquid holdup and the film thickness decreases
- An increase in pressure drop increases the shear stress on the gas-liquid interface and therefore there is improved liquid spreading thus increasing the wetting
- As the liquid velocity increases the liquid holdup and the pressure drop increases improving the wetting efficiency.

Based on these deductions a correlation for the wetting efficiency is determined as in equation 2.52.

$$\eta_{CE} = c\,\mathrm{Re}_L^n \left[\frac{1+(\Delta P/\Delta z)/\rho_L g}{Ga_L}\right]^m \tag{2.52}$$

By performing tracer response analysis and using this data a flowing model (equation 2.52) is formed where c=1.104, n=1/3, m=1/9.

2.5. Prewetting Modes and the Effect of Prewetting

Prewetting of a trickle bed reactor involves the flooding of the reactor bed with the liquid or operating at higher liquid and gas flow rates before obtaining the desired operational specifications. This procedure ensures that all or most of the catalyst particles are wet so as to ensure more efficient operation of the trickle bed reactor. It has been found that the prewetting of a trickle bed reactor can lead to multiple hydrodynamic states, which has major implications for the design and operation of these reactors (Loudon, 2005).

The types of prewetting modes utilised in this study include that of:

- Non-prewetted bed
- Levec-prewetted bed
- Super-prewetted bed

In a non-prewetted bed the name speaks for itself. No flooding of the reactor bed or operation at higher liquid or gas rates is incorporated.

For a Levec-prewetted bed, the bed is flooded for a period of time. For non-porous catalyst particles this period is at least three hours to ensure complete wetting of the particles and to allow any gas pockets to escape. Once the bed is completely flooded, it is allowed to drain until the static and internal holdup has stabilised. It is at this point that the liquid and gas flow is introduced at the desired operational specifications.

A Super-prewetted bed is very similar to that of a Levec-prewetted bed. In this case the bed is flooded for at least three hours to ensure complete wetting of the catalyst particles. Once flooding is complete, the bed is allowed to drain but simultaneously the gas and liquid flows are introduced at the specified operational points.

It is now important to indicate the effect that the different prewetting modes have on the hydrodynamics of trickle bed reactors. Loudon (2005) investigated the effect of prewetting on the liquid holdup and pressure drop.

From his study he concluded that the pressure drop and liquid holdup are functions of the prewetting procedure. Different prewetting procedures resulted in different regions for the hydrodynamic parameters. He stated that the reason for the dependency of hydrodynamic parameters on the prewetting procedure is due to the morphology of liquid flow within a trickle bed reactor. The predominant flow formation encountered in a non-wetted bed is in the form of rivulets whereas in a super prewetted bed it is in the form of films. The flow morphology of a Levec prewetted bed is between that of a non-wetted and Super-wetted bed, i.e. a mixture of films and rivulets and is not dominated by either (Loudon, 2005).

CHAPTER 3

Experimental

Residence time distributions for varying liquid and gas flow rates were obtained at different prewetting procedures. Porous as well as non-porous packing was used during experimental runs. The non-porous packing was used only at the lowest gas flow rate. From the residence time distributions the liquid holdup and in turn the wetting efficiency was determined. The holdup was also obtained by means of the weighing method for purposes of comparison to the RTD holdup. Pressure drop was also recorded during the experimental runs.

3.1. Experimental Setup

Figure 3.1 illustrates the experimental setup that was used. It consists of a reactor packed with catalyst, a liquid feed, low-pressure nitrogen feed and an injection system.

The liquid flow rate is measured with an Endress and Hauser Model PROMAG 10H electromagnetic flow meter and can be changed by opening or closing needle valve, V-1. The flow meter operates within the range 0 – 3.8 ℓ/min, with an accuracy of 0.5% of the measured flow rates above 1 ℓ/min and 1.5% at flow rates above 0.2 ℓ/min. Within the water storage tank, TK-1, a submersible pump (SP-1) and weir are installed in order to provide a constant pressure head to the centrifugal feed pump (CP-1). Ball shut off valves (BV –1 and 2) is installed in order to make it possible for the outlet flow from the reactor to be recycled or drained.

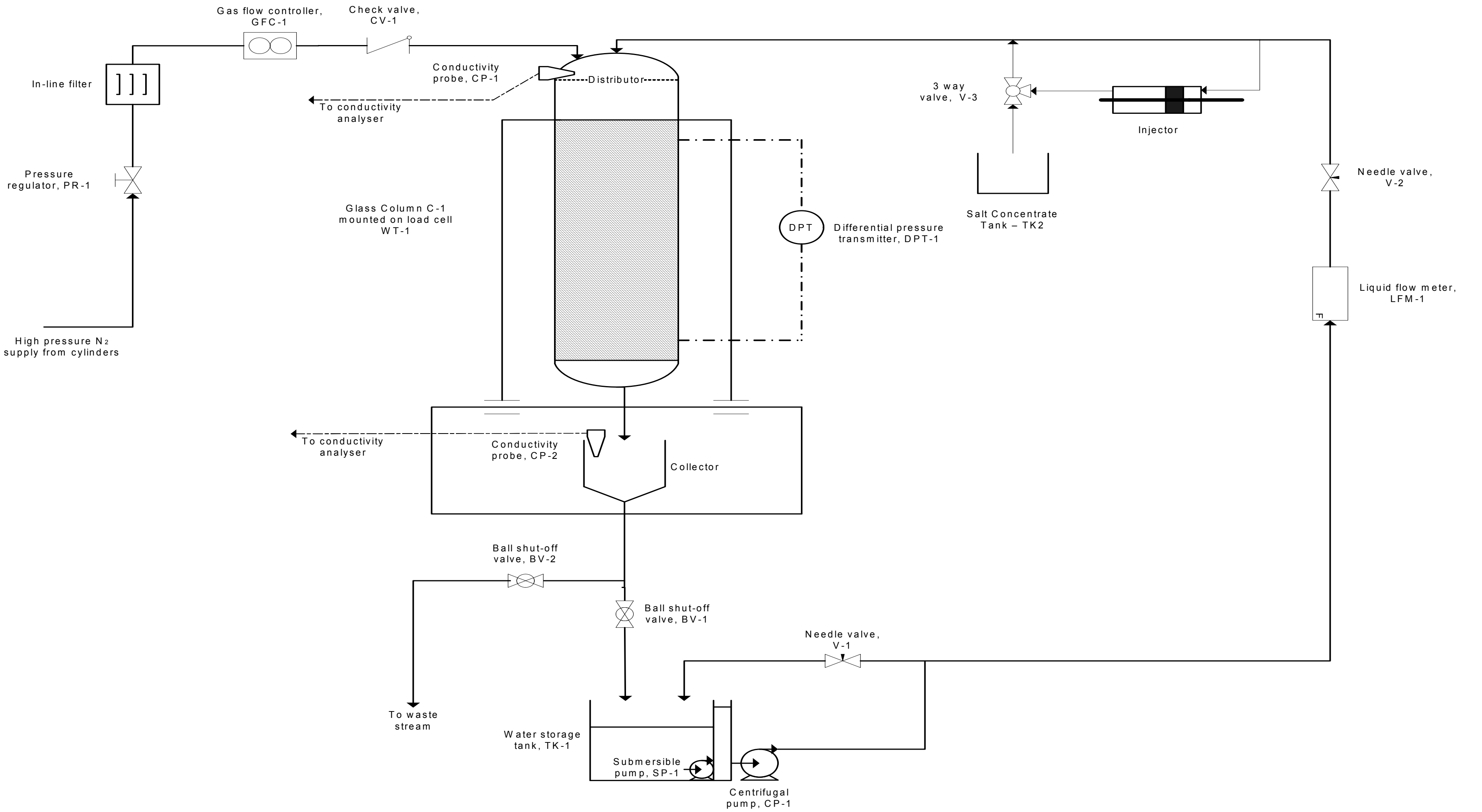

Figure 3.1 - Process flow diagram of the experimental setup

The nitrogen gas is supplied from a high-pressure gas cylinder and is controlled by means of a Brooks Smart mass flow controller, model 5853S. The range of the gas flow controller is 0 – 250 standard ℓ/min with an accuracy of 0.7% of the flow rate. An inline filter F-1 and a check valve CV-1 are installed in the line to protect the controller.

It is very important that the liquid and gas are well distributed throughout the column. To ensure this, a distributor is placed over the top of the packed column. The distributor allows the liquid to be distributed through a plate consisting of a number of holes. Another can replace this plate in order to vary the distribution. Throughout the experiments of this work the same distributor plate was used. It consisted of holes with diameters of 0.5 mm, space 8 mm apart in a square pitch arrangement. This allows for a hole density of 16 000 points/m^2. On the other hand the gas was distributed through three 1/4-inch stainless steel tubes. This was also the same for all experiments performed in this work.

3.1.1. Description of the Reactor and Packing

The reactor consists of a glass column with an internal diameter of 63 mm and a length of 1.0 m. Pressure taps are installed approximately 0.83 m apart which enables one to determine the pressure drop over the reactor. Due to the reactor being made of glass, experiments are limited to atmospheric conditions (101 kPag).

The porous packing that was used during experiments was that of alumina spheres with a diameter of 2.5 mm. The alumina spheres have an internal porosity of 0.46 and a particle density of 1010 kg/m^3. The non-porous packing used was glass spheres with a diameter of 3 mm. During each run the particles were packed to a height of about 0.8 m and the mass thereof was noted for purposes of determining the bed porosity.

3.1.2. Description of Injector and Tracer

In order to perform tracer studies, a volume of tracer needs to be injected into the liquid feed line without disturbing the flow. To ensure this, an injector was constructed that would allow the simultaneous injection of a volume of NaCl solution and the removal of the same volume of clean water already in the feed system. This minimises any disturbances in the flow. The volume of NaCl solution injected for each run is approximately 24.5 ml with a concentration of 20 g/ℓ and is detected with a dual channel Eutech PC 5500 conductivity instrument. The point of injection is approximately 20 cm from the top of the reactor and the conductivity sensors are placed before the distributor and at the exit of the reactor. Locations of the sensors are illustrated in figure 3.2. For access to conductivity data history, data from the conductivity probes are logged on the DeltaV data-logging system.

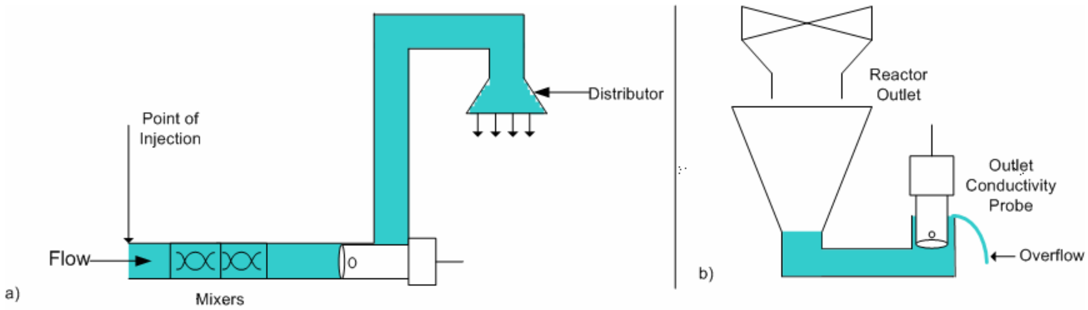

Figure 3.2 - Location of the conductivity probes at a) the inlet of the reactor and b) at the exit of the reactor

3.1.3. Liquid Holdup and Pressure Drop

The column is mounted on a load cell, model 642C3, and thereby enabling continuous measurement of the liquid holdup by weighing the reactor bed during flow. The load cell, calibrated for the range 0 – 20 kg, is connected to a transmitter and allows for continuous holdup data logged onto the DeltaV logging system. The holdup data is also used to verify whether steady-state conditions are obtained. Steady-state conditions are assumed when the standard deviation of 1 or 2 second interval measurements over a total period of at least 5 minutes does not vary.

The pressure drop over the packed column can be measured and is recorded by a Rosemount Model 3051 CD differential pressure transmitter. This pressure transmitter has a range of 0 – 70 Pa, 0.07 – 6.2 kPa and onwards to 62 kPa with an accuracy of 0.1% of the range. At normal operating conditions the accuracy relates to approximately 6 Pa. Data from the differential pressure transmitter is recorded on the DeltaV data logging system, enabling access to any data history.

3.2. Flow Parameters

Different liquid and gas flow parameters were used during experiments to determine the effect of these parameters on the RTD for different prewetting modes. Three different gas and liquid flow rates, as in table 1, were investigated at the three different prewetting modes. The different prewetting modes included that of Non-wetted, Levec-wetted and Super-wetted modes and the experimental procedures for the three modes are discussed in the next section.

Table 1 - Gas and liquid flow rates used during experimental work

U_G (m/s)	U_L (m/s)
0.02	0.002
0.06	0.005
0.1	0.008

These flow parameters fall within the trickle flow regime as opposed to the pulsing regime as evident in figure 3.3. This plot is based on the Trickle-bed Simulator of Larachi et al., (1999).

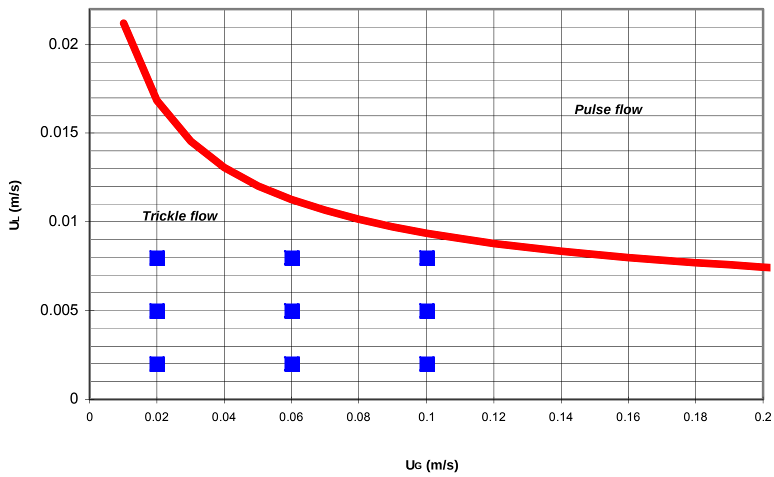

Figure 3.3 - Experimental data points with respect to the trickle-pulse transition boundary

3.3. Experimental Procedure

The glass column is packed with the alumina spheres (porous) or the glass beads (non-porous) to a height of approximately 0.8 m. The mass of the packing placed within the column is noted and therefore the bed porosity can be determined. The packed column is placed on the load cell stand. In order to determine the total liquid holdup, by the weighing method, the load cell is zeroed and therefore eliminates the need to subtract the mass of the bed and the column from the liquid flowing through the bed during operation. In order to incorporate the effect of the prewetting modes different procedures are followed for each prewetting procedure.

3.3.1. Non-prewetted Bed

Once the bed is packed, the gas flow rate is set to the lowest gas flow rate, U_G=0.1 m/s, and the liquid flow rate is then set to the required liquid rate. It is important that the liquid flow rate introduced does not exceed the set point so as to avoid the effects of hysteresis. Once the liquid and gas have been introduced time is allowed for the system to attain steady state. Steady state is achieved when the pressure drop and weighed liquid holdup do not vary. For a non-wetted bed it takes approximately 40 to 60 minutes to reach steady state. At steady state the pressure drop and liquid holdup values are recorded and then the tracer is injected into the system. When tracer has passed through, the liquid holdup and pressure drop readings are again recorded to ensure that steady state had been achieved and that the injection of tracer did not disturb the system. Once the RTD has been obtained at these experimental conditions, the gas flow rate can be increased to the next desired rate. This procedure is then repeated to obtain the RTD's at a certain liquid flow rate and at all gas flow rates. It is important that the gas rate only be increased and not decreased as higher gas rates may have an effect on the liquid distribution and therefore affecting the RTD's.

3.3.2. Super Prewetted Bed

For the Super-prewetted procedure the column is shut off at the bottom of the glass column, by means of a plug, to allow the packed column to be filled with liquid and therefore be flooded. For the porous packing the column is left to be flooded for at least three hours to ensure that the particles are completely wetted. To avoid or minimise the entrainment of gas bubbles the liquid is introduced very slowly. Once the column has been flooded, the liquid and gas flow rates are set to the desired rates and at the same time the column is allowed to drain and therefore irrigation continues throughout the draining period. Once steady state has been achieved, approximately 30 to 40 minutes for this prewetting procedure, pressure drop and holdup values are recorded and the tracer is injected into the system. Once the RTD has been obtained the gas flow rate can be increased to the next desired set point. This procedure is then repeated for the different gas rates to obtain the RTD's at the specific liquid flow rate and all gas flow rates.

3.3.3. Levec Prewetted Bed

The Levec-prewetting procedure is very similar to the Super-prewetting procedure. The only difference is that the column is allowed to drain completely before introducing the liquid and gas flows i.e. during draining the liquid and gas irrigation is stopped. The liquid is only introduced again once the mass or holdup within the column is constant for a period of time. This holdup is known as the residual holdup for non-porous packing and as the static holdup (residual + internal) for porous particles. Once the residual holdup is recorded the liquid and gas rates are set to the desired points allowing steady state to be obtained. At steady state, the pressure drop and liquid holdup are recorded and the tracer is then injected. Once the RTD is obtained the gas flow rate can be increased to the next set point.

3.4. Inlet and Outlet Effects

To eliminate inlet and outlet effects, experiments were performed with and without a packed bed. Without a packed bed the effects of the external system, i.e. injection system, piping and other fittings, are eliminated and corrected for by (3.1), (3.2) and (3.3), assuming linearity of the system.

$$\mu_{1,L} = \mu_{1,total} - \mu_{1,blank} \tag{3.1}$$

$$\sigma_L^2 = \sigma_{L,total}^2 - \sigma_{L,blank}^2 \tag{3.2}$$

$$\tau_L = \tau_{L,total} - \tau_{L,blank} \tag{3.3}$$

Where subscript total refers to the entire system, i.e. the packed bed together with the external system and subscript blank refers to the external system only.

3.5. Deconvolution Procedure

An ideal stimulus is very difficult or even impossible to obtain for tracer analysis. A method of deconvolution is therefore used to determine the tracer response for an ideal pulse from a non-ideal pulse. Due to the non-ideal stimulus, the experimental response data was first normalised and then the method of deconvolution (as described in section 2.1.2) was applied to obtain the response for an ideal stimulus.

3.6. Method of Moments

The method of moments was used to determine the liquid holdup and the wetting efficiency. The liquid holdup is determined using the first moment as in equation 2.5 and the wetting efficiency from the first moment as well as the variance, equation 2.15. The different moments of the residence time distributions were determined using the Simpson rule.

During repeat experimental runs, i.e. at all the same operating conditions, residence time distributions were obtained. Good repeatability was obtained, as discussed in the next section, however when the first and second moments were determined and compared from repeat runs, the moments differed drastically. This is a result of the sensitivity of the moments to the accuracy of the response curve especially in the tail part. The response tail measures the concentration at very low concentrations and therefore a lot of noise is present and introduces inaccuracies. It is for this reason that an exponential decay function was fitted to the tail of the response curve. It has been assumed by workers (Mills & Dudukovic, 1989 and Van der Merwe, 2005) that the decline in the response curve at large times can be assumed to be exponential.

With fitting an exponential function to the response data, it was found that the moments were also very sensitive to where the exponential fit started and how large the range was over which the exponential function was fitted. A sensitivity analysis was performed whereby all possible starting points and ranges, giving a good fit between experimental data and exponential function, were used and the moments determined. A probability curve for the moments was determined and from this the moments were determined for the various response curves. With this analysis, good agreement was found between the various moments for the repeat runs.

3.7. Reproducibility

In order to ensure that the experimental runs are repeatable different runs at the same operating conditions were performed. The repeatability of the experiments was good for all different prewetting modes as well as at the different liquid flow rates as shown in figures 3.4, 3.5 and 3.6.

Any differences observed for the different runs, as in figures 3.4 and 3.6, can be attributed to geometrical differences in the bed, as different beds were used for the different runs.

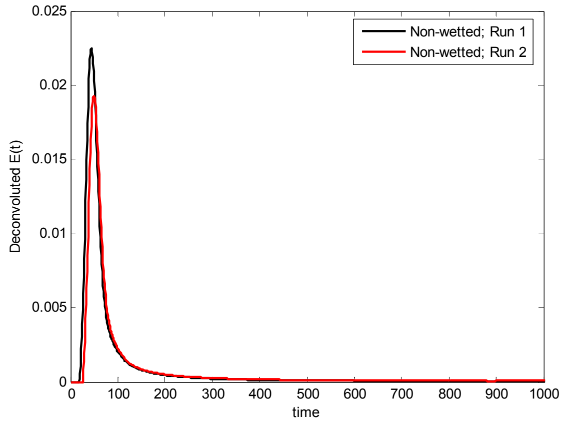

Figure 3.4 - Reproducibility for a non-wetted bed at U_L=2 mm/s

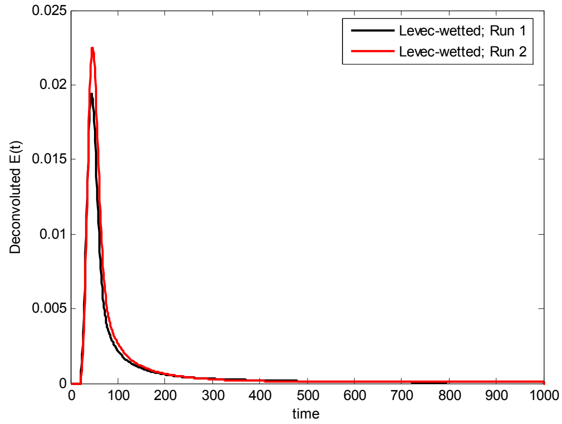

Figure 3.5 - Reproducibility for a Levec-wetted bed at U_L=5 mm/s

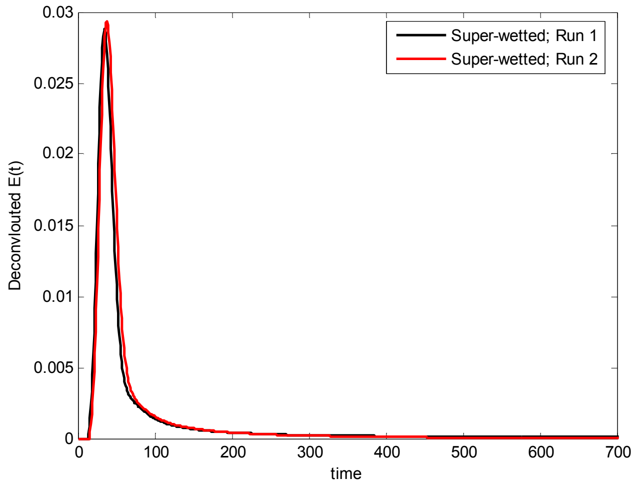

Figure 3.6 - Reproducibility for a Super-wetted bed at U_L=8 mm/s

CHAPTER 4

Results

4.1. RTD Responses

4.1.1. The Effect of Prewetting

The effect of the prewetting on the RTD responses is seen in figure 4.1 and 4.2. The responses for the Levec-wetted and Super-wetted responses are much the same even at higher liquid flow rates.

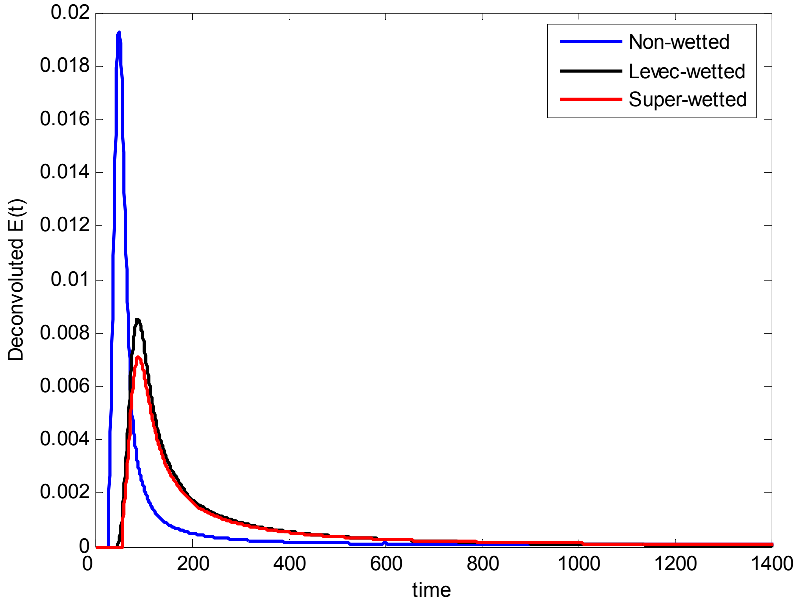

Figure 4.1 - Effect of prewetting at U_L=2 mm/s, U_G=0.02 m/s

Looking at figures 4.1 and 4.2 the following observations could be made:

- The non-wetted response is closer to plug flow than the other prewetting responses
- The tailing effect for the non-wetted response is not as significant as in the Levec and Super-wetted beds
- There is not any difference between the non-wetted responses at higher liquid flow rates respective to the Super and Levec-wetted responses.

- At the lowest liquid flow rate, there is a small difference in the Levec-wetted and Super-wetted: the peak of the Levec-wetted response is slightly higher, however this was not observed for any other gas flow rates
- The dead time for the Levec-wetted and Super-wetted responses is the same, but is more for the non-wetted responses.

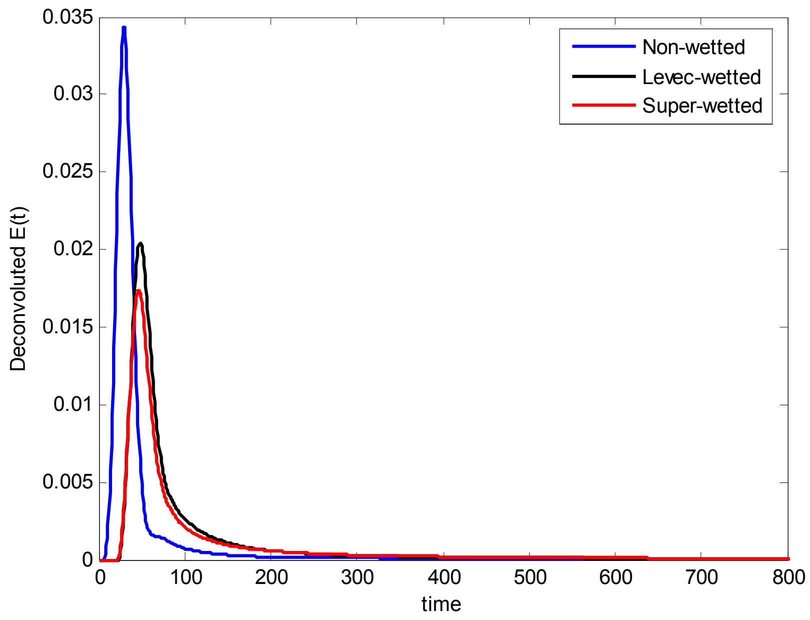

Figure 4.2 - Effect of prewetting at U_L=5 mm/s, U_G=0.02 mm/s

The same trend was observed for a higher liquid flow rate, as seen in appendix A.1.

4.1.2. The Effect of the Liquid flow rate

The effect of the liquid flow rate on the response curves is evident in figures 4.3, 4.4 and 4.5. Each of these figures represents the different prewetting modes. From these figures the following was observed:

- The tracer exits the reactor much quicker with increasing liquid flow rate for all the different modes of prewetting
- The tailing effect becomes more pronounced at lower liquid flow rates
- The dead time of the response curves increases with a decrease in liquid flow rate
- The response curves at higher liquid flow rates are closer to plug flow than at lower liquid flow rates.

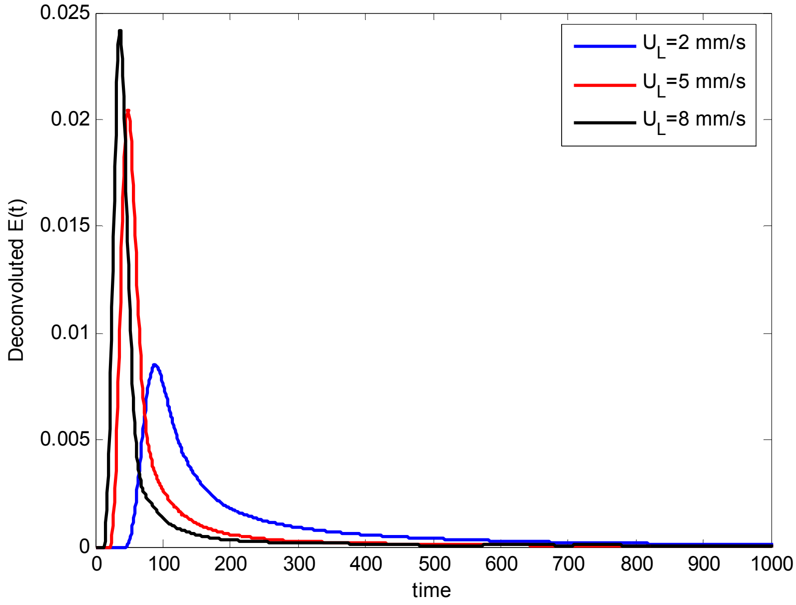

Figure 4.3 - Effect of the liquid flow rate for a non-wetted bed at U_G=0.02 m/s

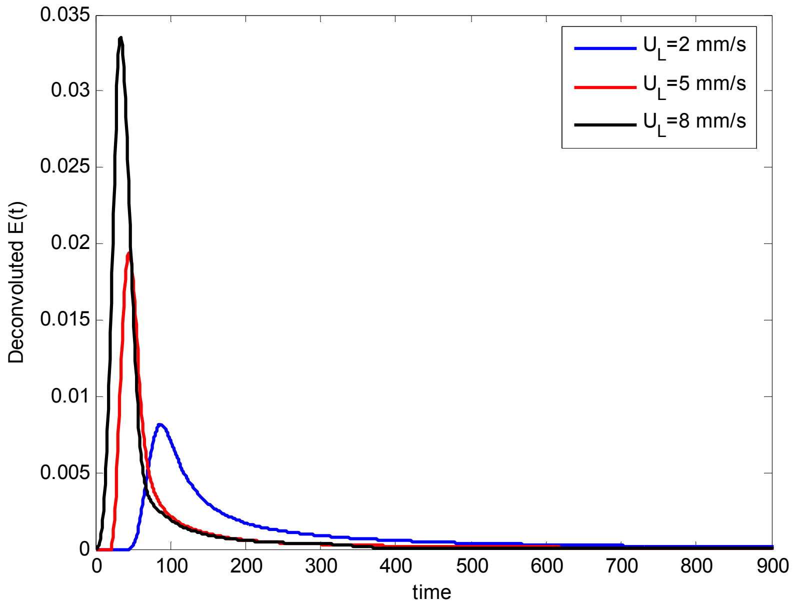

Figure 4.3 - Effect of the liquid flow rate for a Levec-wetted bed at U_G=0.06 m/s

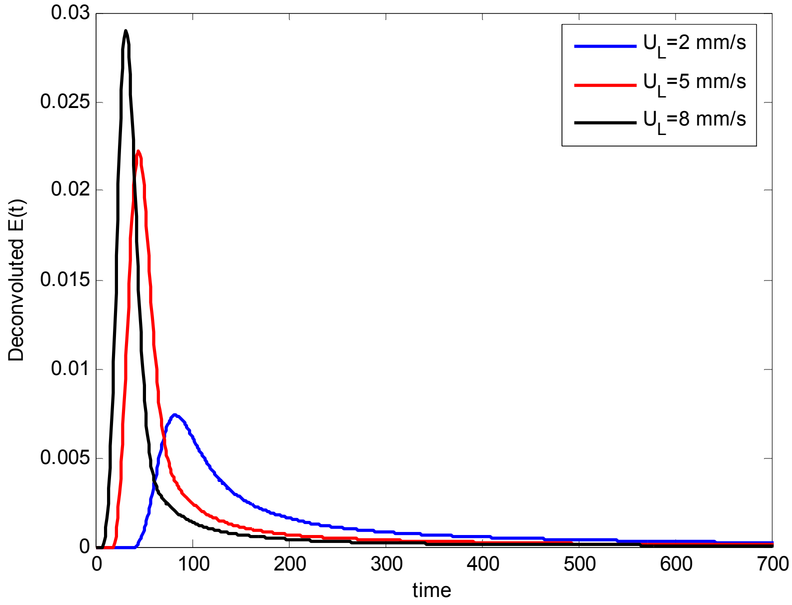

Figure 4.5 - Effect of the liquid flow rate for a Super-wetted bed U_G=0.1 m/s

The same trends were observed at different gas flow rates for the different prewetting modes, appendix A.2.

4.1.3. The Effect of the Gas flow rate

The gas flow rate had no or very little effect on the RTD responses. As evident from figures 4.5 to 4.7, the gas flow rate has a very insignificant effect on the response curves for the different prewetting modes as well as at different liquid flow rates. It is thought that any small differences that may occur could be due to differences in the bed, i.e. the bed geometry.

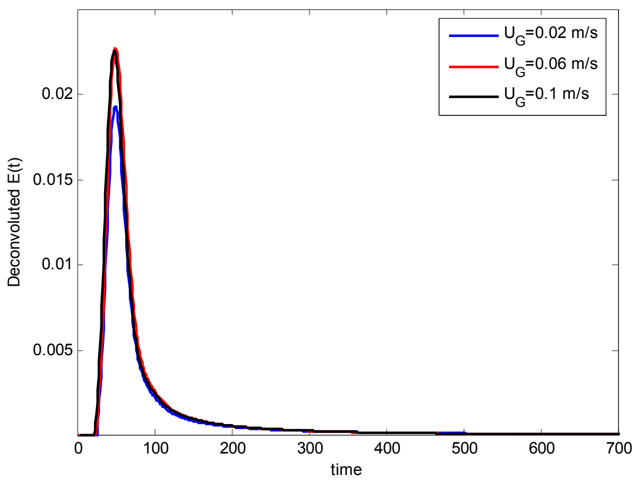

Figure 4.5 - Effect of the gas flow rate for a non-wetted bed at U_L=2 mm/s

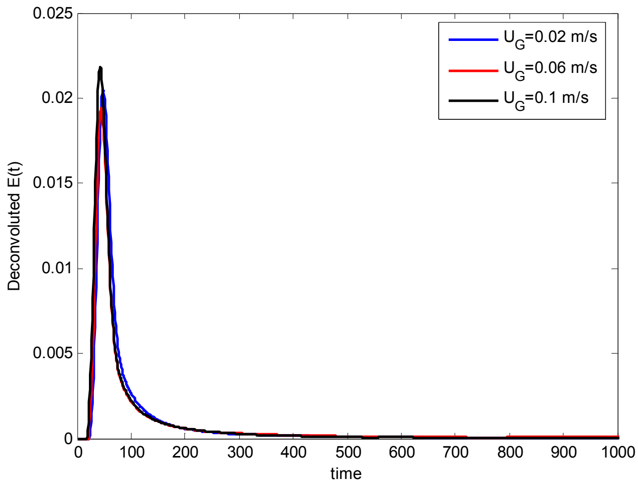

Figure 4.6 - Effect of the gas flow rate for a Levec-wetted bed at U_L=5 mm/s

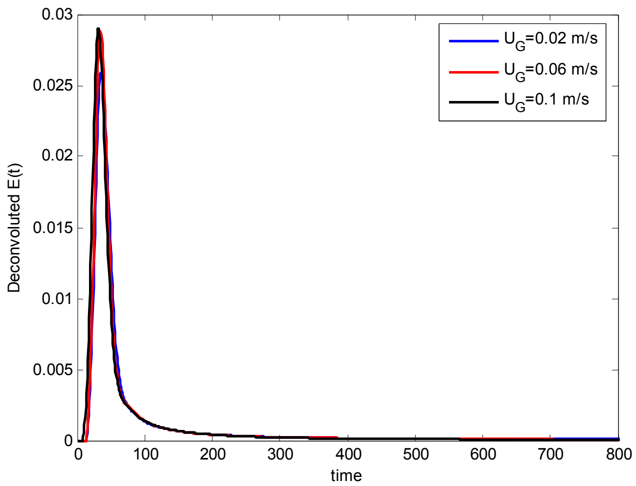

Figure 4.7 - Effect of the gas flow rate for a Super-wetted bed at U_L=8 mm/s

This lack of effect of the gas flow rate was evident at all liquid flow rates for the different prewetting modes.

4.1.4. Differences for Porous and Non-Porous Packing

The effect of the liquid flow rates and the prewetting modes is the same for the porous and non-porous catalyst particles. The differences in the RTD response curves for the porous and non-porous catalyst particles for the different prewetting modes and at all the liquid flow rates and at a gas flow rate of 0.02 m/s are shown in figures 4.8 to 4.10.

The following observations were made from these figures:

- The tailing effect for the non-porous packing is very much less severe than for the porous packing
- At a low liquid flow rate, the non-porous response curves exhibit some tailing, however at the higher liquid flow rates, the tailing effect is non-existent and therefore the closest to plug flow.
- The non-porous response curves for the Levec and Super-wetted responses are similar, however there is a greater difference in this response curves than for the porous response curves
- The peak of the response curves for the non-porous packing is much higher, and is therefore closer to plug flow
- The response curve for the non-porous super-wetted procedure at the lowest liquid flow rate is different to that of the non-porous Levec-wetted procedure, however response curves for these two modes (non-porous) are very similar at higher liquid flow rates
- The dead times corresponding to the same conditions are the same for the porous and non-porous packing.

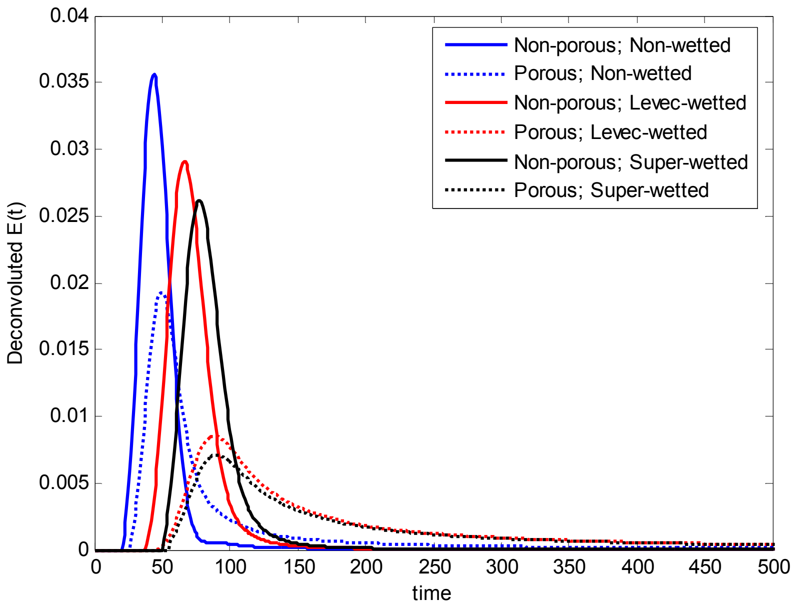

Figure 4.8 – Difference in RTD responses for porous and non-porous packing at U_L=2mm/s, U_G=0.02 m/s

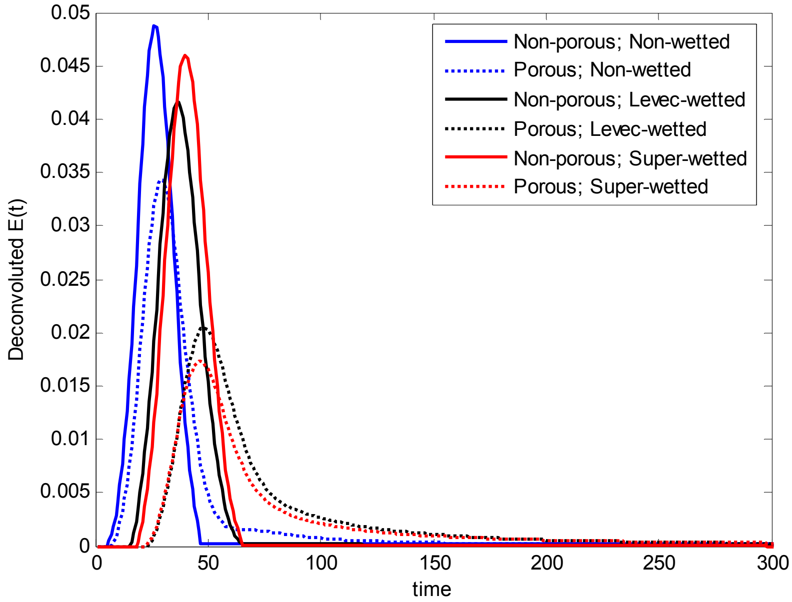

Figure 4.9 - Difference in RTD responses for porous and non-porous packing at U_L=5mm/s, U_G=0.02 m/s

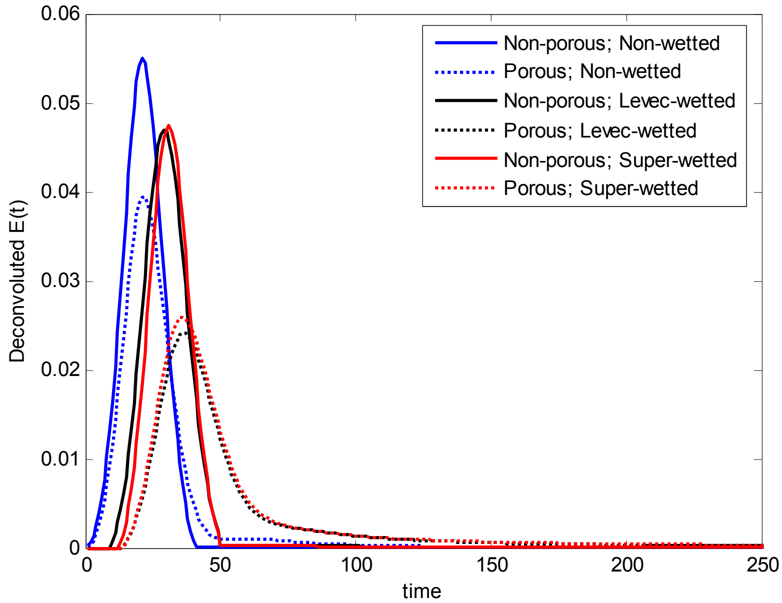

Figure 4.10 - Difference in RTD responses for porous and non-porous packing at U_L=8 mm/s, U_G=0.02 m/s

4.2. Pressure Drop

4.2.1. Effect of Prewetting and Liquid Flow rate

The effect of prewetting on the pressure drop, at constant gas flow rates, is seen in figures 4.11 and 4.12.

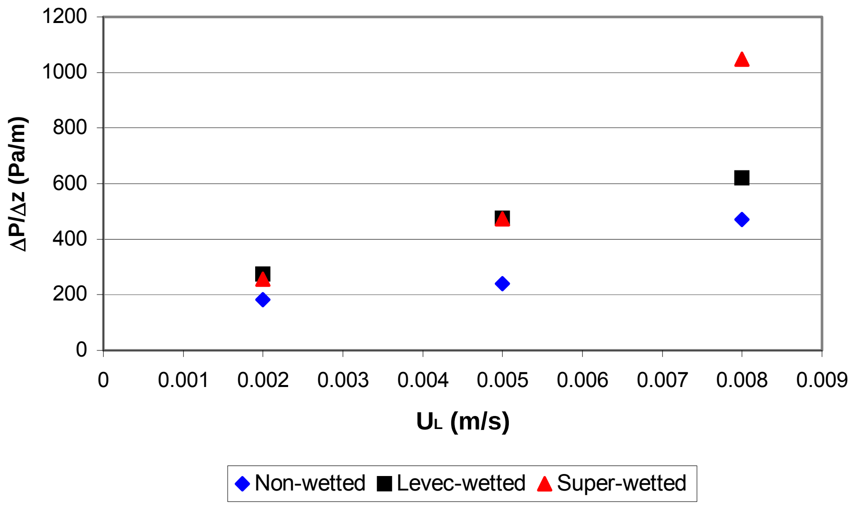

Figure 4.11 – Effect of prewetting on the pressure drop at U_G=0.02 m/s

From these figures the following trends are observed:

- The pressure drop is a function of the liquid flow rate and regardless of the prewetting procedure, the pressure drop increases with the liquid flow rate
- At a gas flow rate of 0.02 m/s the pressure drop for the Levec and Super-wetted procedure is the same, except for at a liquid flow rate of 8 mm/s
- At higher liquid flow rates (5 mm/s and 8 mm/s), the pressure drop for the super-wetted procedure is greater than for the Levec-wetted at U_G=0.06 m/s and 0.1 m/s.
- At a liquid flow rate of 8 mm/s and at all gas rates, the super-wetted procedure results in a much greater pressure drop than for the non-wetted and Levec-wetted procedures.

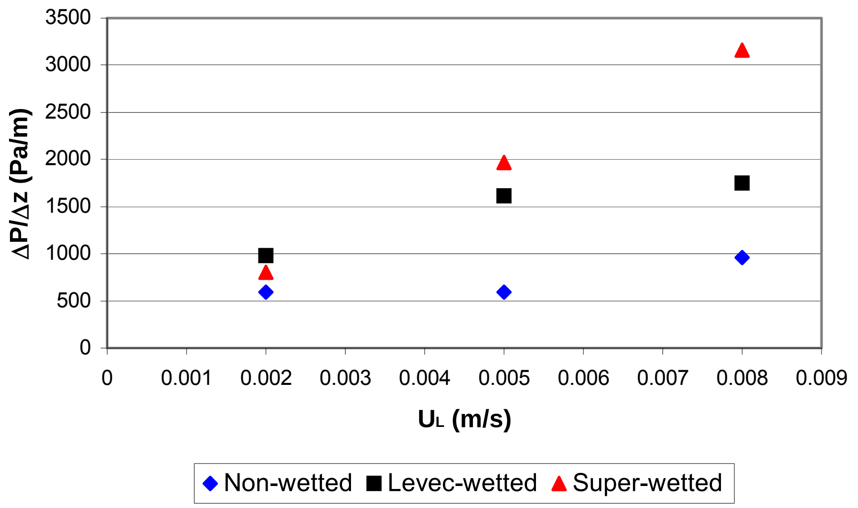

Figure 4.12 - Effect of prewetting on the pressure drop at U_G=0.06 m/s

The pressure drop trend at the higher gas flow rate of 0.1 m/s was similar to that of figure 4.12, and can be seen in appendix A.3.

4.2.2. Effect of Gas Flow rates

In figures 4.13 and 4.14, the effect of the gas flow rate on the pressure drop for the different prewetting procedures can be seen.

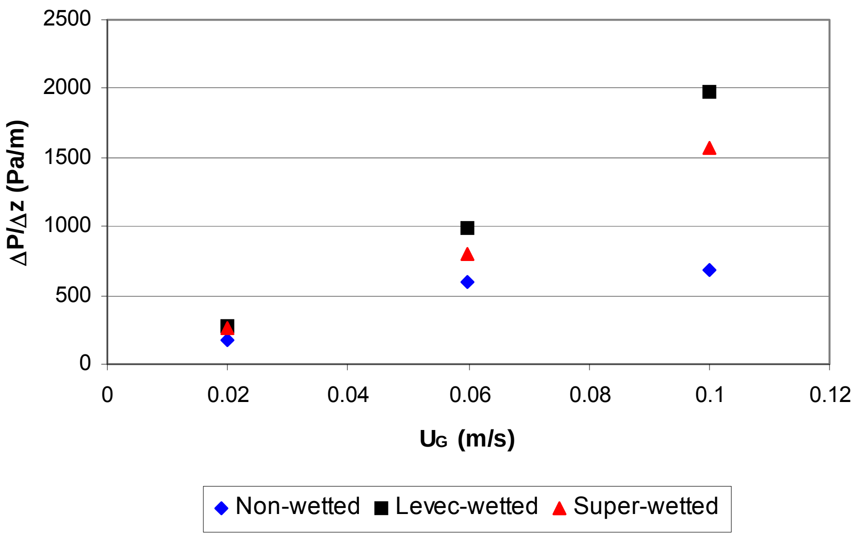

Figure 4.13 - Effect of the gas flow rate on the pressure drop at U_L=2 mm/s

The following trends are observed:

- As expected the pressure drop increases as the gas flow rate increases and for the different prewetting procedures the effect of the gas rate is obvious:

- At a liquid flow rate of 2 mm/s, the pressure drop for the Levec-wetted bed is greater; the opposite is true for higher liquid flow rates.

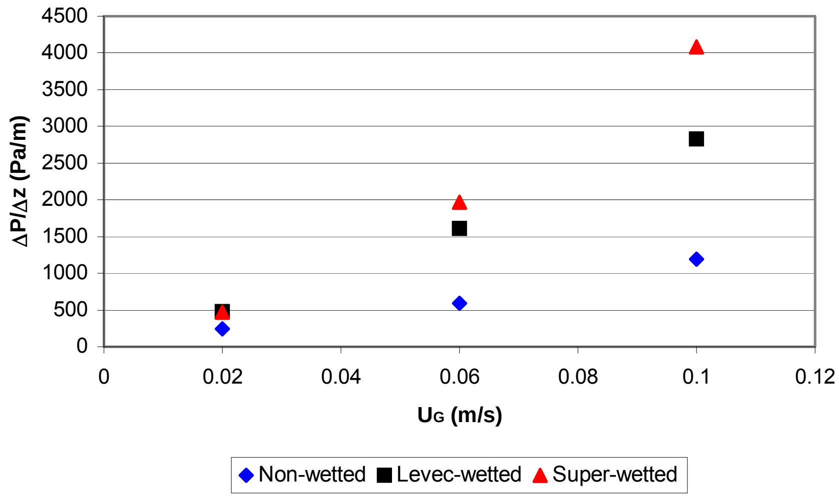

Figure 4.14 - Effect of the gas flow rate on the pressure drop at U_L=5 mm/s

A three dimensional plot of the pressure drop showing the combined effect of the liquid and gas flow rates is shown in figure 4.15

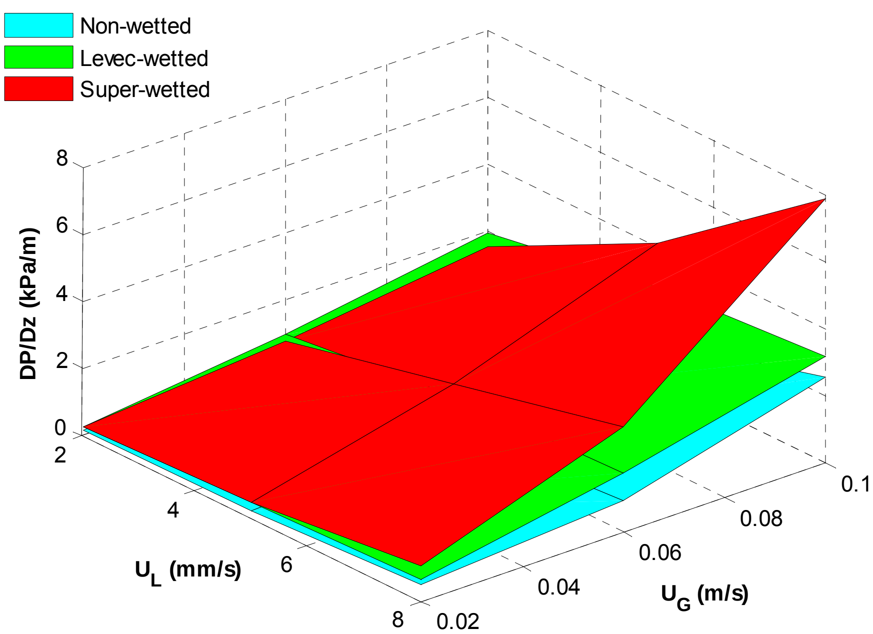

Figure 4.15 - Effect of liquid and gas flow rates on the pressure drop

This figure clearly shows that three distinct regions of pressure drop result from the different prewetting procedures at high liquid and gas flow rates. At low gas and liquid flow rates these regions cannot be distinguished as easily. It is also seen that the gas flow rate has more of an effect on the pressure drop than the liquid flow rate.

4.2.3. Porous versus Non-Porous Packing

The pressure drop for porous and non-porous packing for the different prewetting procedures is shown in figure 4.16.

The following observations were made from figure 4.16:

- The pressure drop for the porous packing is greater than that of the non-porous packing, at the same prewetting procedure
- The pressure drop for the porous, non-wetted procedure is the same as the non-porous, Levec-wetted procedure
- At low liquid flow rates, the difference between pressure drops for the different prewetting procedures is small. This difference increases for the different prewetting procedures and porosity with an increase in the liquid flow rate

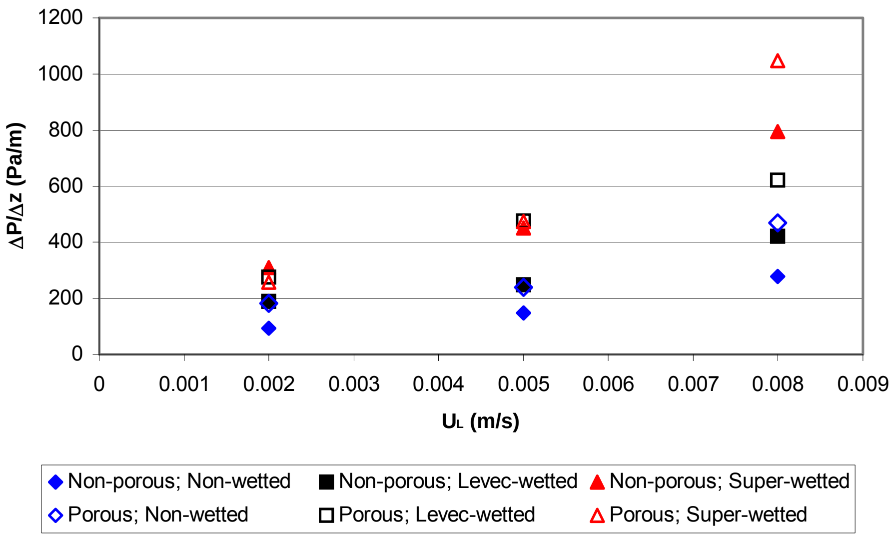

Figure 4.16 – The difference in pressure drops for porous and non-porous packing at U_G=0.02 m/s

4.3. Liquid Holdup

4.3.1. Effect of Prewetting and Liquid Flow rate

The effect of prewetting and the liquid flow rate on the liquid holdup (at constant gas flow rates), as determined from the residence time distributions, can be seen in figures 4.17 and 4.18.

From these figures the following trends were observed:

- The prewetting procedures result in three different regions; these regions come closer together at higher liquid flow rates.
- There is a substantial difference between the Super-wetted and non-wetted regions. The holdup in the Super-wetted bed is three times greater than that of the non-wetted bed at the lower liquid flow rates. At a liquid flow rate of 0.008 mm/s this difference decreases; the holdup in the Super-wetted bed is approximately 1.3 times greater than that of the non-wetted bed
- The holdup in the Super-wetted bed is approximately 1.2 times greater than that of the Levec-wetted bed and this difference decreases only slightly at the highest liquid flow rate
- Regardless of the prewetting procedure, the liquid holdup increases with an increase in the liquid flow rate and has been an observation in the work of many authors (Loudon 2005).

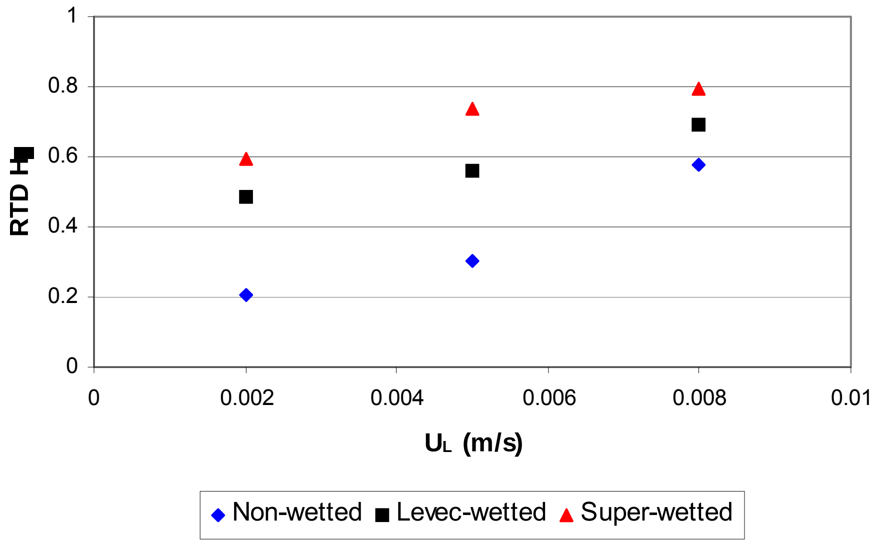

Figure 4.17 – Effect of prewetting on the holdup at U_G=0.02 m/s

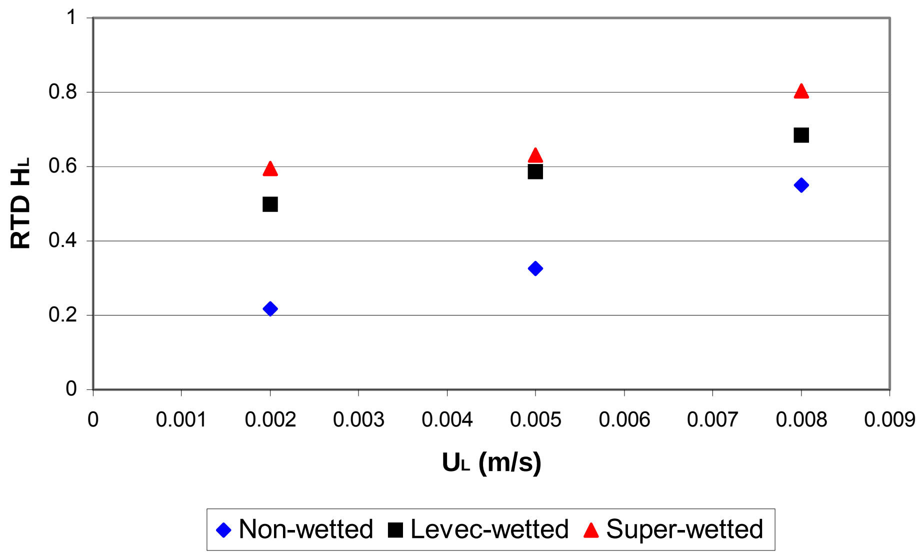

Figure 4.18 - Effect of prewetting on the holdup at U_G=0.06 m/s

At a higher gas flow rate of 0.1 m/s, the holdup trend is the same as for 0.06 m/s (figure 4.18) and can be seen in appendix A.4.

4.3.2. Effect of Gas Flow rates

The effect of the gas flow rate on the liquid holdup, determined from the residence time distribution, is seen in figure 4.19 and 4.20. At a liquid flow rate of 0.002 m/s, it is seen that the gas flow rate does not have a significant effect on the liquid holdup for the different prewetting procedures. However at higher liquid flow rates a small decrease in liquid holdup is observed, especially with increasing gas flow rates and for the Super-wetted beds.

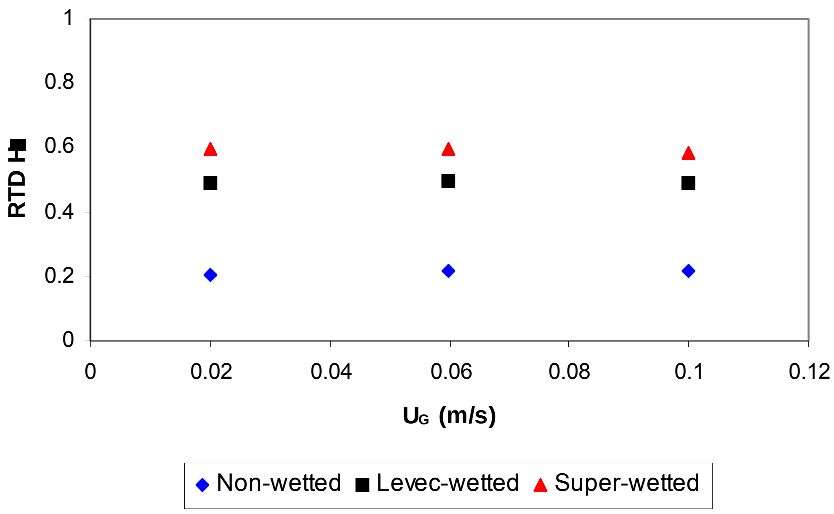

Figure 4.19 –Effect of gas flow rate on the holdup at U_L=0.002 m/s

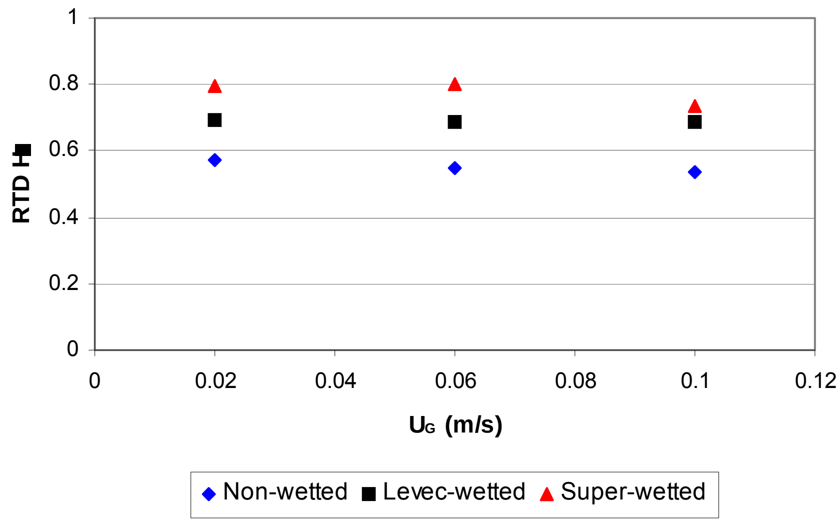

Figure 4.20 - Effect of gas flow rate on the holdup at U_L=0.008 m/s

The combined effect of the liquid flow rate and the gas flow rate for the different prewetting procedures can be seen in the three dimensional figure 4.21. It can be clearly seen that three distinct regions of liquid holdup exist for the different prewetting procedures at all gas and liquid flow rates. The holdup increases with liquid flow rate and stays reasonably constant with an increase in gas flow rate.

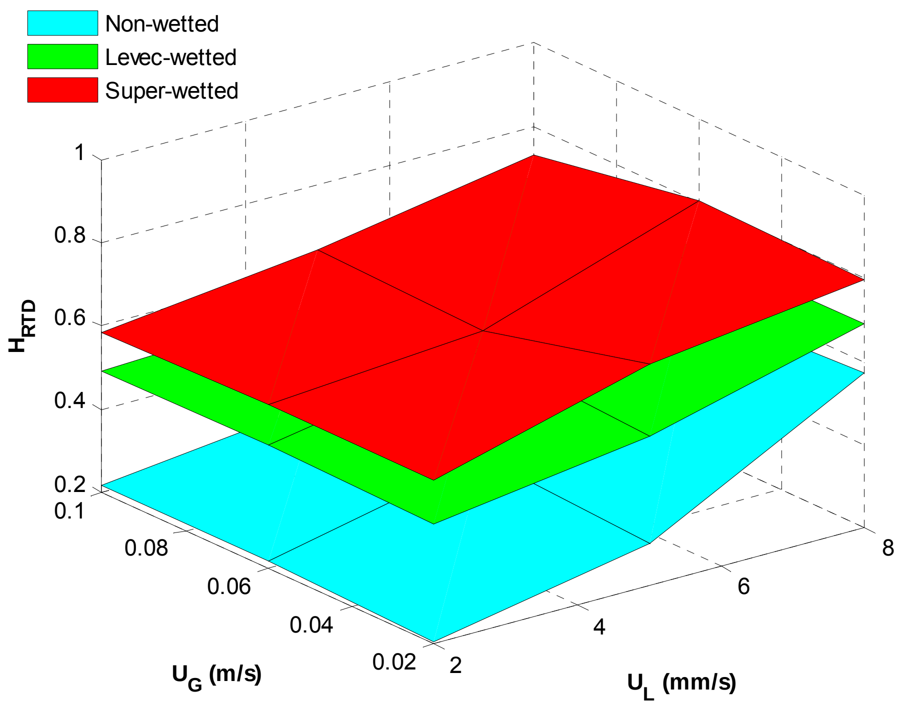

Figure 4.21 - Effect of gas and liquid flow rates on the RTD holdup

4.3.3. Porous versus Non-Porous Packing

The liquid holdup obtained for porous and non-porous packing at a gas flow rate of 0.02 m/s is shown in figure 4.22. The differences in the holdup are also shown for the different prewetting modes.

From figure 4.22 the following observations could be made:

- The difference in holdups for the porous and non-porous packing is very large; the liquid holdup for a porous, Levec and Super-wetted bed is up to four times larger than that of the non-porous packing at high liquid flow rates and up to six times greater than non-porous packing at lower liquid flow rates
- The liquid holdup for non-porous particles is the same for the Levec and Super-wetted beds; thus the difference in holdup for the Levec and Super-wetted, porous beds is due to the internal holdup
- The increase in liquid holdup with an increase in the liquid flow rate is much smaller for the non-porous packing than the porous packing for a non-wetted bed. This indicates that the holdup for a non-wetted bed at the highest liquid flow rate is mainly due to internal holdup

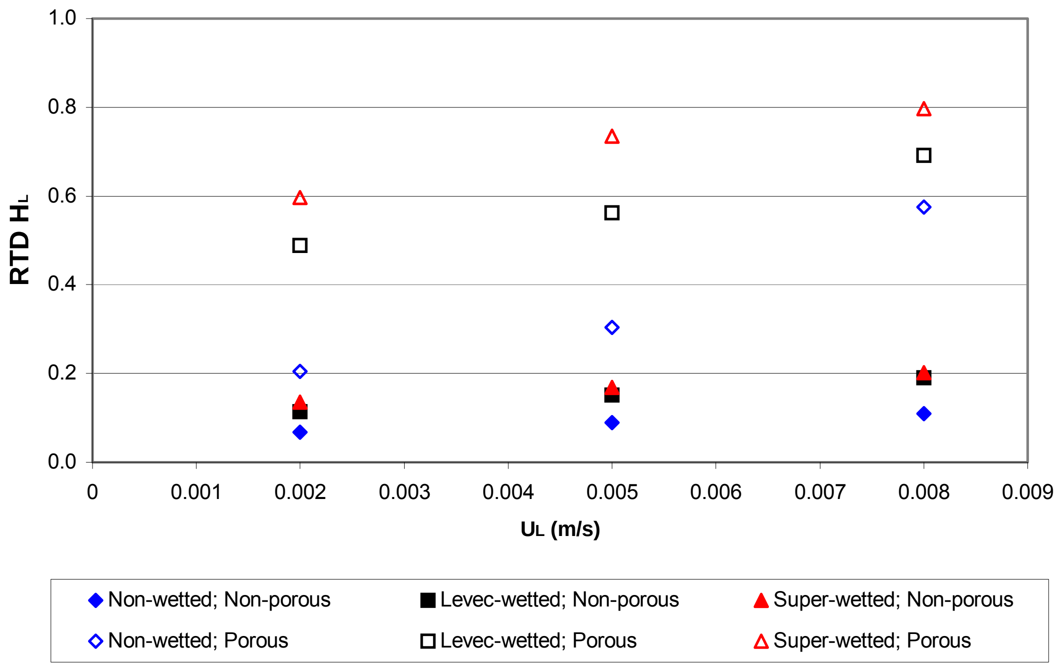

Figure 4.22 - The difference in holdup for porous and non-porous packing at U_G=0.02 m/s

4.3.4. RTD versus Weighed Liquid Holdup

The liquid holdup determined from the residence time distribution was compared to that determined by means of the weighing method. This comparison of liquid holdup is seen in figures 4.23 and 4.24. The following observations could be made from these figures:

- Generally, the liquid holdup determined by means of the weighing method was greater than the holdup determined from the residence time distribution, for all prewetting modes and at all gas flow rates
- At low liquid flow rates the difference in the two holdups was greater than at high liquid flow rates for the non-wetted and Levec-wetted beds
- For the Super-wetted beds, the difference in holdup is not very big at all liquid flow rates.

At a gas flow rate of 0.1 m/s the same trend as in figure 4.22 for the comparison of the holdup is observed, seen in appendix A.5.

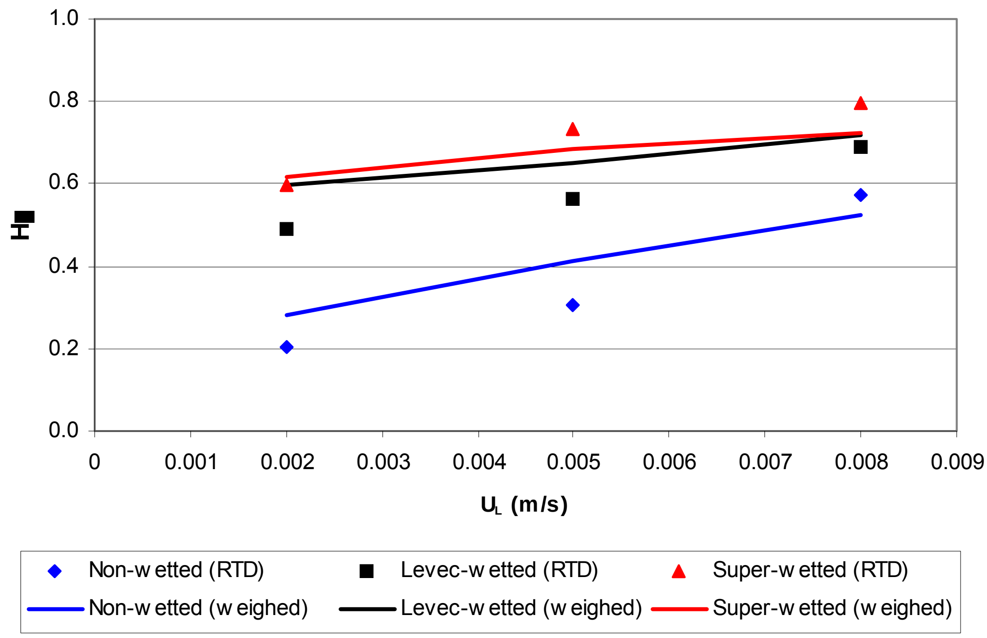

Figure 4.23 - Comparison of RTD and weighed holdup at U_G=0.02 m/s

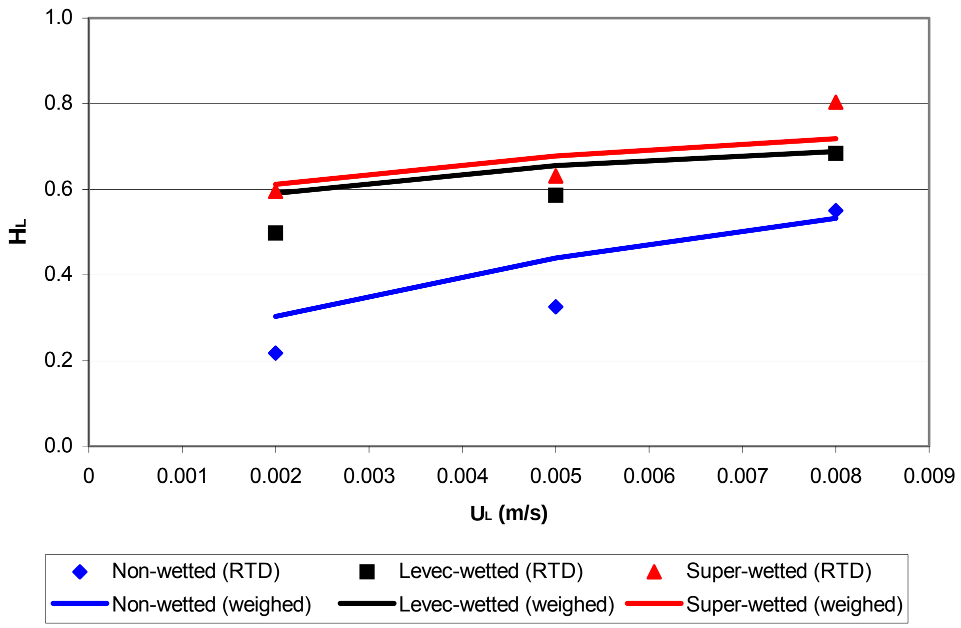

Figure 4.24 - Comparison of RTD and weighed holdup at U_G=0.06 m/s

The absolute average relative error (AARE) was obtained for the liquid holdup determined from the different methods at all liquid flow rates and gas flow rates and is shown in table 4.1. The total AARE is also given where this is the total error over all liquid and gas flow rates.

Table 4.1 – The percentage AARE for the liquid holdup obtained from the different methods for all prewetted procedures

	Non-wetted			Levec-wetted			Super-wetted		
	U_L (mm/s)								
U_G (m/s)	2	5	8	2	5	8	2	5	8
0.02	36.7	35.1	8.80	22.5	15.9	3.8	3.6	6.9	9.2
0.06	39.8	34.8	3.10	18.7	11.8	0.5	2.7	7.5	10.7
0.01	44.4	66.6	7.40	18.6	26.5	0.3	4.6	4.0	0.7
Total	30.7			13.2			5.5		

To illustrate the differences between the holdup determined from the residence time distributions and that determined from the weighing method the ratio of these holdups for the different prewetting procedures and at all gas and liquid flow rates was determined. This comparison is shown in figure 4.25. When the holdup ratio is greater than 1, it means that the liquid holdup determined from the weighing method is greater than that determined from the RTD. As seen in figure 4.25, the following trends are observed:

- The holdup ratio is greater than one at low liquid flow rates and is not influenced by the gas flow rates.
- The holdup ratio decreases to 1 and less (especially for the non-wetted procedure) at higher liquid flow rates meaning that the RTD liquid holdup is equal to or more than that determined by means of the weighing method.
- For the Super-wetted procedure the holdup ratio is very close to one and only decreases to approximately 0.9.
- Over the entire range of operating conditions, the holdup ratio varies between 1.7 and 0.9, meaning that the liquid holdup determined from the weighing method is 1.7 to 0.9 times that of the liquid holdup determined from the RTD.

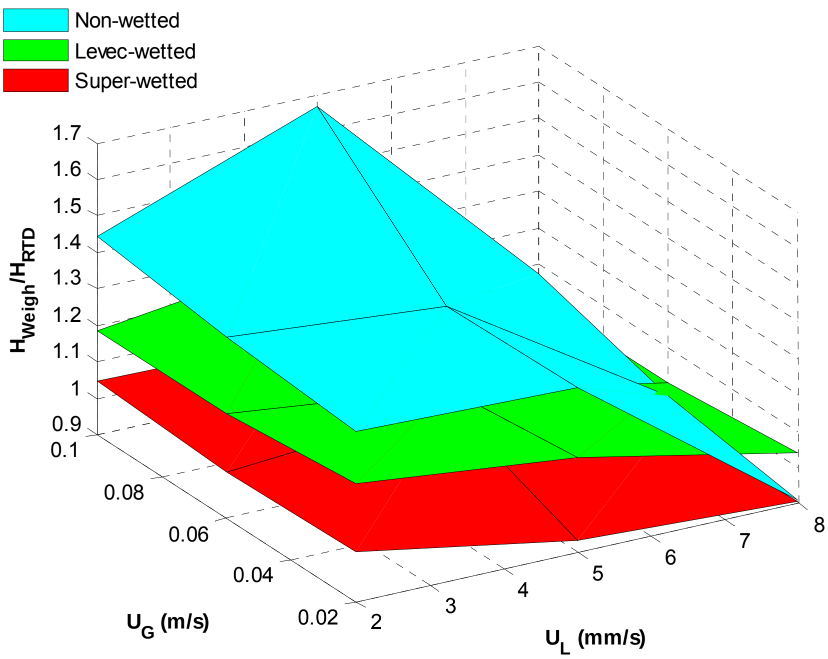

Figure 4.25 - Comparison of the RTD and weighed holdup at varying gas and liquid flow rates for porous packing

4.4. Wetting Efficiency

The wetting efficiency was determined by the method of Mills & Dudukovic (1981), section 2.4.2. This method makes use of the first moment and the variance to determine the effective diffusivity, which in turn is used to determine the wetting efficiency as in equation 2.45. In order to use this method the equilibrium adsorbtion constant (K_A) needs to be determined. In this work, this constant was determined experimentally and was found to be $4x10^{-04}$ m^3/kg.

To determine the wetting efficiency from equation 2.45, it is required to know the effective diffusivity for a liquid filled reactor. In this work it was assumed that for a Super-wetted bed at the highest liquid flow rate, the wetting is complete, i.e. the particles are internally and externally completely wetted, and therefore the effective diffusivity for this bed would be that for a liquid filled bed. This assumption is seemed reasonable in that authors have reported complete wetting, η_{ce} = 1, at high liquid flow rates (Al-Dahhan & Dudukovic, 1995) and most correlations predict η_{ce} = 1 at these high flow rates.

4.4.1. The Effect of Prewetting and Liquid Flow Rate

The effect of prewetting and liquid flow rate on the wetting efficiency can be seen in figures 4.26 and 4.27, at constant gas flow rates. From these figures the following observations were made:

- Two distinct regions of wetting efficiency can be distinguished. These regions are for the non-wetted beds and for the Levec/Super-wetted beds
- The wetting efficiency is approximately the same for the Levec-wetted and Super-wetted beds
- The wetting efficiency for the Super-wetted beds appears to remain constant at higher liquid flow rates (U_L=0.005 and 0.008 m/s) and higher gas rates (U_G=0.06 and 0.1 m/s). It can therefore be stated that

total wetting is already obtainable at U_L=0.005 m/s and U_G=0.06 m/s for the Levec and Super-wetted procedures.

- Wetting efficiency increases with the liquid flow rate and is constant with gas flow rate
- A decrease in wetting efficiency with an increase in liquid flow rate from 0.005 to 0.008 m/s at low gas rates for the non-wetted beds is observed. It is thought that this could be due to the sensitivity of the wetting efficiency to the variance of the residence time distributions and is therefore an inaccurate measure of wetting efficiency.

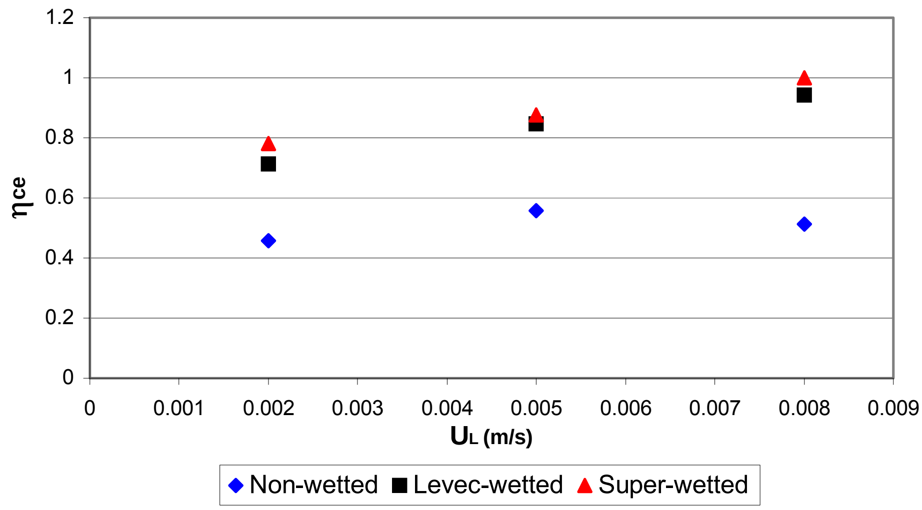

Figure 4.26 – Effect of prewetting and liquid flow rate on the wetting efficiency at U_G=0.02 m/s

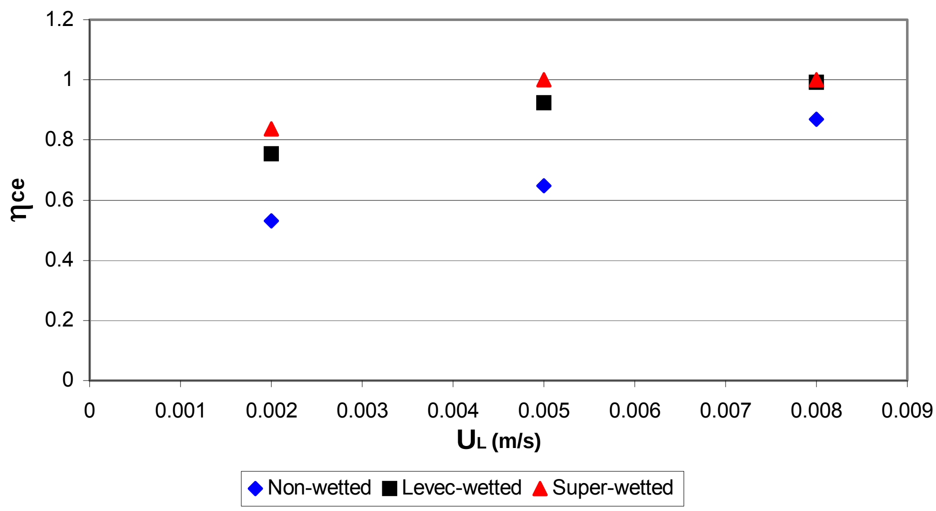

Figure 4.27 – Effect of prewetting and liquid flow rate on the wetting efficiency at U_G=0.1 m/s

The effect of prewetting and liquid flow rate on the wetting efficiency for an intermediate gas flow rate can be seen in appendix A.6.

4.5. Correlations

Various correlations for pressure drop, liquid holdup and wetting efficiency were tested against data obtained from this work. The pressure drop correlations of Sato et al., (1973) and Ellman et al., (1998), the liquid holdup correlations of Ellman et al., (1990), Holub et al., (1992), Larachi et al., (1991), Specchia & Baldi (1191) and Nemec & Levec (2005), and wetting efficiency correlation of Al-Dahhan & Dudukovic (1995) were tested whether it could predict the hydrodynamic parameters for the different prewetting procedures.

4.5.1. Pressure Drop Correlations

The results for the prediction of pressure drop correlations, for constant gas flow rates, are shown in figures 4.28 and 4.29.

It is obvious that the correlation best describing the pressure drop at U_G=0.02 m/s is that of Sato et al., (1973). The correlation best predicts a pressure drop for that of a non-wetted, porous bed and Levec-wetted, non-porous bed. It could be said that this correlation gives an estimate of the pressure drop average for a non-wetted, porous or non-porous bed and a Levec-wetted, non-porous bed. In addition, this correlation best predicts at lower liquid flow rates. The correlation of Ellman et al., (1988) predicts a pressure drop much lower than that obtained for any of the prewetting procedures, liquid flow rates and gas flow rates.

At higher gas flow rates (U_G=0.06 and 0.1 m/s) the correlation of Sato et al., (1973) did not predict accurately the pressure drop and was much lower than that obtained for any of the prewetting procedures.

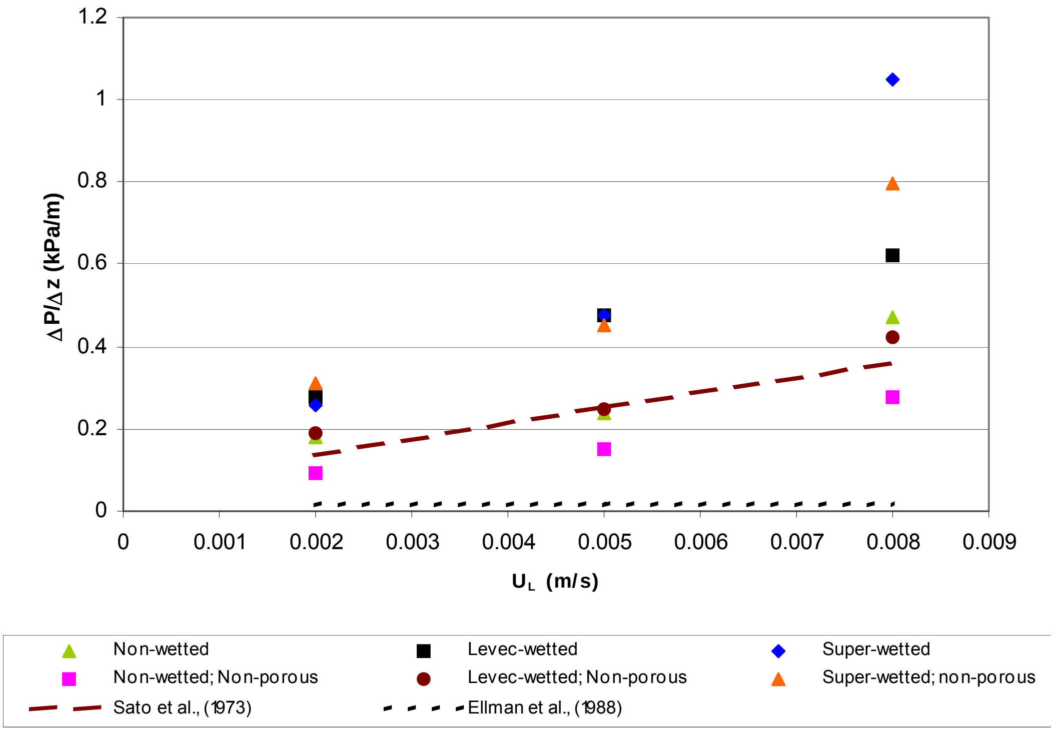

Figure 4.28 – The performance of pressure drop correlations at U_G=0.02 m/s

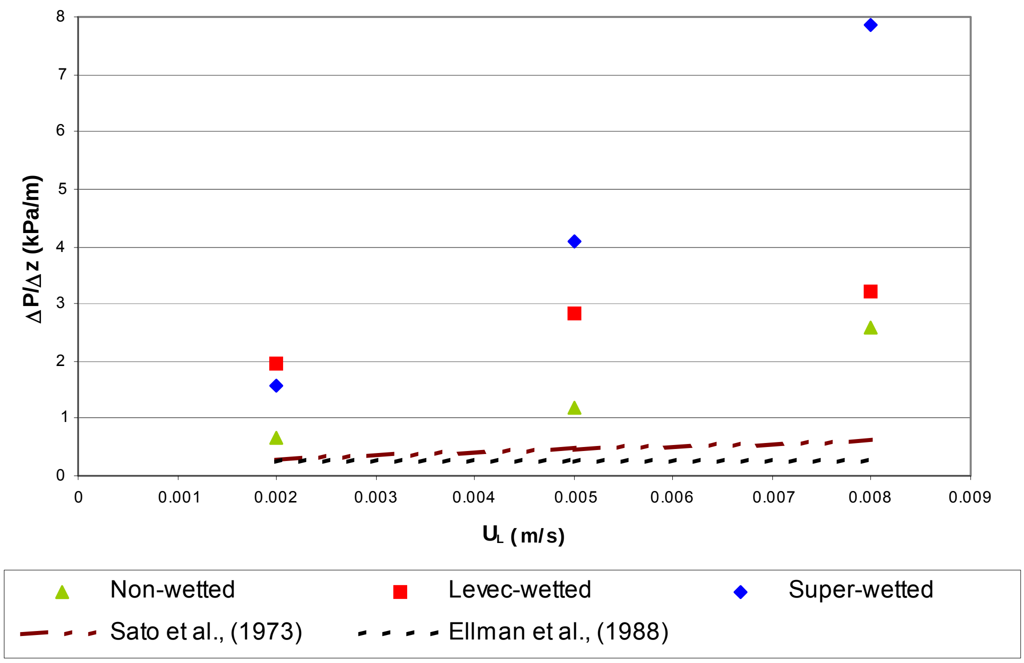

Figure 4.29 – The performance of pressure drop correlations at U_G=0.1 m/s

4.5.2. Liquid Holdup Correlations

The prediction of liquid holdup correlations, at constant gas flow rates, is shown in figures 4.30 and 4.31.

It can be seen that the correlation of Ellman et al., (1990) accurately predicts liquid hold determined from RTD data for a Super-wetted bed especially at higher gas flow rates and lower liquid flow rates. Another correlation predicting the RTD liquid holdup is that of Nemec and Levec (2005) and predicts holdup accurately for a Levec-wetted bed at lower liquid flow rates.

The other liquid holdup correlations tested against the experimental liquid holdup did not accurately predict liquid holdup. These correlations predicted much lower liquid holdup values than that determined by means of the residence time distribution.

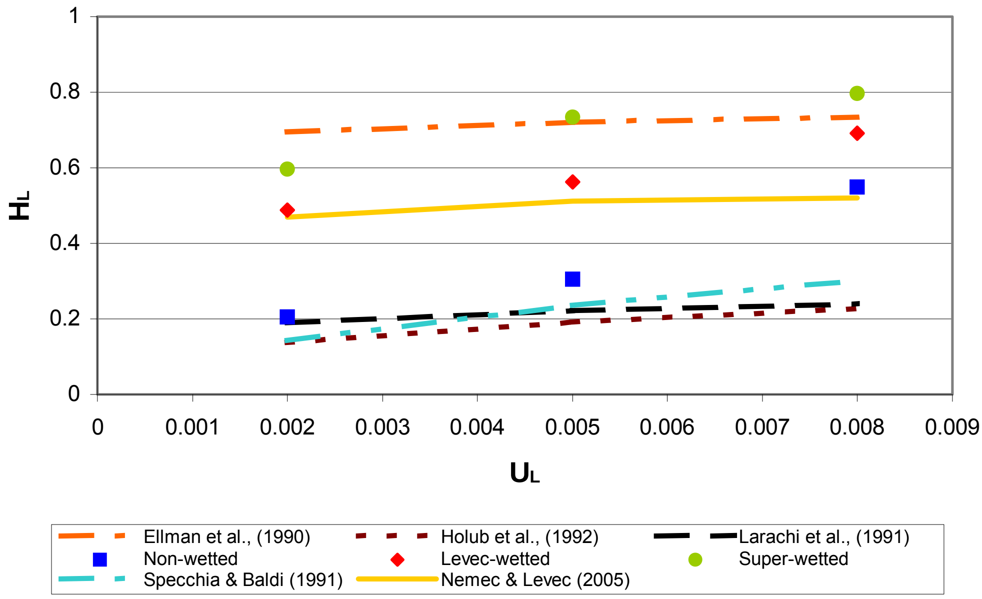

Figure 4.30 - The performance of liquid holdup correlations at U_G=0.02 m/s

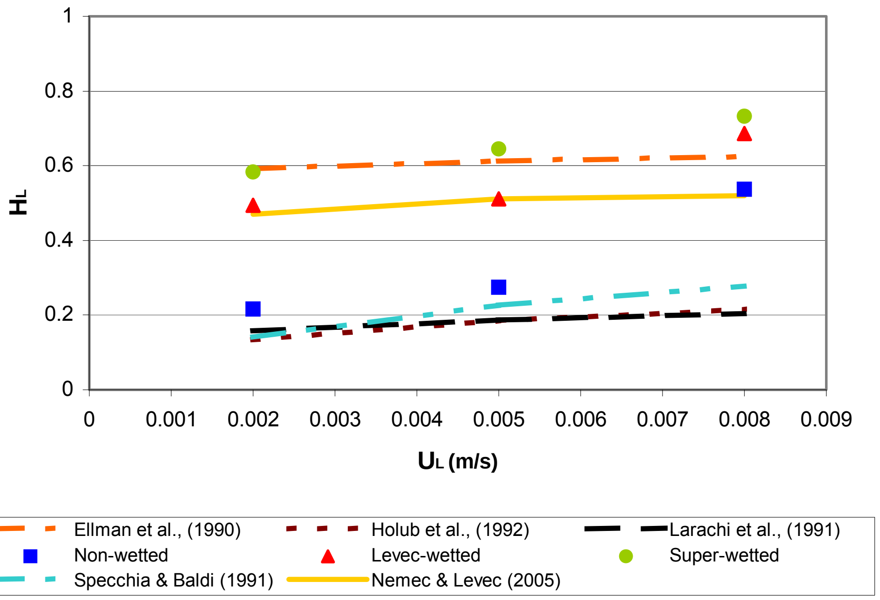

Figure 4.31 - The performance of liquid holdup correlations at U_G=0.1 m/s

It was thought that the correlations that under predicted the liquid holdup for the porous packing might accurately predict the liquid holdup for the non-porous packing. These correlations are shown in figure 4.32. It is seen that the correlation of Holub et al., (1992) accurately predicts the liquid holdup for the Super-wetted, non-porous bed. The correlations of Larachi et al., (1991) and Specchia & Baldi (1991) did not accurately predict holdup for the different prewetting procedures.

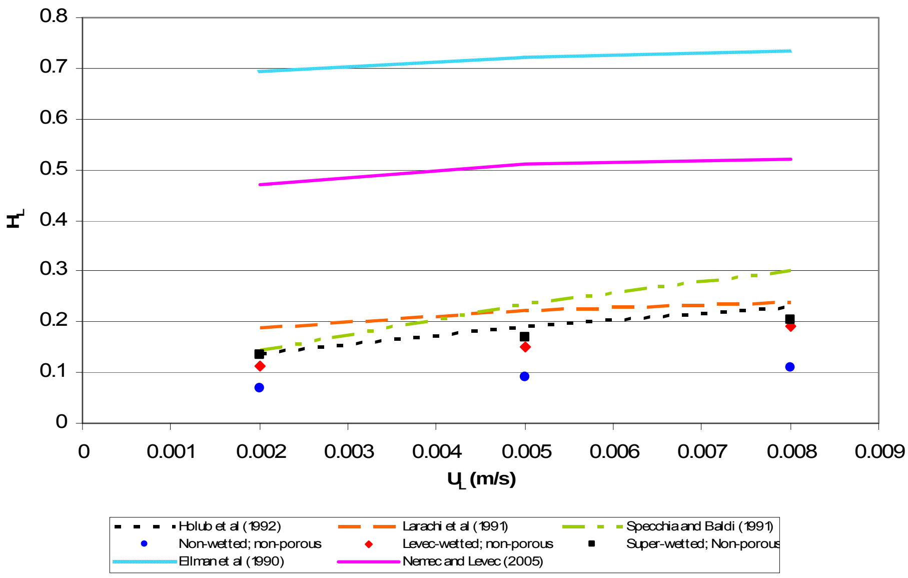

Figure 4.32 - The performance of liquid holdup correlations for non-porous packing at U_G=0.02 m/s

4.5.3. Wetting Efficiency Correlation

The performance of the Al-Dahhan and Dudukovic (1995) correlation is shown at high and low liquid flow rates in figures 4.33 and 4.34, for all prewetting procedures. At an intermediate liquid flow rate the same results were obtained.

It can be seen that the correlation of Al-Dahhan and Dudukovic (1995) does not predict the wetting efficiency for all the prewetted modes at all liquid and gas flow rates. The predicted wetting efficiency is much greater than that obtained from the experimental results. A single point, i.e. at the lowest liquid flow rate for the Super-wetted bed, was best predicted by the correlation. The correlation predicts total wetting at a liquid flow rate of approximately 3 mm/s for all prewetted procedures. This is definitely not the case for the experimental results obtained in this work. At a liquid flow rate of 3 mm/s, the non-wetted bed is far from complete wetting even at the highest liquid flow rate the non-wetted bed is no where near to complete wetting.

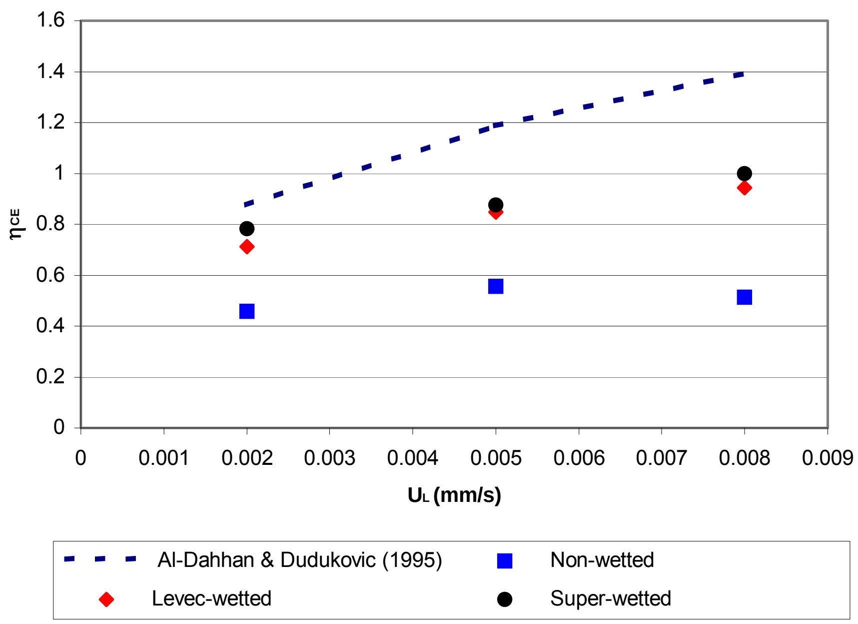

Figure 4.33 - The performance of wetting efficiency correlations for porous packing at U_G=0.02 m/s

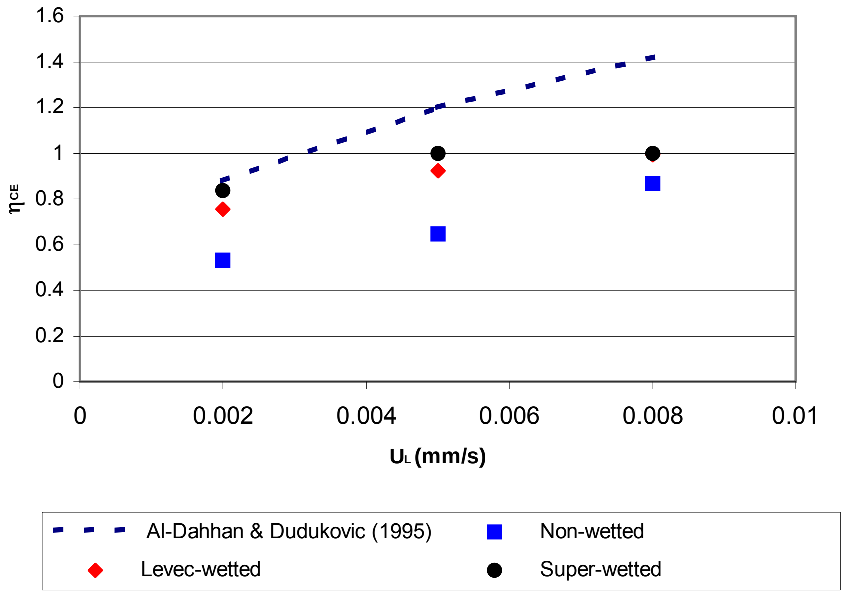

Figure 4.34 - The performance of wetting efficiency correlations for porous packing at U_G=0.1 m/s

4.6. Fitting Residence Time Distributions

The Piston dispersion exchange (PDE) model was fitted to the residence time distribution data that was obtained. The parameters are used to fit this model include the Peclet number (Pe), the number of transfer units (N) between the dynamic and static liquid holdup, the ratio of the dynamic to total liquid holdup (H) and the mean residence time (τ). These parameters are defined as follows:

$$Pe = \frac{U_L Z}{D_A}; \; N = \frac{\alpha_m Z}{H v_D}; \; H = \frac{h_D}{h_L}$$

These parameters are incorporated into the PDE model (equations 2.10 and 2.11) by changing to dimensionless form.

The PDE model was fitted to the data for porous and non-porous beds at all liquid flow rates and a gas flow rate of 0.02 m/s for all the prewetting procedures. The fit between experimental data and the PDE model is shown in figures 4.35 to 4.38.

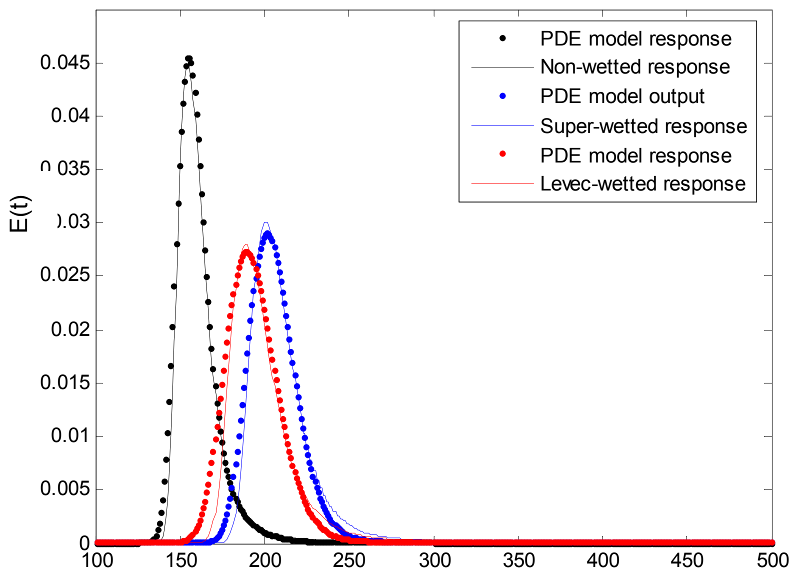

Figure 4.35 - PDE model response fitted to experimental responses for non-porous packing at U_L=2 mm/s

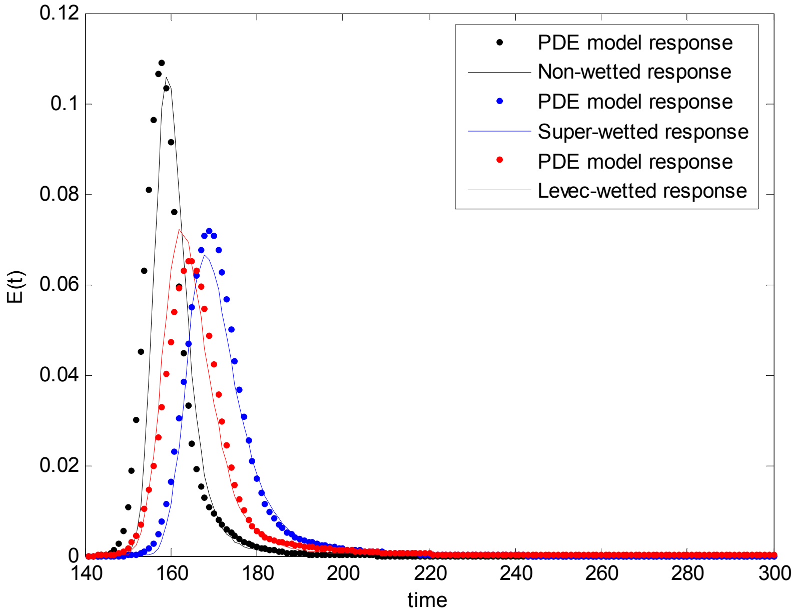

Figure 4.36 - PDE model response fitted to experimental responses for non-porous packing at U_L=5 mm/s

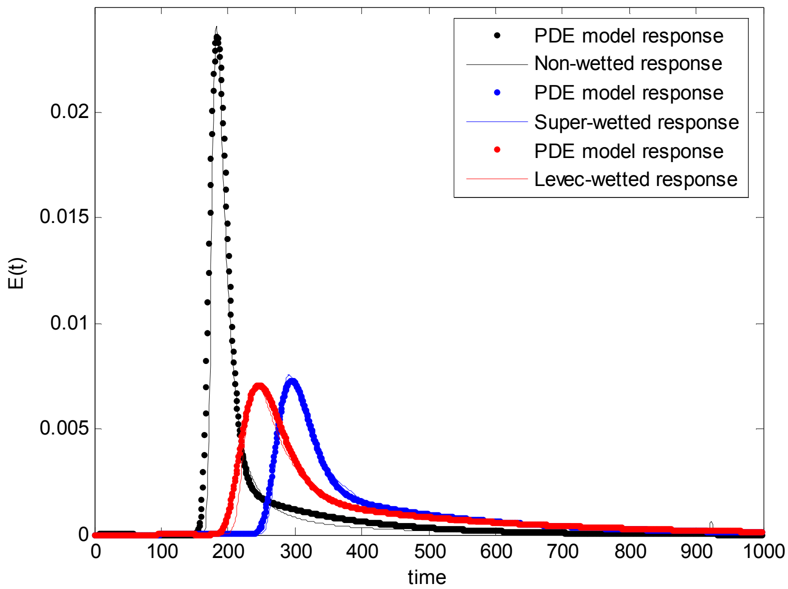

Figure 4.37 - PDE model response fitted to experimental responses for porous packing at U_L=2 mm/s

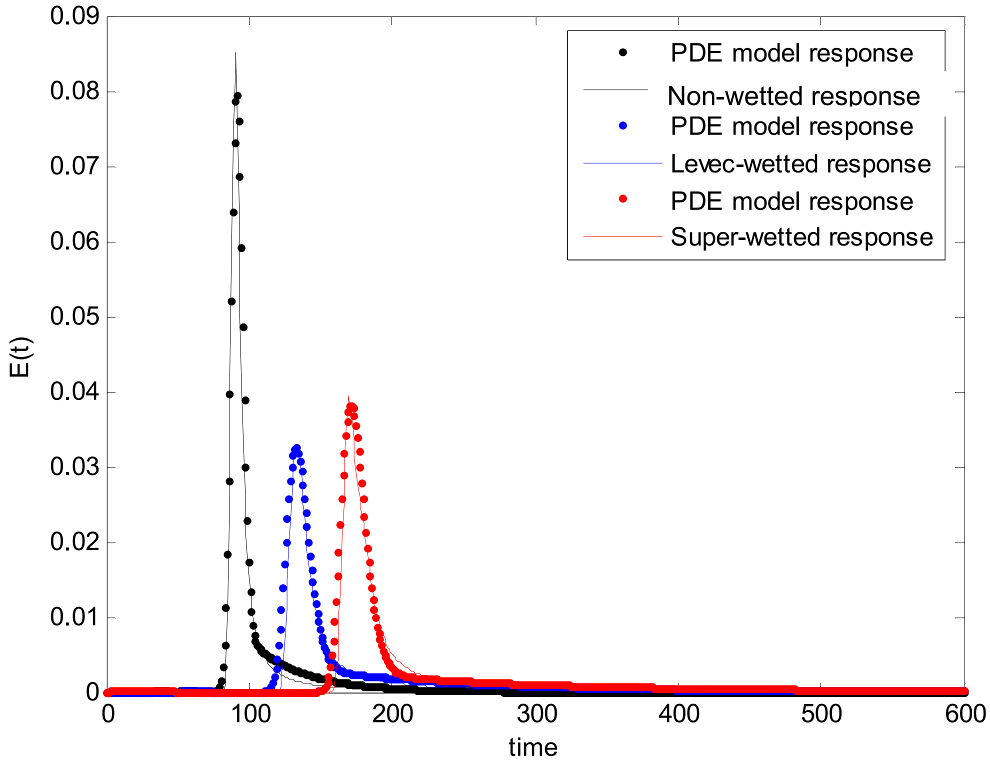

Figure 4.38 - PDE model response fitted to experimental responses for porous packing at U_L=8 mm/s

It can be seen that reasonably good fits were obtainable for the porous as well as non-porous packing. The PDE model did not always fit the tail of the response curves very well. This was expected, as the PDE model does not incorporate the effects of internal diffusion as well as the effects of prewetting.

The model parameters as well as the error between fitted data for the different prewetting procedures and for the porous and non-porous packing are shown in tables 4.1 and 4.2.

Table 4.2 - PDE model parameters for the non-porous packing at U_G=0.02 m/s

	Non-wetted			Levec-wetted			Super-wetted		
	U_L (mm/s)								
	2	5	8	2	5	8	2	5	8
Pe	69	120	158	55	95	110	59	100	105
N	0.279	0.341	0.436	0	0.200	0.387	0	0.157	0.268
H	0.939	0.928	0.866	0.982	0.946	0.909	0.999	0.955	0.947
τ	47	26	21	71	39	30	81	44	32
Error	0.087	0.138	0.164	0.127	0.122	0.173	0.177	0.261	0.418

Table 4.3 - PDE model parameters for the porous packing at U_G=0.02 m/s

	Non-wetted			Levec-wetted			Super-wetted		
	U_L (mm/s)								
	2	5	8	2	5	8	2	5	8
Pe	28	69	81	24	47	39	16	24	35
N	0.408	0.397	0.338	0.771	0.589	0.452	0.715	0.509	0.354
H	0.507	0.715	0.711	0.493	0.593	0.491	0.463	0.412	0.462
τ	107	40	36	216	84	77	252	128	83
Error	0.246	0.241	0.251	0.081	0.188	0.234	0.122	0.269	0.261

4.6.1. Effect of Prewetting and Liquid Flow Rate on PDE Parameters

The effect of prewetting and the liquid flow rate on the PDE parameters can be seen in figures 4.39 and 4.40.

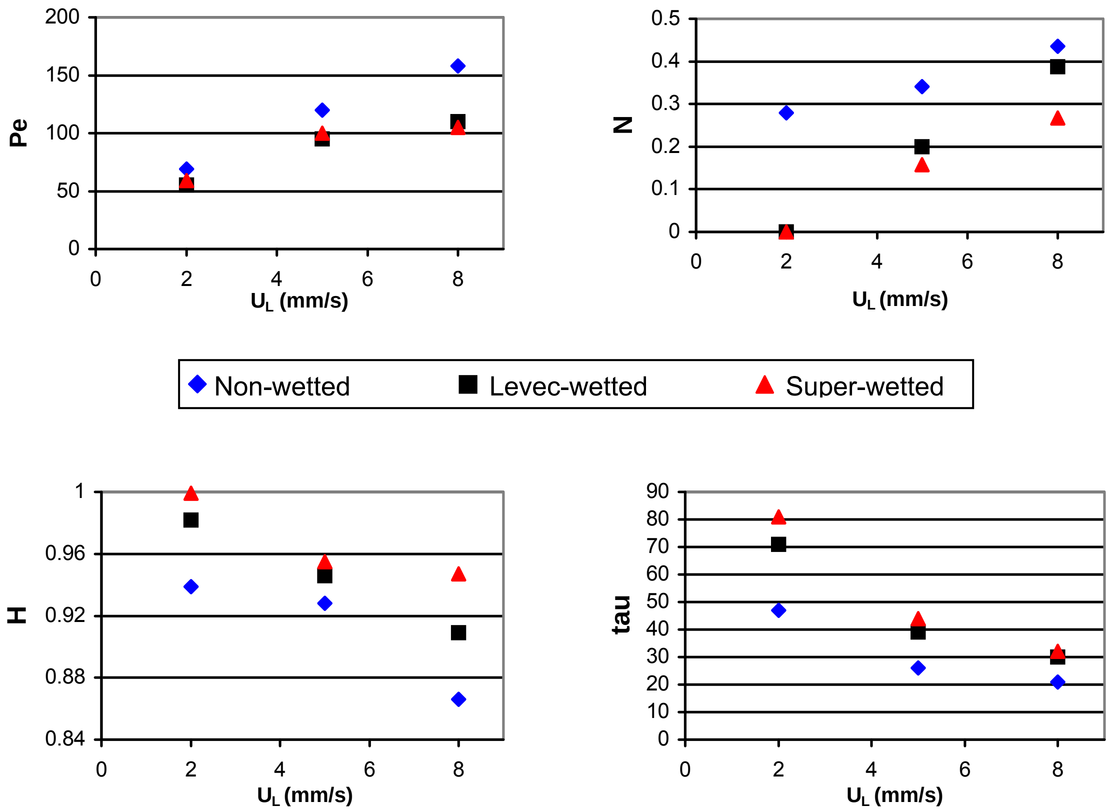

Figure 4.39 – Effect of prewetting and liquid flow rate on PDE parameters for non-porous packing

From these figures the following observations can be made:

- The Peclet number (Pe) increases with an increase in liquid flow rate
- The general trend is that the Peclet number is greater for a non-wetted bed and decreases with prewetting. This implies that the dispersion increases with prewetting
- The number of transfer unit behaves differently for the porous and non-porous packing: for the non-porous packing an increase in the number of transfer units with liquid flow rate is observed. For the porous packing the opposite is true: the number of transfer units decreases with an increase in liquid flow rate
- The number of transfer units (N) increases with prewetting for the porous packing, indicating more rapid mass transfer between dynamic and static liquid, and decreases with prewetting for the non-porous, indicating slower mass transfer
- The ratio of dynamic to total holdup (H) also behaves differently for the porous and non-porous packing. For the non-porous packing the holdup ratio decreases with an increase in liquid flow rate and for the porous packing the holdup ratio behaves erratically but there seems to be an increasing trend with liquid flow rate
- The holdup ratio for the non-porous packing increases with prewetting indicating an increase in the dynamic holdup. The holdup ratio for the porous packing decreases with prewetting indicating a decrease in the dynamic holdup
- The average residence time (τ) decreases with an increase in the liquid flow rate for both porous and non-porous packing
- The average residence time increases with prewetting for both porous and non-porous packing.

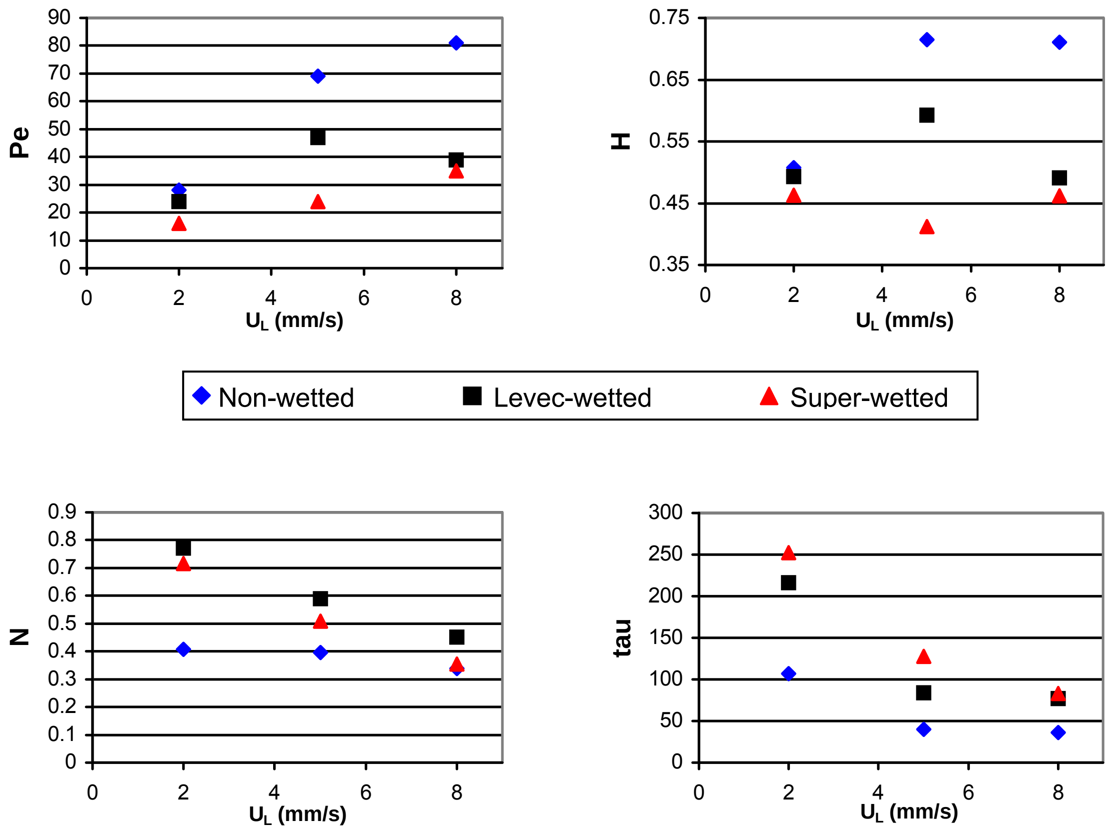

Figure 4.40 – Effect of prewetting and liquid flow rate on PDE parameters for porous packing

4.6.1.1. The Effect on the Dispersion Coefficient

The dispersion coefficient was determined from the Peclet numbers for the porous and non-porous packing. The effect of prewetting and the liquid flow rate on the dispersion coefficients are shown in figures 4.41 and 4.42.

The following trends were observed from these figures:

- The dispersion coefficient increases with an increase in liquid flow rate for the porous and non-porous packing
- The dispersion coefficient increases with prewetting
- For the non-porous packing two distinct regions of dispersion occur that is for non-wetted beds and prewetted (Levec and Super wetted) beds.
- For the porous packing however, three distinct regions of dispersion can be distinguished that is for each of the prewetted procedures

- The dispersion coefficient is greater for the porous packing than for the non-porous packing, as expected.

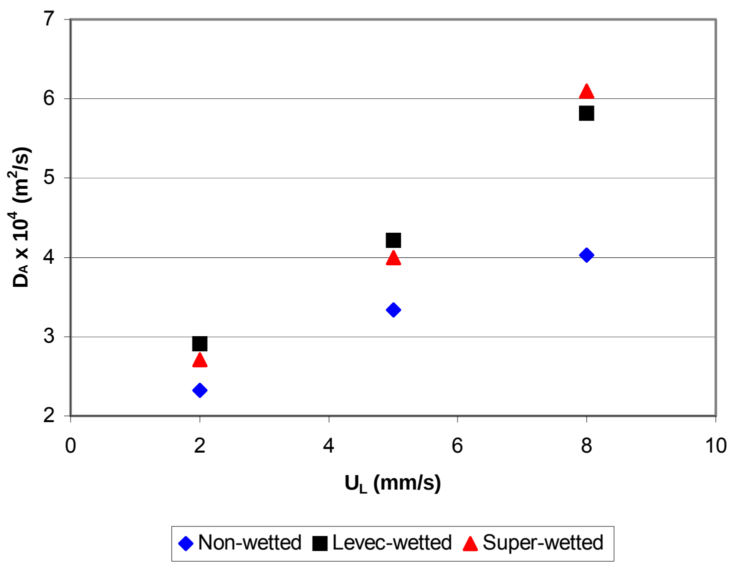

Figure 4.41 – Effect of prewetting and liquid flow rate on the dispersion coefficient for non-porous packing

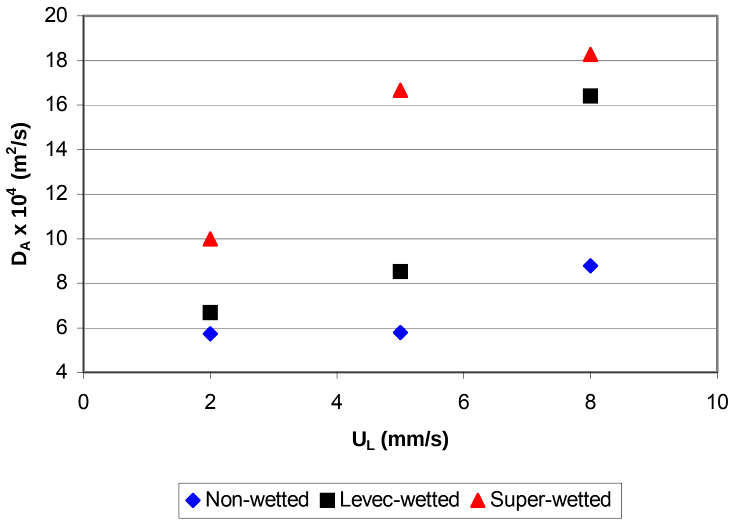

Figure 4.42 - Effect of prewetting and liquid flow rate on the dispersion coefficient for porous packing

4.6.1.2. The Effect on the Dynamic Liquid Holdup

The effect of prewetting and liquid flow rate on the dynamic holdup, as determined from the liquid holdup ratio, is shown in figures 4.43 and 4.44.

The following observations for the porous and non-porous packing were made regarding the dynamic and static liquid holdup:

- The dynamic holdup increases with an increase in the liquid flow rate
- The dynamic holdup is also greater for prewetted beds than for non-wetted beds
- From the dynamic holdup and the dynamic to total holdup ratio it can be said that the static holdup is greater for the porous packing than for the non-porous. This static holdup for the porous particles takes into account the internal liquid holdup and therefore would be greater than that of the non-porous packing
- The holdup ratio indicates that even though the static holdup also increases with liquid flow rate, this increase is very small compared to the increase in the dynamic holdup

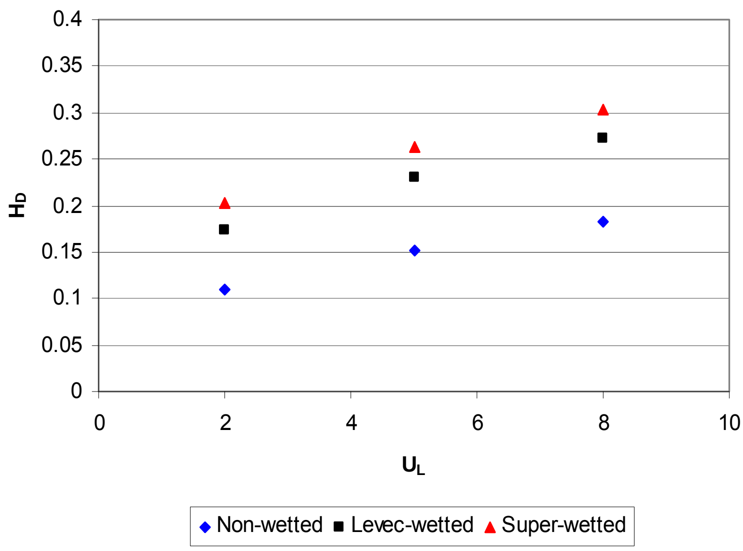

Figure 4.43 – Effect of prewetting and liquid flow rate on the dynamic holdup for non-porous packing

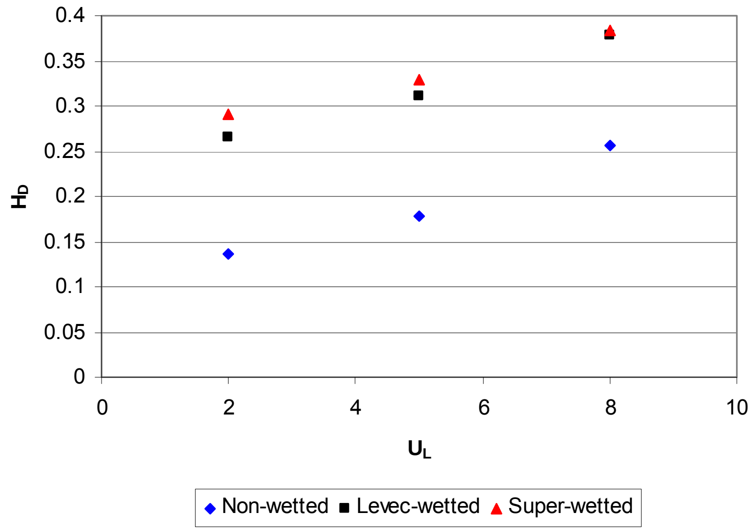

Figure 4.44 - Effect of prewetting and liquid flow rate on the dynamic holdup for porous packing

4.6.1.3. The Effect on the Mass Transfer Coefficient

The effect of prewetting and the liquid flow rate on the mass transfer coefficient, k_La, is shown in figures 4.45 and 4.46. The mass transfer coefficient was determined from the number of transfer units (N). It is observed that the mass transfer is very slow between the dynamic and static liquid holdup volumes.

The following trends can be seen in figures 4.45 and 4.46:

- The mass transfer between dynamic and static liquid increases with the liquid flow rate
- The mass transfer coefficient is less for prewetted beds than for non-wetted beds
- For the non-porous packing, at a low liquid flow rate, the mass transfer is zero for the prewetted beds (Levec and Super)
- Mass transfer is generally slower for the porous packing when compared to that of the non-porous packing.

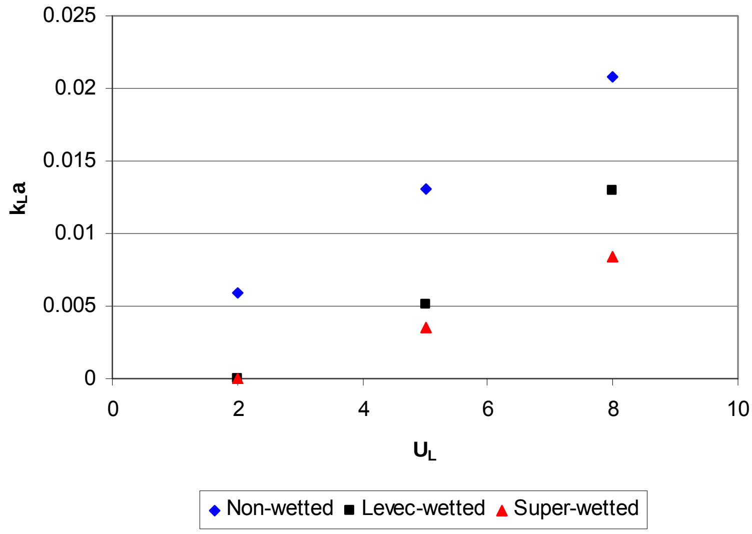

Figure 4.45 - Effect of prewetting and liquid flow rate on the mass transfer coefficient for non-porous packing

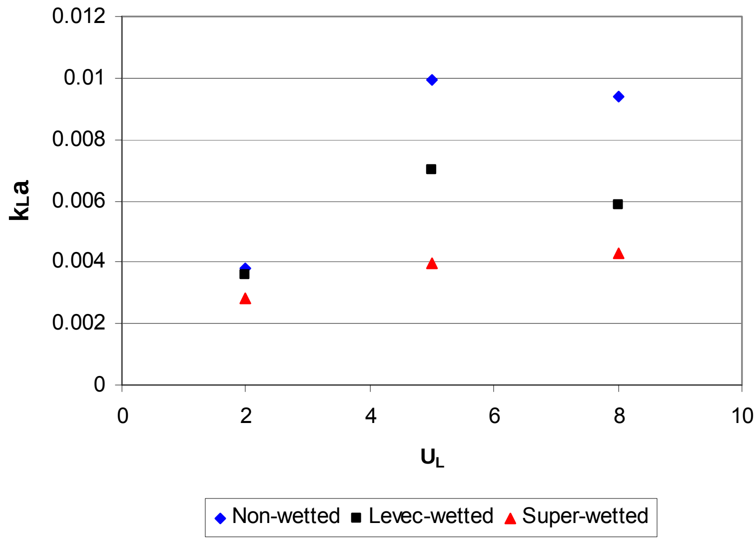

Figure 4.46 - Effect of prewetting and liquid flow rate on the mass transfer coefficient for porous packing

To eliminate the effect of the holdup and therefore the superficial velocity in the dynamic phase, the product of k_La and $H_D{}^n$ were determined. According to Gianetto et al., (1973), quoted by Loudon (2005), the mass transfer coefficient is proportional to the liquid velocity and therefore the liquid holdup. The equation governing this is:

$$k_L \propto U_D^{3/2} \propto H_D^{3/2} \qquad (4.1)$$

From equation 4.1, it can therefore be said that the product of k_La and $H_D^{3/2}$ for the different prewetted beds should be equal, if the difference in holdup is the sole cause of the k_La trends observed for different prewetting, provided that the specific interfacial area between dynamic and static phases (a) is the same, i.e. equation 4.2.

$$\left(k_L a H_D^{3/2}\right)_{Super} = \left(k_L a H_D^{3/2}\right)_{Levec} = \left(k_L a H_D^{3/2}\right)_{Non-wetted} \tag{4.2}$$

The effect of prewetting and liquid flow rate on k_La ($H_D^{3/2}$) is shown in figures 4.47 and 4.48 for the different types of packing.

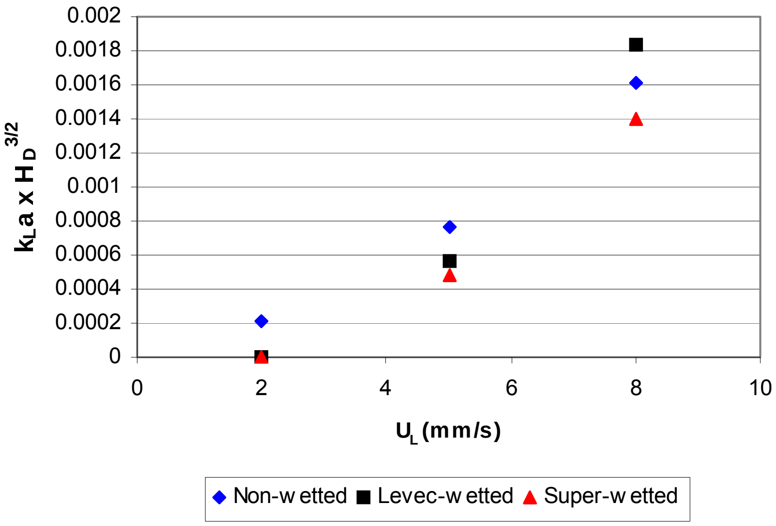

Figure 4.47 - Effect of prewetting and liquid flow rate on the product of mass transfer and dynamic holdup for non-porous packing

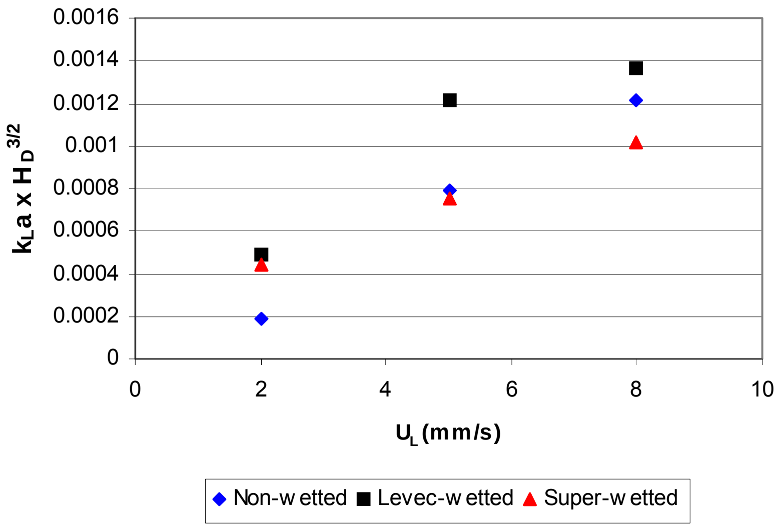

Figure 4.48 - Effect of prewetting and liquid flow rate on the product of mass transfer and dynamic holdup for porous packing

It can be seen that the general trend for k_La ($H_D^{3/2}$) does not differ from that of k_La for the non-porous packing whereas the trend for the porous packing is that the mass transfer product for the non-wetted bed shifted downwards with regards to that of the Levec and Super-wetted beds.

4.6.2. Comparison of Residence Times obtained from Best-fit Method and Method of Moments

By determining parameters by two different methods allows one to compare these methods and can therefore give an indication of the accuracy of the methods. The average residence times obtained from the best-fit method and the method of moments were compared and the results can be seen in figure 4.49 and 4.50.

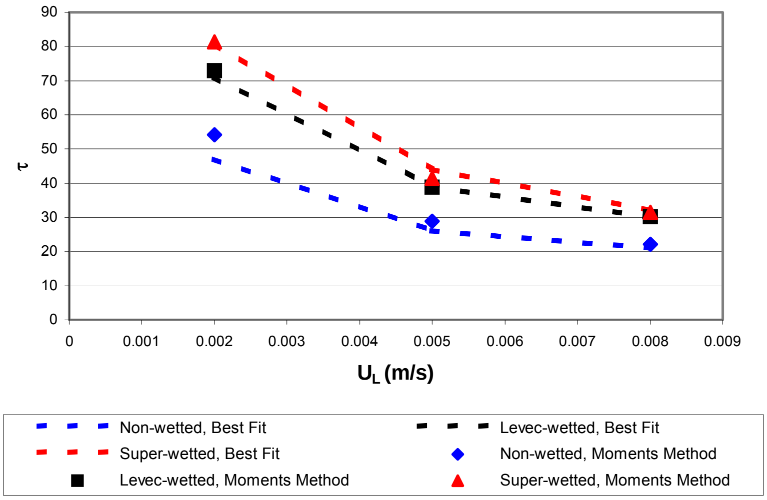

Figure 4.49 - Comparison of average residence times obtained from best fit and moment methods for non-porous packing

There is very good agreement between these two methods. The differences in residence times improve with prewetting and are very good at all liquid flow rates. For the non-wetted beds the differences in residence times are greater than the other prewetting procedures, however this difference is reasonable.

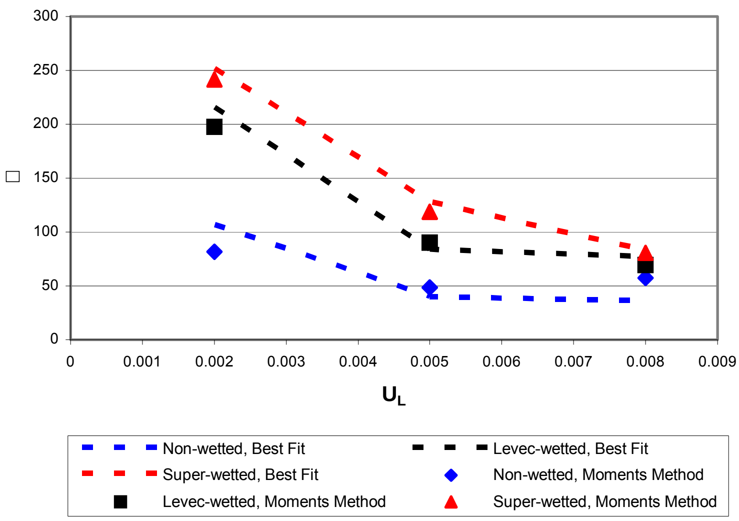

Figure 4.50– Comparison of average residence times obtained from best fit and moment methods for porous packing

The absolute average relative error (AARE) for the residence times of the different methods is shown in table 4.3. It can be seen that the AARE is smaller for the non-porous packing and therefore both methods is suitable for determining parameters for non-porous packing. The AARE increases for the porous packing but good agreement is obtained for the prewetted beds.

Table 4.4 – The percentage AARE for the residence times obtained from different methods

	Non-wetted	Levec-wetted	Super-wetted
Porous	35	8.5	4.7
Non-porous	10.8	1.3	2.7

CHAPTER 5

Discussion

5.1. The Effect of Prewetting

The effect of prewetting on residence time distributions, liquid holdup, pressure drop and wetting efficiency is evident from the results in the previous chapter. The prewetting procedure can drastically change these hydrodynamic parameters. The pressure drop can increase by as much as four times for a prewetted bed as that for a non-wetted bed. The difference between a Levec and Super-wetted bed is less severe. Liquid holdup is also evidence that prewetting does affect trickle bed operation and performance. Liquid holdup in Super-wetted bed can be as much as three times greater than that for a non-wetted bed. With different prewetting procedures the solid-liquid contacting efficiency is also largely affected. At the same conditions, the wetting can be partial (approximately 60 % wetting efficiency) for a non-wetted bed and wetting can be complete (100%) for a Super-wetted bed.

These differences due to prewetting have been attributed to the flow morphology in the beds by a number of authors (Loudon, 2005 and Christensen et al., 1986). Christensen et al., (1986), quoted by Loudon, 2005, stated that the flow in a non-wetted bed is dominated by rivulets whereas the flow in prewetted beds is dominated by film flow.

The results for the liquid holdup, pressure drop and wetting efficiency confirm this statement of dominant flow patterns for the different prewetting procedures. The Super and Levec-wetted beds have much higher liquid holdups and pressures drops than that of the non-wetted beds and can be explained by means of flow morphology and liquid distribution within the bed.

Due to the presence of rivulets in a non-wetted bed, the catalyst packing is not entirely wetted and parts of the bed are completely dry as evidenced by the wetting efficiency always less than one. With prewetting the beds, the dry areas would now become wetted as liquid fills these areas and partially wetted catalyst can now become totally wetted. The wetting efficiency results show that even with prewetting total wetting is not always achieved. It is only at high liquid flow rates that the wetting is complete. With dry areas being filled with liquid, the liquid holdup increases and liquid distribution increases forcing liquid flow into the form of films. The flow morphology therefore changes from being predominantly rivulet flow to film flow.

The pressure drop tells the same story. With prewetting the bed there is greater liquid distribution due to film flow and therefore the area available for the gas to pass through is decreased thus increasing the pressure drop. The increase in pressure drop can also be argued by means of increased gas-liquid shear forces due to the increased liquid area. From figure 4.11, it is seen that the pressure drop for the Levec and Super-wetted beds are the same at the lower liquid flow rates. It is proposed that the reason for this is due to the flow morphology. At these conditions the flow morphology for the Levec and Super-wetted beds is assumed to be the same, i.e. film flow. However due to the low liquid flow rate the film around the catalyst particle thins out causing rupturing of the film and thus results in flow morphology similar to that of a non-wetted bed. Wammes et al., (1991) stated that at low liquid flow rates the film thickness decreases and can decrease to a point where the film ruptures thereby forming rivulets. Therefore at low liquid flow rates the flow morphology in a prewetted bed is that of rivulet flow as well as film flow. This describes comparable pressure drops and differing liquid holdup for the various prewetting procedures as well as non-wetted beds, at low liquid flow rates.

Ravindra et al., (1977) stated that rupturing of liquid films forming rivulets is a result of the draining process during different prewetting procedures. The differences in the Levec and Super-wetted beds is due to the draining procedures in the Levec-wetted bed and therefore the rupturing of films around the catalyst particles results in lower liquid holdup, wetting efficiency and pressure drop for the Levec-wetted beds as compared to the Super-wetted beds.

Similar conclusions were made in the work of Loudon (2005). Loudon (2005) investigated the effect of prewetting on the various hydrodynamic parameters for non-porous catalyst packing.

This difference in flow morphology for the prewetted beds can also be deduced from the residence time distributions for the different prewetting procedures. The effect of prewetting on residence time distributions is seen in figures 4.1 and 4.2. A clear distinction can be made between the non-wetted beds and the prewetted beds. For the non-wetted bed the peak of the response curve is much higher thus indicating that less tailing occurs in the non-wetted bed than for the prewetted beds. Even though the difference in the residence time distribution curves for the Levec and Super-wetted beds is very small, there is a difference in the peak of the response curve. A lower peak in the response curve for the Super-prewetted bed indicates a greater tailing effect.

The more pronounced tailing in the prewetted beds indicates that the flow morphology is indeed film flow. When the predominant flow pattern is films, the tracer needs to pass through this film for each wetted particle to the centre of the particle and then exits the particle. This process results in a delayed or longer exiting time for the tracer and thus tailing of the response curve results. For the non-wetted bed, the predominant flow being rivulets, the tracer only passes to the wetted particles by means of the liquid rivulets and its path is not hindered by the presence of liquid films, whereby it needs to diffuse through, around the particles and therefore the time taken for the tracer to pass through the bed is much quicker and the tailing effect is limited for the non-wetted bed.

The tailing effect being a result of the flow morphology cannot be argued for increased liquid flow rates. It can be argued that at higher liquid flow rates, the wetting of catalyst particles improves thereby increasing film flow. This could result in the tracer having to pass through more films surrounding particles therefore slowing the tracer resulting in a more pronounced tailing effect. This is however not the case shown by the experimental results. The tailing effect due to liquid morphology is somewhat overcome by increased liquid velocity. In figures 4.3, 4.4 and 4.5, the effect of the liquid flow rate for the different prewetting procedures can be seen. At higher liquid flow rates the tailing effect becomes less and at lower liquid flow rates the tailing of the residence time distribution curves becomes more prominent. This would mean that the tracer follows the path of the free or externally flowing liquid more closely and any internal or external diffusion rates are very fast, even negligible. At low liquid flow rates the flow morphology becomes a more predominant factor in creating the tailing effect present in residence time distribution response curves.

Authors have stated (Illiuta et al., 1999d) that the internal or intraparticle diffusion through the porous catalyst particles result in the tailing effect of response curves. This would translate as follows: in the presence of rivulet flow therefore partial wetting (such as in a non-wetted bed) the internal diffusion would be limiting and would result in the ‘delayed’ exit of any tracer. This is illustrated by figure 5.1.

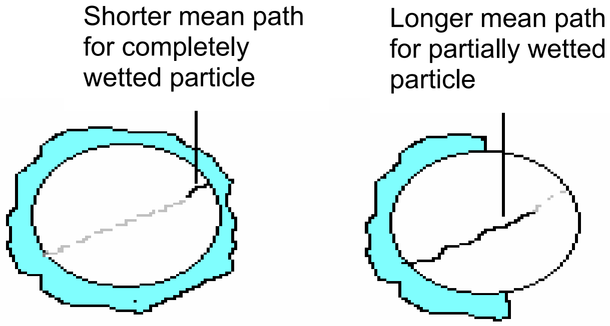

Figure 5.1 – Effect of catalyst wetting on intraparticle diffusion path.

With partial wetting the internal diffusivity would be greater due to the path travelled by a tracer molecule is that from the wetted area through the particle to an active site and then exiting at the wetted area. This internal diffusion resistance would create tailing in the response curves. With increased wetting of film flow the mean path travelled by a tracer molecule decreases resulting in less tailing in the response curves. This would mean that a greater tailing effect would be observed for a non-wetted bed and less tailing for prewetted beds. This contradicts the results obtained in this work. For this reason it can be said that the tailing effect present in residence time distribution curves can be a result of both internal diffusion as well as the flow morphology present in the reactor bed, where the effect of the flow morphology is more dominant. This can also be concluded from figure 4.8 whereby the residence time distribution curves for porous and non-porous packing is compared. For the non-porous residence time distribution curves some tailing is evident and cannot be a result of internal diffusion effects and is therefore due to the flow morphology.

The small effect that the gas flow rate has on the liquid holdup for prewetted beds further substantiates different flow morphologies for prewetted beds. In figure 4.20, the effect of the gas flow rate on the liquid holdup shows a slight decrease in holdup for the prewetted beds. This is due to the flow morphology being predominantly film flow. Increased gas flow rates results in increased liquid distribution thus causing liquid films to be thinned out and therefore the liquid holdup decreases. Loudon (2005) stated that the absence of the effect of the gas flow rate for non-wetted beds is due to less gas-liquid interaction when the dominant flow formation is rivulets.

5.2. Trickle Bed Analysis by Residence Time Distributions

In this work, the use of residence time distributions to determine a number of hydrodynamic parameters proved to be very useful. In addition, it was shown that the residence time distributions could be used to determine the effect of prewetting. By just looking at the response curves a lot can be said regarding prewetting of packed bed reactors.

Two methods of determining parameters were used in this work, namely that of the method of moments and a best-fit method. Both methods have proven to work well for trickle bed reactors however each has its own drawbacks. The method of moments gave good results however the moments determined are very sensitive to the accuracy of the response curves especially at very low concentrations. The best-fit method also performs well but it is a very tedious method especially for large data sets. In order for this method to be accurate a model describing all phenomena occurring in the system needs to be developed. The parameters determined from the best-fit method will be subject to the criteria of optimisation. The results obtained for each method will be discussed in the next sections.

5.2.1. Method of Moments

The method of moments was used to determine the liquid holdup and the wetting efficiency.

5.2.1.1. Liquid Holdup

The use of the first moment to determine the liquid holdup gave good results. There was a small difference in the holdup determined from the first moment and that from the weighing method especially at low liquid flow rates. At high liquid flow rates and for the Super-wetted beds there was very good agreement between these methods in terms of liquid holdup.

This difference for the different methods is due to the tracer not being accessible to all the liquid holdup volume and becomes more accessible as the liquid flow rate increases. This can be an indication of differences in the liquid holdup and the degree of mixing for the different prewetting procedures. These differences can be attributed to the different flow morphologies of the prewetted beds (as discussed in section 5.1).

5.2.1.2. Wetting Efficiency

The wetting efficiency was determined using the method of moments and as described in the work of Mills & Dudukovic (1981). In order to determine the wetting efficiency assumptions had to be made. Assumptions made were:

- Internal holdup or pore filling is complete due to capillary forces for all prewetted beds. This assumption is inaccurate for non-wetted beds, however the amount of internal holdup did not largely, if at all, affect the wetting efficiency
- The amount of dispersion is very small when compared to the amount of diffusivity and therefore the Peclet number is very large
- The mass transfer to the catalyst pellets is much greater or faster than the internal diffusion and therefore the internal diffusion is the limiting step.

The wetting efficiency was found to increase with liquid flow rate and with prewetting. The wetting efficiency for the Levec and Super-wetted beds were very much the same. The increased wetting efficiency, at the same liquid flow rate, for prewetted beds can be attributed to the flow morphology or flow pattern existing in prewetted beds. Low and incomplete wetting efficiency in a non-wetted bed indicates that catalyst particles are partially wetted and that parts of the bed can be entirely dry. If the predominant flow pattern in a dry bed is in the form of rivulets, it will be the case that parts of the bed are not reached by the flowing liquid resulting incomplete wetting. Increased and even total wetting efficiency in prewetted beds would be explained by increased liquid distribution and therefore film flow being the dominant flow pattern.

5.2.2. Best-Fit Method

For the best-fit method the Piston Dispersion Exchange Model was used to determine the Peclet number, the number of transfer units between the dynamic and static holdup, the ratio of dynamic to total liquid holdup and the average residence time.

5.2.2.1. Peclet Number

The Peclet number, an indication of the amount of dispersion occurring in the system, was determined for the porous and non-porous packing. With both types of packing the same trend in Peclet number was observed with prewetting and liquid flow rate. As expected, the Peclet number increases with liquid flow rate due to the rate of transport by means of convection increasing within the system. What is more interesting is the decrease in the Peclet number with prewetting, showing that the rate of transport by dispersion increased from a non-wetted bed to a Levec and Super-wetted bed. This increase in dispersion coefficient indicates that the amount micro mixing (such as radial and axial mixing effects) is different for the different prewetting modes.

The difference in the degree of mixing can once again be attributed to different flow morphologies present in the different prewetted beds. In a non-wetted bed it has been proposed that the flow pattern is predominantly rivulets. With rivulets flowing down a packed bed there is limited, if any, interaction between different rivulets and therefore due to this detachment, liquid molecules do not mix and disperse over a large scale. The rate of transport within these rivulets will mostly be due to convection. The opposite will be true if film flow was the dominant flow pattern such as in prewetted beds.

5.2.2.2. Average Residence Time

With an increase in liquid flow rate the average residence time decreases due to the tracer molecules exiting the packed bed much quicker as the liquid holdup is less. The increase in residence time with prewetting was observed for both methods of parameter estimation. Greater residence times for prewetted beds indicates increased liquid holdup (as was observed in the experimental results) and the average time spent by each tracer molecule is longer therefore the tracer is more accessible to the liquid volume within the bed. Interaction between molecules and catalyst would be greater suggesting that film flow will predominantly occur in prewetted beds.

The average residence time determined from the best fit method and the method of moments were compared for the porous and non-porous packing. It was seen that the residence times compared well for the non-porous packing and become even better with prewetting. Comparison for the porous packing was not as good as for the non-porous packing however it is still perceived as being good. For the porous packing the residence time determined from the PDE model was generally greater than that of the method of moments. This discrepancy is due to the fact that the PDE model does not incorporate the effects of internal diffusion and internal liquid holdup such as occurring in porous particles.

5.2.2.3. Dynamic Liquid Holdup

The dynamic to total liquid holdup ratio was used to determine the dynamic holdup. Even though the trends observed for the holdup ratio was different for the different types of packing, the trend in the dynamic holdup was increasing with increasing liquid flow rate. The dynamic holdup also increases with prewetting. The increase in the dynamic holdup, with prewetting, is another indication that the flow morphology for prewetted beds is different to that of non-wetted beds. The dynamic holdup for the non-wetted bed is the lowest when compared to the Levec and Super-wetted beds. This would be an indication that the flow pattern in these beds is mainly dominated by rivulets and as the beds are prewetted the liquid holdup increases as liquid fills any void spaces and previously non-wetted areas become wetted. The liquid distribution therefore increased and changed from rivulet flow to film flow with prewetting.

It was also noted that the dynamic liquid holdup determined for the porous particles was very high. The reason for this could be due to the fact that the

PDE model does not consider any internal liquid holdup and therefore the dynamic holdup determined from the PDE model includes some internal liquid holdup.

5.2.2.4. Dynamic-Static Mass Transfer Coefficient

The dynamic-static mass transfer coefficient was determined by means of the number of transfer units. It was observed that the mass transfer decreased with prewetting the beds. This could be due to two reasons:

- The liquid holdup for the prewetted beds is greater and therefore the superficial velocity is lower for the prewetted beds. With the lower superficial velocity the mass transfer is slower between the static and dynamic liquid holdup
- The tracer does not take part in non-wetted areas of a packed bed resulting in the tracer taking up less time to exit the bed. For the non-wetted bed (consisting of non-wetted areas) it therefore seems as if the mass transfer is faster but rather the tracer exits the bed quicker due to dry areas existing in the bed.

To eliminate the first reason for slower static-dynamic mass transfer for prewetted beds, the effect of prewetting on the product of the mass transfer coefficient and the dynamic holdup, i.e. $k_L a\ H_D^{3/2}$, was determined. This can be seen in figures 4.47 and 4.48. It is observed that $k_L a\ H_D^{3/2}$ decreases with prewetting for the non-porous packing, thereby indicating that the second reason (as mentioned above) is the cause of decreased mass transfer for prewetted beds. For the porous packing the same trend is observed for the Levec and Super-wetted beds, i.e. the mass transfer for the Levec-wetted bed is faster than that of the Super-wetted bed due to the tracer not taking part in non-wetted areas of the Levec-wetted bed. The slower mass transfer observed for a non-wetted bed for the porous packing, in relation to the prewetted beds, cannot be explained by the above reason. It is thought that the dynamic holdup for the porous particles is not accurate due to the absence of internal liquid holdup in the PDE model and therefore results in inaccurate results of $k_L a\ H_D^{3/2}$, as in figure 4.48.

5.3. Correlations

A number of correlations predicting liquid holdup, wetting efficiency and pressure drop were tested against the experimental values of these hydrodynamic parameters obtained in this study. It was found that very few of these correlations could accurately predict the hydrodynamic parameters obtained for different prewetting procedures.

The lack of agreement between the correlations and the experimental values is an indication that existing correlations do not account for different prewetting procedures. Due to the great differences observed in the liquid holdup, wetting efficiency and pressure drop for the different prewetted beds and non-wetted beds, it is very important to include the effect of prewetting in any correlations.

Many authors neglect to state which prewetting procedure, if any, was used in their work and this contributes to the exclusion of the effect of prewetting. For example in the work of authors such as Ellman et al., (1988) and Larachi et al., (1991), the correlations were based on a number of experimental results obtained from a number of authors, where no mention was made of which prewetting procedure was used. These correlations would then result in only giving an average value between the different prewetted beds.

The pressure drop correlation best predicting experimental results was that of Sato et al., (1973). The experimental conditions of Sato et al., (1973) were much the same as that used in this work. Sato et al., (1973) performed experiments on an air-water system for different size of non-porous glass packing, with no prewetting. It is then expected that this correlation would predict pressure drop for the non-wetted, non-porous beds, which was not the case. This correlation predicted well for the non-porous, Levec-wetted and porous, non-wetted beds.

The liquid holdup correlation of Nemec and Levec allowed for the prediction of liquid holdup in Levec-wetted beds and good agreement was obtained between this correlation and the experimental Levec-wetted liquid holdup obtained from this work. In the work of Nemec and Levec (2005), they used the concept of relative permeability and it was reasoned that the relative permeabilities of the gas and liquid phases are functions of the corresponding phase saturations. Furthermore, from their investigation, they revealed that the phase saturation changed with the transition of rivulet flow to that of film flow. It can therefore be said that with the inclusion of the relative permeabilities of the various phases into correlations, liquid holdup and other hydrodynamic parameters can perhaps be better predicted for different prewetting procedures.

CHAPTER 6

Conclusions and Recommendations

In this study, it was shown that prewetting procedures can have a tremendous effect on various hydrodynamic parameters such as liquid holdup, pressure drop and wetting efficiency for porous and non-porous packing. It was concluded that the differences in the hydrodynamic parameters due to prewetting is a result of different flow morphologies in the beds, i.e. the dominant flow morphology for a non-wetted bed is that of rivulets and for prewetted beds that of film flow. It was also found that at low liquid flow rates the flow morphology in prewetted beds changes from film flow to a combination of rivulet and film flow. This is a result of the thinning or rupturing of liquid films around catalyst particles, at low liquid flow rates.

The conclusion of different flow morphologies for prewetted and non prewetted beds was confirmed by the residence time distributions and various parameters obtained there from. The more pronounced tailing in the prewetted beds is an indication that the flow morphology is predominantly film flow. This tailing effect of the residence time distributions being a result of flow morphology could not be explained at higher liquid flow rates and therefore at these high liquid flow rates the liquid velocity overcame the effects of the flow morphology. It could therefore be concluded that at low liquid flow rates the flow morphology becomes a more predominant factor in creating the tailing effect present in residence time distribution for prewetted beds.

The presence of internal diffusion has been attributed to creating the tailing effect occurring in tracer response curves and this is seemed accurate, however, this phenomenon does not explain the tailing effect in non-porous catalysts. In addition the effect of internal diffusion did not explain the results obtained in this work, on the contrary it contradicted the results obtained from the residence time distributions. It was therefore concluded that the tailing effect in residence time distributions is a result of both internal diffusion and liquid flow morphology, where the liquid flow morphology is the more dominant one. Furthermore, the effect of the gas flow rate on the liquid holdup confirmed the presence of different liquid flow morphologies for prewetted and non-prewetted beds.

The use of residence time distributions to determine a number of hydrodynamic parameters proved to be very useful and accurate. The method of moments and the best-fit method were used. Both methods proved to work well and good agreement was obtained between these methods. The PDE model was used for the best-fit method. It is important to note that when the method of moments is used, it must be ensured that the response curves are very accurate especially at low concentrations, as the moments are very sensitive to these inaccuracies.

The following conclusions could be made from the various parameters obtained from the different methods:

- Method of Moments
    - *Liquid Holdup*. The differences in the liquid holdup determined from the method of moments and the weighing method confirmed that tracer molecules is not always accessible to all the liquid holdup but increases with prewetting, thereby confirming a different flow morphology for prewetted beds.
- Best-fit Method
    - *Peclet Number/ Dispersion Coefficient*. An increase in the dispersion coefficient with prewetting was observed and indicates that the amount of micro mixing is different for the different prewetted beds.
    - *Residence Time*. Differences in the residence times, obtained from different methods, for the porous packing confirmed that the PDE model does not model well the porous packing, response curves due to the lack of internal diffusion and internal holdup in this model.

- *Dynamic Liquid Holdup*. The dynamic liquid holdup determined for the porous particles were very high and is due to the inaccuracy of the PDE model, i.e. lack of consideration of internal holdup, for porous particles.
- *Dynamic-Static Mass Transfer Coefficient*. It was confirmed through the determination of the dynamic-static mass transfer that film flow, as in prewetted beds, results in an apparently slower mass transfer as opposed to rivulet flow, due to non-wetted areas not taking part in this mass transfer. From this it can be concluded that prewetting results in different flow morphologies.

From the results obtained from the best-fit method, it is recommended that a residence time distribution model be used or developed that incorporates the effects of internal diffusion and internal holdup as present in porous catalyst particles.

Numerous correlations were tested against the data obtained in this study in order to predict liquid holdup, pressure drop and wetting efficiency. It was found that very few correlations could accurately predict the parameters due to the absence of the effect of prewetting. It is therefore recommended that correlations be developed for the hydrodynamic parameters that incorporate the effect of prewetting and as such the presence of different flow morphologies.

References

Al-Dahhan, M. and Dudukovic, M. (1995) 'Catalyst Wetting Efficiency in Trickle Bed Reactors at high Pressures' Chemical Engineering Science, 50(15), 2377-2389.

Al-Dahhan, M.H. and Dudukovic, M.P. (1995) 'Catalyst Wetting Efficiency in Trickle Bed Reactors at High Pressure' Chemical Engineering Science, 50(15), 2377-2389.

Baussaron, L., Julcour-Lebigue, C., Wilhelm, A.M., Boyer, C. and Delmas, H. (2005) 'Partial Wetting in Trickle Bed Reactors: Measurement Techniques and Global Wetting Efficiency' Chemical Engineering Science.

Buffham, B.A. (1983) 'Internal and External Residence Time Distributions' Chem. Eng. Communication, 22, 105-117.

Buffham, B.A. and Mason, G. (1993) 'Holdup and Dispersion: Tracer Residence Times, Moments and Inventory Measurements' Chemical Engineering Science, 48(23), 3879-3887.

Charpentier, J.C. and Reynier, J.P. (1971) 'Holdup Prediction in Packed Columns for Cocurrent Gas-Liquid Downflow' Chemical Engineering Science, 26, 1783-1784.

Christensen, G., McGovern, S.J. and Sundaresan, S. (1986) 'Cocurrent Downflow of Air and Water in a Two-Dimensional Packed Column' AIChE Journal, 32(10), 1677-1689.

Colombo, A.J., Baldi, G. and Sicardi, S. (1976) 'Solid-Liquid Contacting Effectiveness in Trickle Bed Reactors' Chemical Engineering Science, 31, 1101-1108.

Danckwerts, P.V. (1953) ‘Continuous Flow Systems: Distribution of Residence Times’ Chem. Eng. Sci., 2(1), 1-13.

Dudukovic, M.P. (1977) ‘Catalyst Effectiveness Factor and Contacting Efficiency in Trickle Bed Reactors’ AIChE Journal, 23(6), 940-944.

Ellman, M.J., Midoux, N., Laurent, A. and Charpentier, J.C. (1988) ‘A New Improved Pressure Drop Correlation for Trickle Bed Reactors’ Chemical Engineering Science, 43, 2201-2210.

Ellman, M.J., Midoux, N., Laurent, A. and Charpentier, J.C. (1990) ‘A New Improved Liquid Holdup Correlation for Trickle Bed Reactors’, Chemical Engineering Science, 45, 1677-1684.

Fogler, H.S. (1999) Elements of Chemical Reaction Engineering, Prentice-Hall International, New Jersey.

Gianetto, A., Baldi, G., Specchia, V. and Sicardi, S. (1978) ‘Hydrodynamics and Solid-Liquid Contacting Effectiveness in Trickle Bed Reactors’ AICHE Journal, 24 (6), 1087-1104.

Henry, H.C. and Gilbert, J.B. (1973) ‘Scale Up of Pilot Plant Data for Catalytic Hydroprocessing’ Ind. Eng. Chem. Process Des. Develop., 12(3), 328-334.

Holub, R.A., Dudukovic, M.P. and Ramachandran, P.A. (1992) ‘A Phenomenological Model for Pressure Drop, Liquid Holdup and Flow Regime Transition in Gas-Liquid Trickle Flow’, Chemical Engineering Science, 47, 2343-2348.

Iliuta, I. and Larachi, F. (2000) ‘Double Slit Model for Partially Wetted Trickle Flow Hydrodynamics’ AIChE Journal, 46(3), 597-609.

Iliuta, I. and Thyrion, F.C. (1997) ‘Flow Regimes, Liquid Holdups and Two-Phase Pressure Drop for Two-Phase Cocurrent Downflow and Upflow through packed Beds: Air/Newtonian and Non-Newtonian Liquid Systems' Chemical Engineering Science, 52(21/22), 4045-4053.

Illiuta, I., Larachi, F. and Grandjean, B. (1999) 'Residence Time, Mass Transfer and Backmixing of the Liquid in Trickle Flow Reactors containing Porous Particles' Chemical Engineering Science, 54, 4099-4109.

Illiuta, I., Thyrion, F.C. and Muntean, O. (1996) 'Hydrodynamic Characteristics of Two Phase Flow Through Fixed Beds: Air/Newtonian and Non-Newtonian Liquids' Chemical Engineering Science, 51(22), 4987-4995.

Julcour-Lebique, C., Baussaron, L., Delmas, H. and Wilhelm, A.M. (2006) 'Theoretical Analysis of Tracer Method for the Measurement of Wetting Efficiency' Chemical Engineering Science, Manuscript Draft.

Kan, K.M. and Greenfield, P.F. (1979) 'Pressure Drop and Holdup in Two-Phase Cocurrent Trickle flow through Packed Beds' Ind. Eng. Chem. Process Des. Dev., 18, 740-745.

Larachi, F., Grandjean, B., Iliuta, I., Bensetiti, Z., Andre, A., Wild, G. and Chen, M. (1999) Excel Worksheet Simulators for Packed Bed Reactors, http://www.gch.ulaval.ca/bgrandjean/pbrsimul/pbrsimul.html, [2006, October 25].

Larachi, F., Laurent, A., Midoux, N. and Wild, G. (1991) 'Experimental Study of Trickle Bed Reactor Operating at high Pressure: Two-Phase Pressure Drop and Liquid Saturation' Chemical Engineering Science, 46, 1233-1246.

Loudon, D. (2005) The Effect of Prewetting on the Pressure Drop, Liquid Holdup and Gas-Liquid Mass Transfer in Trickle Bed Reactors, Masters Dissertation, Department of Chemical Engineering, University of Pretoria, Pretoria, South Africa.

Midoux, N. and Charpentier, J.C. (1973) 'Apparent Diffusivity and Tortuosity in Liquid Filled Porous Catalyst used for Hydrodesulphurisation of Petroleum Products' Chemical Engineering Science, 28, 2108-2111.

Mills, P.L. and Dudukovic, M.P. (1981) 'Evaluation of Liquid-Solid Contacting in Trickle Bed Reactors by Tracer Methods' AICHE Journal, 27(6), 893-903.

Mills, P.L. and Dudukovic, M.P. (1989) 'Convolution and Deconvolution of Non Ideal Tracer Response Data with Application to Three Phase Packed Beds' Computers Chem. Eng. 13(8), 881-898.

Naor, P. and Shinnar, R. (1963) 'Representation and Evaluation of Residence Time Distributions' I&EC Fundamentals, 2(4), 278-286.

Nemec, D. and Levec, J. (2005) 'Flow through Packed Bed Reactors 2: Two Phase Concurrent Downflow' Chemical Engineering Science, 60, 6958-6970.

Nigam, K.D.P., Illuita, I. and Larachi, F. (2002) 'Liquid Back Mixing and Mass Transfer Effects in Trickle Bed Reactor filled with Porous Catalyst Particles' Chem. Eng. and Processing, 41, 365-371.

Ramachandran, P.A., Dudukovic, M.P. and Mills, P.L. (1986) 'A New Model for Assessment of External Liquid-Solid Contacting in Trickle-Bed Reactors from Tracer Response Measurements' Chemical Engineering Science, 28, 855-860.

Ravindra, P.V., Rao, D.P. and Sao, M.S. (1997) 'Liquid Flow Texture in Trickle Bed Reactors: An Experimental Study' Ind. Eng. Chem. Research, 36, 5133-5145.

Robinson, B.A. and Tester, J.W. (1986) 'Characterisation of Flow Maldistribution Using Inlet-Outlet Tracer Technique: An Application of Internal Residence Time Distributions' Chemical Engineering Science, 41(3), 469-483.

Sato, Y., Hirose, T., Takahashi, F. and Toda, M. (1973) 'Pressure Loss and Liquid Holdup in a Packed Bed Reactor with Cocurrent Gas-Liquid Downflow' Journal of Chem. Eng. Japan, 6(2), 147-152.

Sicardi, S., Baldi, G. and Specchia, V. (1980) 'Hydrodynamic Models for the Interpretation of the Liquid Flow in Trickle Bed Reactors' Chemical Engineering Science, 35, 1775-1782.

Sicardi, S., Baldi, G. Gianetto, A. and Specchia, V. (1980) 'Catalyst Areas Wetted by Flowing and Semistagnant Liquid in Trickle Bed Reactors' Chemical Engineering Science, 35, 67-73.

Specchia, V. and Baldi, G. (1977) 'Pressure drop and Liquid Holdup for Two Phase Concurrent Flow in Packed Beds' Chemical Engineering Science, 32, 515-523.

Tsamatsoulis, D. and Papyannakos, N. (1994) 'Axial Dispersion and Holdup in a Bench-Scale Trickle Bed Reactor at Operating Conditions' Chemical Engineering Science, 49(4), 523-529.

Van Deemter, J.J. (1961) 'Skewed Holding Time Distributions' Chemical Engineering Science, 13(3), 190-191.

Van der Merwe, W. (2004) The Morphology of Trickle Flow Liquid Holdup Masters Dissertation, Department of Chemical Engineering, University of Pretoria, Pretoria, South Africa.

Van Houwelingen, A. (2005) The Morphology of Solid-Liquid Contacting Efficiency in Trickle Bed Reactors Masters Dissertation, Department of Chemical Engineering, University of Pretoria, Pretoria, South Africa.

Van Swaaij, W.P.M. (1969) 'Residence Time Distribution in the Liquid Phase of Trickle Flow in Packed Columns' Chemical Engineering Science, 24(7), 1083-1095.

Wammes , W.J.A., Middlekamp, J., Huisman, W.J., De Baas, C.M. and Westerterp, K.R. (1991) ‘Hydrodynamics in a Cocurrent Gas-Liquid Trickle Bed at Elevated Pressures’ AIChE Journal, 37, 1849-1862.

Appendix

A.1. The Effect of Prewetting on the RTD Response

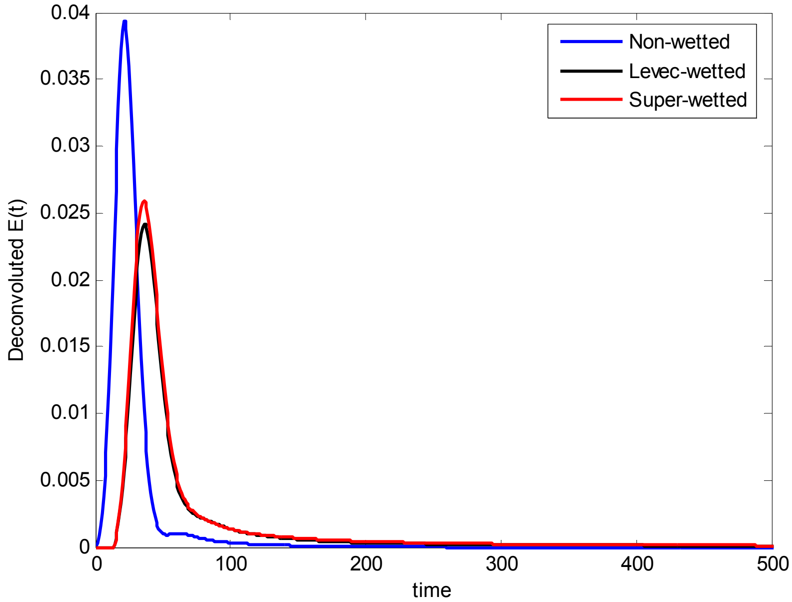

Figure A.1 - Effect of prewetting at U_L=8 mm/s, U_G=0.02 mm/s

A.2. The Effect of the Liquid Flow Rate on the RTD Response

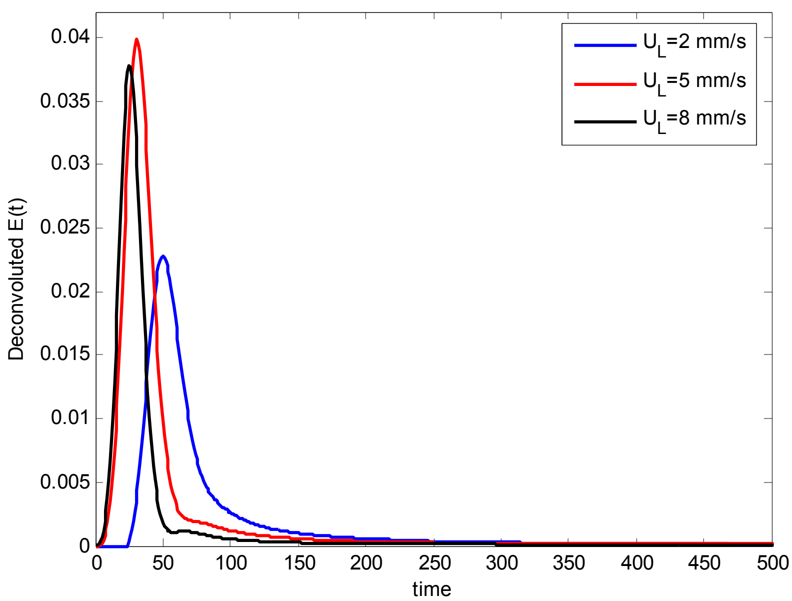

Figure A.2 - Effect of the liquid Flow rate for a non-wetted bed at U_G=0.06 m/s

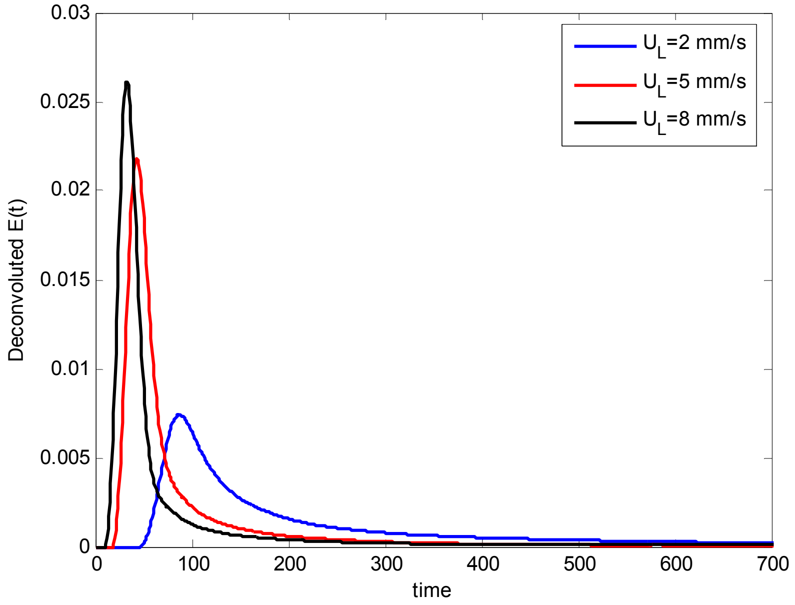

Figure A.3 - Effect of the liquid flow rate for a Levec-wetted bed at U_G=0.1 m/s

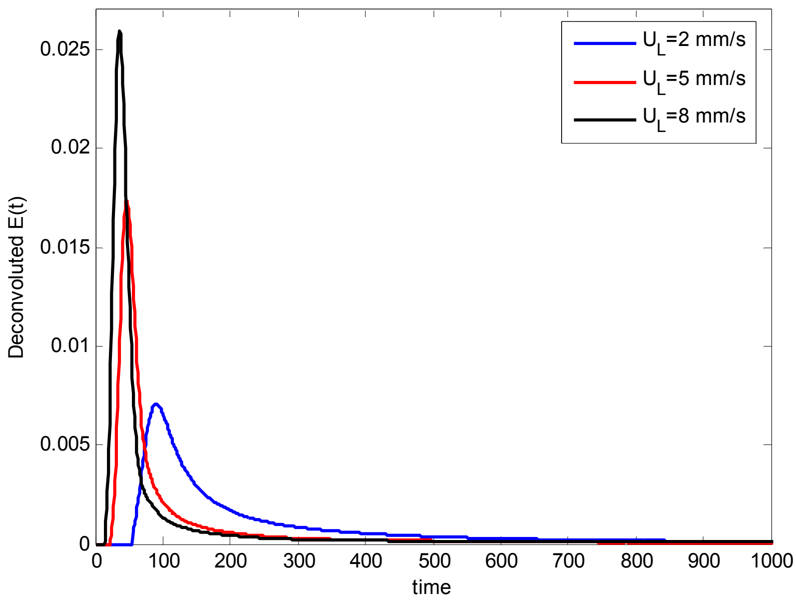

Figure A.4 - Effect of the liquid flow rate for a Super-wetted bed U_G=0.02 m/s

A.3. The Effect of the Prewetting and Liquid Flow Rate on the Pressure Drop

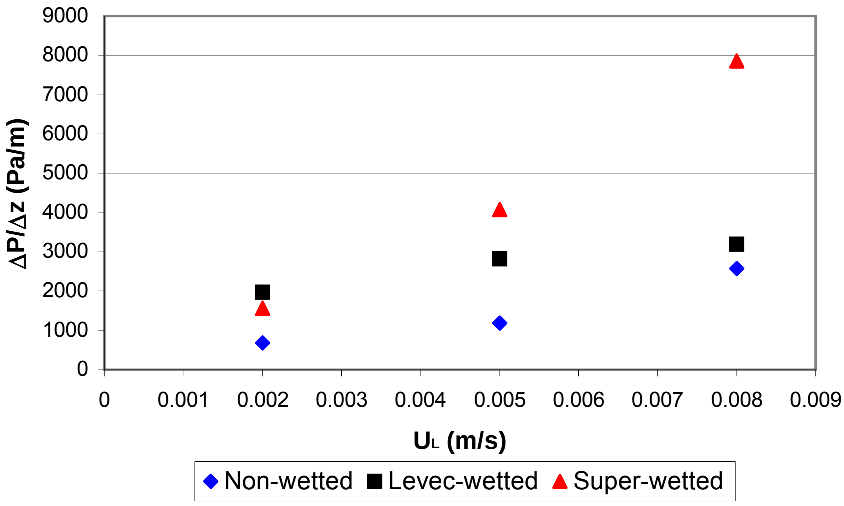

Figure A.5 - The effect of Prewetting on the Pressure Drop at U_G=0.1 m/s

A.4. The Effect of the Prewetting and Liquid Flow Rate on the Liquid Holdup

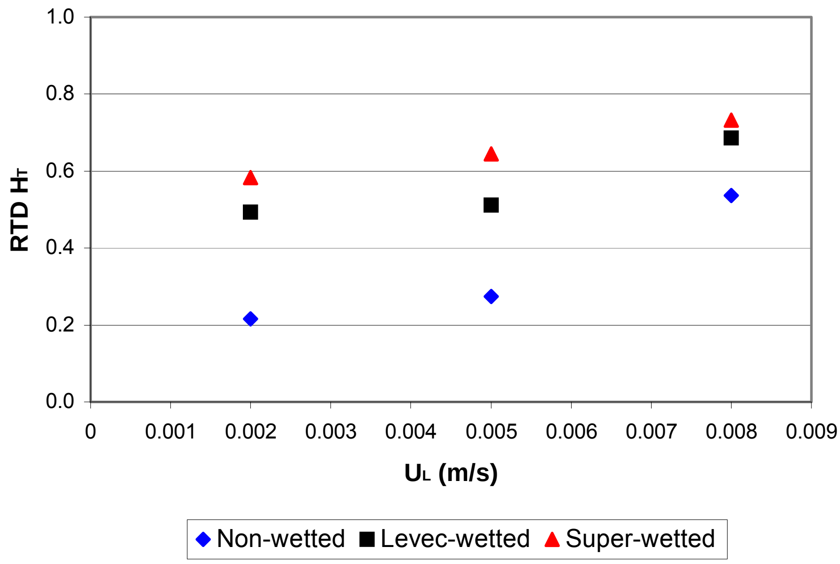

Figure A.6 - Effect of prewetting on the holdup at U_G=0.1 m/s

A.5. The Difference in the RTD and Weighed Liquid Holdup

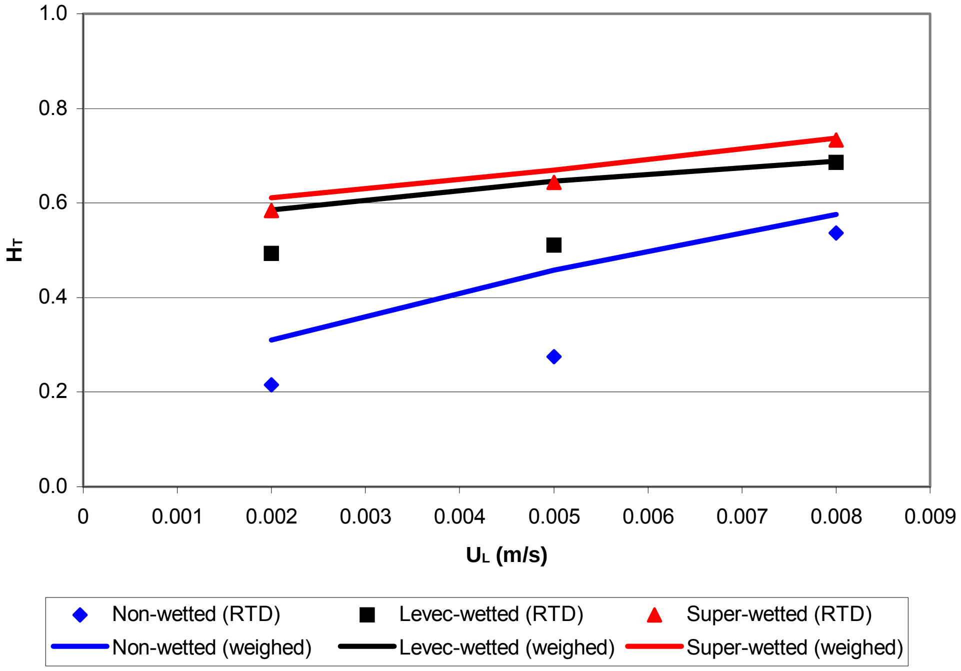

Figure A.7 - Comparison of RTD and weighed holdup at U_G=0.1 m/s

A.6. The Effect of Prewetting and Liquid Flow Rate on the Wetting Efficiency

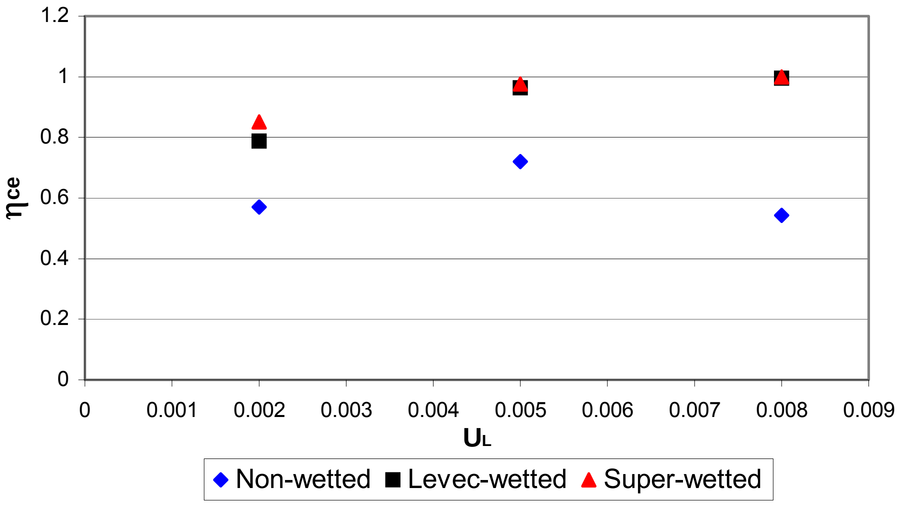

Figure A.8 - Effect of prewetting and liquid flow rate on the wetting efficiency at U_G=0.06 m/s